Doctoral Thesis

Study on Angiogenic Cytokine Production in Human Skeletal Muscle Cell Sheet

Thummarati Parichut

September 2021

Graduate School of Engineering

Osaka University

Contents

Abstract

Skeletal muscle mainly consists of a heterogeneous population of myoblasts and fibroblasts. The skeletal muscle cells have been studied for cardiac regeneration to apply for autologous transplantation in the patient's heart with ischemia. Plenty of angiogenic cytokines secreted from the skeletal muscle cells have been shown to recover the damaged heart tissue, possibly through angiogenesis induction. While research on cell sheet technology has expanded, the impacts of human skeletal muscle fibroblast (HSMF) co-cultured with skeletal muscle myoblast (HSMM) on angiogenic cytokine balance and its implication have not been yet clarified. In this study, mono-culture and co-culture of HSMM and HSMF as monolayers (two-dimensional structure) and multilayers (three-dimensional structure) in various conditions and their respective outcomes were investigated to understand the angiogenic cytokine balance and endothelial network formation regulation.

In chapter 2, the effect of HSMF co-culture in skeletal muscle cell sheet on the productivity of angiogenic cytokines and angiogenesis was elucidated. First, the skeletal muscle cells from the original source were isolated into HSMM and HSMF populations. These cells were then prepared by mono-culture and co-culture as monolayers. The culture media were collected and measure the angiogenic cytokine productivity. Time-lapse observation and cell tracking system was applied to understand the paradigms of physiological interactions implicating the cytokine production from monolayers with different HSMF. Moreover, the effect of heterogeneous populations of skeletal muscle cells on angiogenesis was evaluated using 3D *in vitro* culture system imitating *in vivo* angiogenesis, in which green fluorescent protein-expressing human umbilical vein endothelial cells (GFP-HUVECs) were cultured under the fabricated multilayered human skeletal muscle cells with various proportions of HSMF.

In chapter 3, the role of FGF-2 in endothelial behaviors to promote endothelial network formation in the human skeletal muscle cell sheets were studied. A culture system comprising five-layered sheets

of human skeletal muscle cells co-incubated on GFP-HUVECs mimicking *in vivo* angiogenesis was prepared, and exogenous FGF-2 was added in culture media of a treated group of the cell sheet. The endothelial network images from the local and whole area inside the cell sheet were captured and analyzed the network length, tip number, and connectivity to understand the extension of the endothelial network. The quantitative analysis method of endothelial network formation was modified from the previous study to measure the network from the whole sheet area. The numbers of medium and long endothelial networks in the cell sheet were measured, and time-lapse observation of endothelial cells during network formation was applied to elucidate the precise role of FGF-2 on endothelial functions during network extension.

Overall, this study provides insight into the impact of HSMF co-cultured in skeletal muscle cell sheet on the production of angiogenic cytokines (VEGF, HGF, and FGF-2) and its implication on angiogenesis. This study also creates cultural conditions to enhance endothelial network formation, which are regarded as necessary in multilayer skeletal muscle cell sheets and other tissue engineering approaches.

Chapter 1

General introduction

1.1 Regenerative medicine and cell sheet engineering

The term “tissue engineering” was only officially coined in the last few decades. In 1993, Dr. Langer and Dr. Vacanti first proposed tissue engineering defined as "*an interdisciplinary field that applies the principles of engineering and life sciences toward the development of biological substitutes that restore, maintain, or improve tissue function or a whole organ*" (Langer et al. 1993). Subsequently, tissue engineering has been combined with other subjects, such as cell-based therapy, stem cell biology, biomechanics prosthetics, and biochemistry, and has been termed regenerative medicine.

The promising field of regenerative medicine aims to replace, repair, or regenerate various tissues and organs to cure patients suffering from several diseases or traumas. Although various techniques and cell sources are available for regenerative medicine, it is still challenging to establish new approaches to overcome the technical limitations of cell therapy from the conventional approaches. For example, intravenous injection of cells for myocardial infarction treatment has been shown to have low cell retention after cell delivery. It has been reported that less than 0.1% of injected cells reached the heart, but most cells were diffused to other organs (Freyman et al. 2006). Therefore, a high dose of cells is required to increase the efficiency of treating some diseases. Combining seeded cells with scaffolds or other tissue is another engineering approach and widely advanced in regenerative medicine to improve both cell retention and therapeutic efficiency after cell delivery. Several cell types, such as hematopoietic progenitor cells for the treatment of leukemia (Koehl et al. 2002), brain cells for the treatment of Parkinson's disease (Olanow et al. 2003), hepatocytes for the treatment of liver diseases (Iansante et al. 2018), and human neural stem cells to treat chronic ischemic stroke (Kalladka et al. 2016) have been transplanted into human patients using this approach. However, it is limited to a small range of diseases where a relatively small number of cells are sufficient for treatment, although lack of donors is not a

major criticism of this method compared to organ transplantation. However, the use of cell-loaded scaffolds tends to have certain adverse effects, such as material-associated infections and immune reactions to the implant (Boehler et al. 2011).

Facilitation of cell-to-cell interactions and extracellular matrix (ECM) development are necessary for tissue maintenance. Harvesting cell suspensions with trypsin often damages cell surface proteins that are important for cell-to-cell and cell-to-ECM interactions. The negative result impairs cell adhesion and proliferation, leading to uneven distribution and low repair efficiency after transplantation. Conventional tissue engineering with scaffold-seeded cells also has some limitations due to high cell death or loss due to various factors such as inflammation at the graft site, autoimmunity, and mechanical injury. Engineering of scaffold-free tissue with induction of angiogenic cytokines to promote angiogenesis could improve cell survival and therapeutic efficiency.

Cell sheet technology is a scaffold-free tissue engineering technique in which transplanted cells can be fully preserved by forming cell-cell junctions and extracellular matrix proteins. Cell sheet composition resembles that of natural tissues, and therefore, avoids limitations associated with scaffold degradation. Moreover, cell sheet harvesting is possible without enzyme treatment; cell-cell interactions and cell sheet structure are well preserved. Moreover, this technology enables the delivery of the therapeutic cell population into the target tissue without the cell leaking through the injection channel or washing out to the bloodstream or becoming apoptosis due to lack of cell adhesion. Therefore, the development of cell sheet technology improves regenerative capacity and increases the potential applications for biological research.

The development of cell sheet technology was first reported by Takezawa et al. as the poly N-isopropyl acrylamide (PIPAAm) polymer was used to coat cell culture surfaces (Takezawa et al. 1990). This polymer exhibits the interesting character of a temperature-responsive reversible transition that leads to a change in its hydrophobic/hydrophilic properties (Kenji K. 1990; Nagase et al. 2018).

Therefore, the cells can be harvested simply by changing the temperature without enzymatic treatment. At a temperature above 32°C, the culture surface is hydrophobic, allowing cells to attach and proliferate. Lowering the culture temperature to 20°C then makes the surface hydrophilic, allowing cells to be easily detached from the surface and producing biologically active and functional uniform cell sheets (**Fig. 1-1A**). Since cell sheets contain ECM and cell membrane proteins, cell sheets can be attached to other cell sheets, and three-dimensional tissues can be easily prepared by simply layering cell sheets without immunological scaffolds (**Fig. 1-1B**).

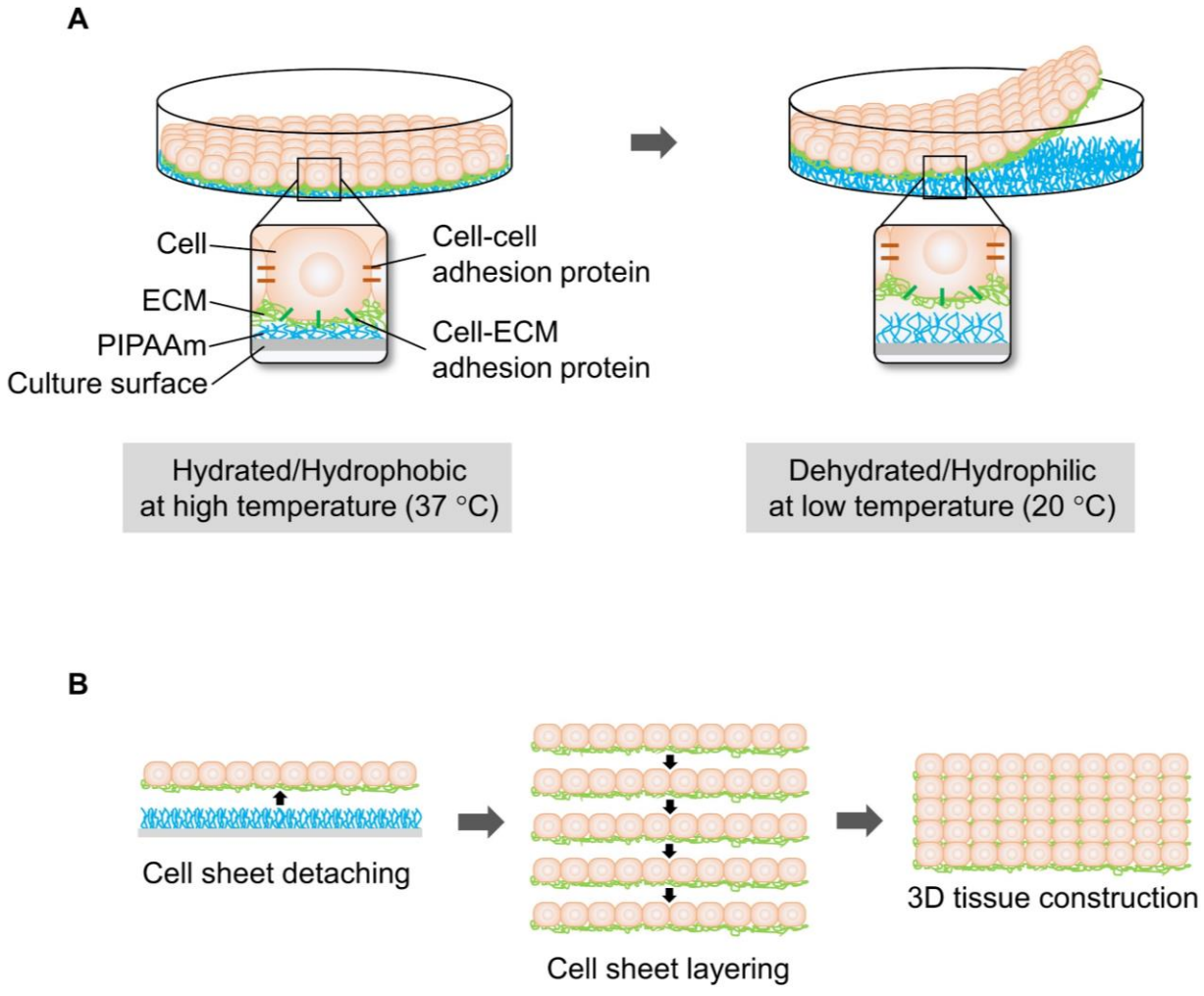

Fig. 1-1 Schematic diagram of cell sheet technology using the temperature-responsive surface. (A) By lowering the temperature, cultured cells are harvested on a temperature-dependent surface coated with a poly(N-isopropyl acrylamide) (PIPAAm) as a confluent cell sheet, preserving cell-cell junctions cell

surface proteins, and the extracellular matrix (ECM). (B) Fabrication of three-dimensional tissue by layering cell sheet.

The potential of cell sheet technology was first demonstrated by Nishida et al. in transplantation using autologous oral mucosal epithelial cells for corneal regeneration (Nishida et al. 2004). Since then, numerous cell types, including epidermal keratinocytes (Matsumine et al. 2019), vascular endothelial cells (Sumide et al. 2006), periodontal ligaments (PDLs) (Hasegawa et al. 2005), cardiomyocytes (Guo et al. 2020), and skeletal muscle cells (Sawa et al. 2015), have been investigated as cell sheets for regenerative medicine. Cell sheet technology has not only been applied in the field of tissue transplantation but also provides multicellular three-dimensional models for biological research (Nagamori et al. 2013; Li et al. 2017; Lee et al. 2018) (**Fig. 1-2**).

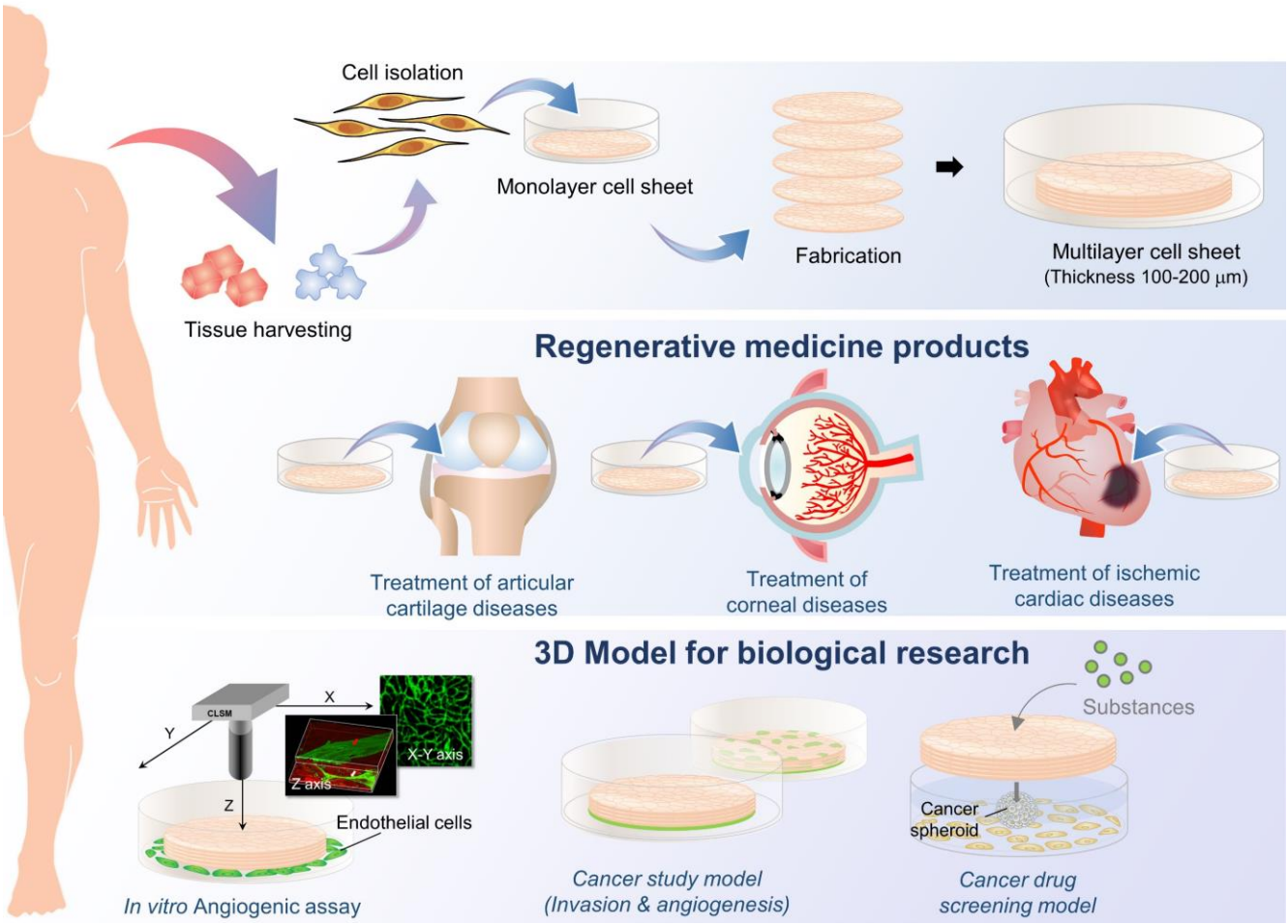

Fig. 1-2 Applications of cell sheet technology engineering for regenerative medicine and biological research.

1.2 Application of the skeletal muscle cells for myocardial infarction treatment

Myocardial infarction (MI) or heart attack is a condition that results in irreversible death of heart tissue secondary to prolonged ischemia. Today, MI remains a leading cause of death worldwide (Cleland et al. 1999). Treatment of MI including drugs to improve blood flow and dissolve the clot and surgical procedures to treat blood vessels narrowed by atherosclerosis. However, these methods have only been able to halt the progression of the disease (Kwon et al. 2010). Therefore, new therapies are needed to regenerate damaged hearts and overcome the poor prognosis of the patients. Heart transplantation is the most effective method to treat patients with MI; however, the lack of organ supply is still a major problem. Besides, the use of artificial hearts for transplantation in late-stage disease is associated with problems due to complications such as infection, bleeding, and thrombosis (Cook et al. 2015). Recently, cell transplantation for MI has gained attention as a promising therapy to overcome the transplant challenge. This therapy involves the direct intramyocardial injection of stem cells or skeletal muscle myoblasts (Taylor et al. 1998; Orlic et al. 2001). From the previous report, intramyocardial skeletal muscle transplantation has been shown to improve heart function after infarction (Menasche et al. 2001; Menasche 2007). Since autologous skeletal muscle myoblasts isolated from patients were transplantated successfully with no rejection and complication (Siminiak et al. 2004). However, this method still has some disadvantages including cell loss from the leakage of injected cells from myocardium (Pagani et al. 2003) and poor survival of graft cells and myocardial damage (Suzuki et al. 2004).

In the last decade, tissue engineering has been made considerable progress and appealing as an emerging field that restores or improves damaged tissue or whole organ function. Tissue engineering for skeletal muscle myoblast transplantation is the most appealing and clinical straightforward to pursue cardiac tissue replacement (Chen et al. 2015).

Recently, innovative tissue engineering for transplantation has been developed as cell sheet technology. This approach can be manufactured without biomaterials, and the tissues prepared from this approach are preserved in their intercellular and extracellular structures essential for cell function during transplantation. Besides, such technology enables the delivery of the therapeutic cell population into the

target tissue without cell loss by leakage through the injection channel or washout to the circulation, or apoptosis by failure to adhere, called anoikis (Yang et al. 2005).

Myoblast sheet was firstly established using autologous skeletal muscle myoblast by Okano's group at Tokyo Woman's Medical University, Japan (Memon et al. 2005; Matsuura et al. 2013). The first trial of autologous human skeletal muscle myoblast sheet transplantation by *in vivo* dilated cardiomyopathy confirmed the feasibility, safety, and therapeutic efficiency of the cell sheet (Sawa et al. 2013). For treatment mechanism, the myoblasts sheet might produce several cytokines such as vascular endothelial growth factor (VEGF), hepatocyte growth factor (HGF), fibroblast growth factor-2 (FGF-2), which are essential factors to promote angiogenesis actively in the infarcted area and attract the progenitors to come and improve the damaged part resulting in the induction of cardiac tissue (Ahmad et al. 2015). Before that evidence, it was reported that implantation of multilayered myoblast sheets such as three and five-layered sheets promoted favorable results with better induction of angiogenesis, presence of more elastic fibers, and less fibrosis compared with a monolayer sheet, most probably due to more cytokine secretion from the HSMMs (Sekiya et al. 2009). From these findings, it is easily feasible that, thicker skeletal muscle cell sheet could more induce angiogenesis in the infarcted area and recover the heart functions due to high secretion of angiogenic inducible factors.

1.3 Angiogenic growth factors

Several potent growth factors, including vascular endothelial growth factor (VEGF), hepatocyte growth factor (HGF), and basic fibroblast growth factor (bFGF or FGF-2) are reported as primary angiogenic simulators in ischemic areas. These growth factors are also experimentally demonstrated to improve cardiac functions (Fallah et al. 2019; Laddha et al. 2019). VEGF exerts its biological functions through binding to two homologous VEGF receptors expressed on the surface of the endothelial cells (Carmeliet 2005; Fallah et al. 2019). After binding, VEGF directly acts on the endothelial cells to promote migration, increase permeability, and enhance survival during vascularization and angiogenesis (Zachary et al. 2001). From previous studies, injection of skeletal myoblasts with genetic modifications

to upregulate VEGF expression was reported to effectively treat acute myocardial infarction by promoting vasodilatory and angiogenic effects (Suzuki et al. 2001; Haider et al. 2004). However, this therapeutic strategy of gene transfer is associated with viral vectors; therefore, adverse effects and ethical concerns need to be concerned (Kim et al. 2001).

HGF is one of the most potential angiogenic stimuli. It has been reported to be involved in various cell types, including endothelial cells, by promoting motility, cell-to-cell interaction, branching, and/or tubular morphogenesis (Morimoto et al. 1991; Rosen et al. 1997). Moreover, previous studies have investigated the effects of HGF for the treatment of myocardial infarction by *in vivo* study (Nakamura et al. 2000; Ueda et al. 2001; Jin et al. 2003; Liu et al. 2016). This study demonstrated that the HGF-engineered skeletal myoblasts promote angiogenesis, reduce myocardial fibrosis, and decrease cardiomyocytes' apoptosis (Yuan et al. 2008; Madonna et al. 2015).

Previously, FGF-2 is also reported to exert therapeutic effects in ischemia by regulating angiogenesis through the regulation of various cell-cell interactions (Murakami et al. 2008), and incorporation with other growth factors or chemokines such as VEGF (Masaki et al. 2002; Kanda et al. 2004) and HGF (Onimaru et al. 2002).

1.4 Research outline

This study aimed to investigate the productivity of angiogenic growth factors, including VEGF, HGF, and FGF-2, by skeletal muscle cells, HSMMs and HSMFs, and cell behaviors in the cell sheet to promote angiogenesis. Primary human skeletal muscle cells containing HSMF and HSMM were used to construct monolayers and 3D multilayers cell sheets. Then, cytokine levels in cultured media, cell migration, and endothelial network formation were analyzed (**Fig. 1-3**).

Chapter 1 focused on the effect of HSMF co-cultured with HSMM in cell sheet on angiogenic cytokine production and angiogenesis. The VEGF, HGF, and FGF-2 in culture media of monolayers prepared from various proportions (co-culture) and cell densities (mono-culture) of HSMMs and HSMFs were measured. The mechanism underlying VEGF production in co-culture was investigated by

examining the dynamic behaviors of cells in monolayers to analyze the effect of HSMFs on myoblast-to myoblast contact. After that, the effect of heterogeneous populations of skeletal muscle cells on angiogenesis was evaluated using green fluorescence protein-expressing human umbilical vein endothelial cells (GFP-HUVECs) incubated with fabricated multilayer HSMM sheets comprising various proportions of HSMFs. This understanding can be applied to design engineered tissues, including skeletal muscle cell sheets, to improve the therapeutic potential for myocardial infarction.

Chapter 2 focused on the precise role of FGF-2 in endothelial function to promote angiogenesis after transplantation. In this study, a culture system comprising a five-layered sheet of human skeletal muscle cells co-incubated on GFP-HUVECs mimicking *in vivo* angiogenesis was used. The cultured media from the skeletal muscle cell sheets was measured the basal level of endogenous FGF-2. Then, the endothelial network formation in the cell sheets treated with or without exogenous FGF-2 after prolonged culture was analyzed. The time-lapse observation was used to monitor dynamic endothelial behaviors during network formation in the five-layered cell sheet. Moreover, the effect of FGF-2 on survival and proliferation of GFP-HUVECs outside the cell sheet was also demonstrated. In the present study, the results suggested the precise roles of FGF-2 to maintain endothelial connection and extent endothelial network in skeletal muscle cell sheets.

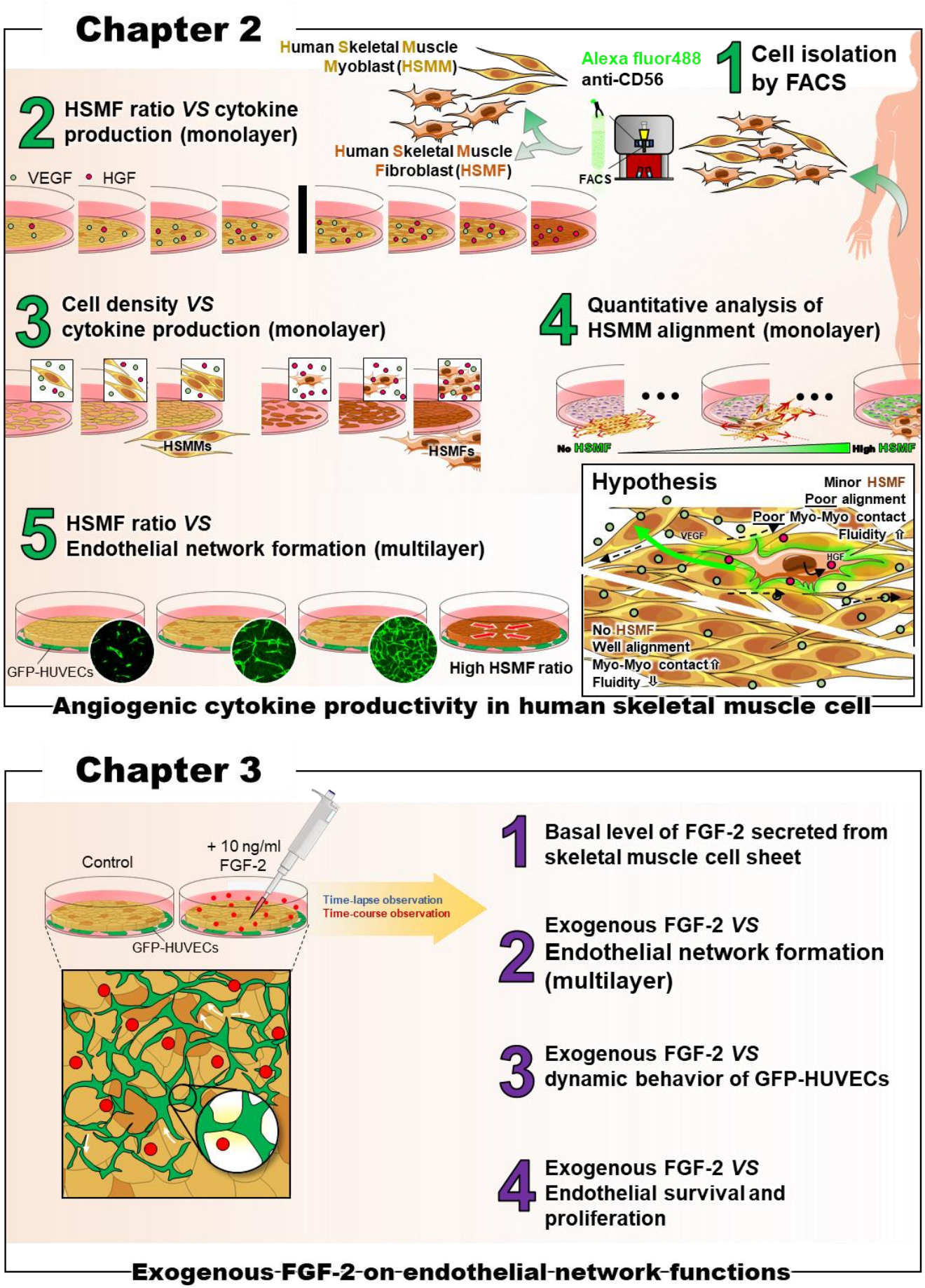

Fig. 1-3 Schematic diagram showing an outline of this study

Chapter 2

Angiogenic cytokine productivity in human skeletal muscle cells

2.1 Introduction

Angiogenesis is a fundamental process in animal development and restoration of damaged tissues (Felmeden et al. 2003). This process is forming new blood vessels from the existing ones by increasing vessel density, network length, and branching (Durand et al. 2017). During the angiogenic process, endothelial cells from the existing blood vessel are activated and stimulated by various growth factors such as VEGF and HGF. The activated cells are destabilized from the existing vessel, and they are engaged for invasion, migration, proliferation following cell-to-cell connection, and tube formation for blood vessel maturation (Papetti et al. 2002).

Efficient establishment of vascularization achieved by stimulation of angiogenesis is the key challenge for tissue engineering. The survival of cells in the middle of the thick three-dimensional tissue construct depends on a vascular supply of oxygen and nutrient (Santos et al. 2010). Accordingly, the induction of angiogenic factors to promote blood vessel formation for engineered tissue constructs is a major challenge to pave the way for broad clinical use of tissue engineering applications. Several approaches, which may improve vascular growth into implanted tissue constructs, are currently under investigation (Anderson et al. 2004; Rucker et al. 2006).

For the model of *in vitro* angiogenesis, human umbilical vein endothelial cell (HUVEC), isolated from the umbilical cord, has been commonly used for vascular biology research due to the simple isolation, human source availability, and low cost (Baudin et al. 2007; Lei et al. 2016). Moreover, HUVEC transfected to express a green fluorescent protein (GFP) provides a classic cell tracking model to investigate many aspects of endothelial functions in the angiogenic process (Liu et al. 2016; Andree et al. 2019). In cell sheet technology, GFP-HUVECs have been used to co-culture with multilayer human skeletal muscle cell sheets, allowing examining the dynamic endothelial behaviors that mimic the *in vivo*

angiogenesis. This system can evaluate the endothelial network formation, which is considered to be a promising *in vitro* angiogenesis model (Nagamori et al. 2013).

Ischemic heart disease is the leading cause of mortality of people over the world. The disease occurs when the blood flow to the myocardial tissue is obstructed by plaque or blood clotting. After myocardial infarction, millions of myocardial cells die and lose from the infarcted site because of the lack of oxygen and blood supply (2010; Severino et al. 2020). Several therapeutic approaches based on tissue engineering are available to rescue the ischemic heart to replace losing cells and induce angiogenesis. Human skeletal muscle myoblast transplantation is being perceived as one of the potential alternatives for treating myocardial infarction (Pagani et al. 2003). The advantages of using skeletal muscle myoblast are availability and the lack of immunologic barriers to the transplantation process (Dib et al. 2005; Menasche 2007). Furthermore, transplantation of autologous skeletal myoblast into the human heart was proved for safety and efficiency (Menasche et al. 2001; Durrani et al. 2010). Several studies have revealed that skeletal muscle myoblasts provide various essential factors capable of angiogenesis induction and recruit the progenitors to the infarcted area resulting in the induction of cardiac tissue and recovery of heart functions (Suzuki et al. 2001; Murtuza et al. 2004; Memon et al. 2005; Shirasaka et al. 2013). Besides, implantation of multilayered skeletal myoblast sheets promoted favorable results with better induction of angiogenesis by *in vitro* (Ngo et al. 2013) and *in vivo* studies (Sekiya et al. 2009; Miyagawa et al. 2017).

Fibroblasts are the most abundant cell type found in the connective tissues, which able to synthesize and secrete pro-angiogenic growth factors, such as vascular endothelial growth factor (VEGF), hepatocyte growth factor (HGF), and fibroblast growth factor-2 (bFGF or FGF-2) (Newman et al. 2011; Kendall et al. 2014; Chapman et al. 2016). Additionally, fibroblasts also synthesize extracellular matrix (ECM) components such as collagen, fibronectin, and proteoglycans to support angiogenesis (Newman et al. 2011; Chapman et al. 2016). Nevertheless, an uncontrolled number of fibroblasts can cause fibrosis due to excessive deposition of ECM (Mann et al. 2011; Kendall et al. 2014). Thus, co-transplantation of skeletal myoblasts with a small proportion of fibroblasts can be a potential approach for ischemic myocardium regeneration. From the viewpoint of application, the fibroblasts and myoblast

proportion, which may vary depending on tissue source, should influence transplantation's therapeutic efficiency. The detail of the heterogeneous population of skeletal myoblast and fibroblast for maintaining cytokine production and angiogenesis has not been completely understood.

A variety of potent growth factors has been identified as angiogenic simulators in ischemic areas. Among these factors, VEGF (VEGF-A), HGF, and FGF-2 are direct pro-angiogenic markers to promote angiogenesis (Fallah et al. 2019; Laddha et al. 2019). Moreover, these growth factors have been experimentally shown improvement of myocardial cardiac functions. The combined delivery of HGF and VEGF to infarcted myocardium showed increasing wall thickness of left ventricle (LV) and capillary density, reducing the infarction size and improving the dilatation index (Makarevich et al. 2018). Moreover, clinical trials have demonstrated that the myocardial perfusion was enhanced, leading to improve cardiac function and well-tolerated after treatment with VEGF, HGF, and FGF-2 (Atluri et al. 2008). VEGF functions are mediated by binding to two homologous VEGF receptors expressed on vascular endothelial cells (Carmeliet 2005; Fallah et al. 2019). VEGF directly acts on endothelial cells to enhance migration, increase permeability, enhance survival during vascularization and angiogenesis (Zachary et al. 2001). Injection of skeletal myoblasts with genetic modification to upregulated VEGF demonstrated the effective treatment of acute myocardial infarction through vasodilatation and angiogenesis effects (Suzuki et al. 2001; Haider et al. 2004). However, these studies involve viral vectors for therapeutic gene transfer, which the adverse effects and ethical considerations are concerned (Kim et al. 2001). HGF is a potent mitogen for several cell types, including endothelial cells, by promoting endothelial cell motility, interaction, branching morphogenesis, and tubular morphogenesis during angiogenesis and vascularization (Morimoto et al. 1991; Rosen et al. 1997). Furthermore, previous evidence has been proved the therapeutic effects of HGF on myocardial infarction by *in vivo* study (Nakamura et al. 2000; Ueda et al. 2001; Jin et al. 2003; Liu et al. 2016). HGF-engineered skeletal myoblasts promoted angiogenesis, reduce myocardial fibrosis, and decreased cardiomyocytes (Yuan et al. 2008; Madonna et al. 2015). In addition to VEGFs and HGF, FGF-2 can control angiogenesis by regulating various cell-cell interactions and influencing other growth factor or chemokines, including

VEGF (Masaki et al. 2002; Kanda et al. 2004) and HGF, provide a beneficial effect for the treatment of ischemia (Onimaru et al. 2002).

Cells isolated from muscle tissues comprise the major population of myoblast and fibroblasts. The specific markers such as CD56 (also known as neural cell adhesion molecule), expressed on myogenic cells but not in fibroblasts, are commonly used to isolate fibroblast and myoblast from a mixed population. In this study, the human skeletal muscle cells were used to isolate fibroblast and myoblast. The study aims to investigate the impact of HSMF co-culture in HSMM sheets on cytokine balance and evaluate the consequence of angiogenesis *in vitro*. Angiogenic cytokine productivity was measured from monolayers prepared from the uni-culture and co-culture of HSMF and HSMM with various ratios and initial seeding density. Dynamic observation of cells in monolayer was performed to understand the cytokine production mechanism in the skeletal muscle cells. Using in *vitro angiogenesis* mimicking transplantation area, the effect of HSMFs co-culture in HSMM sheet on angiogenesis was also demonstrated (**Fig. 2-1**).

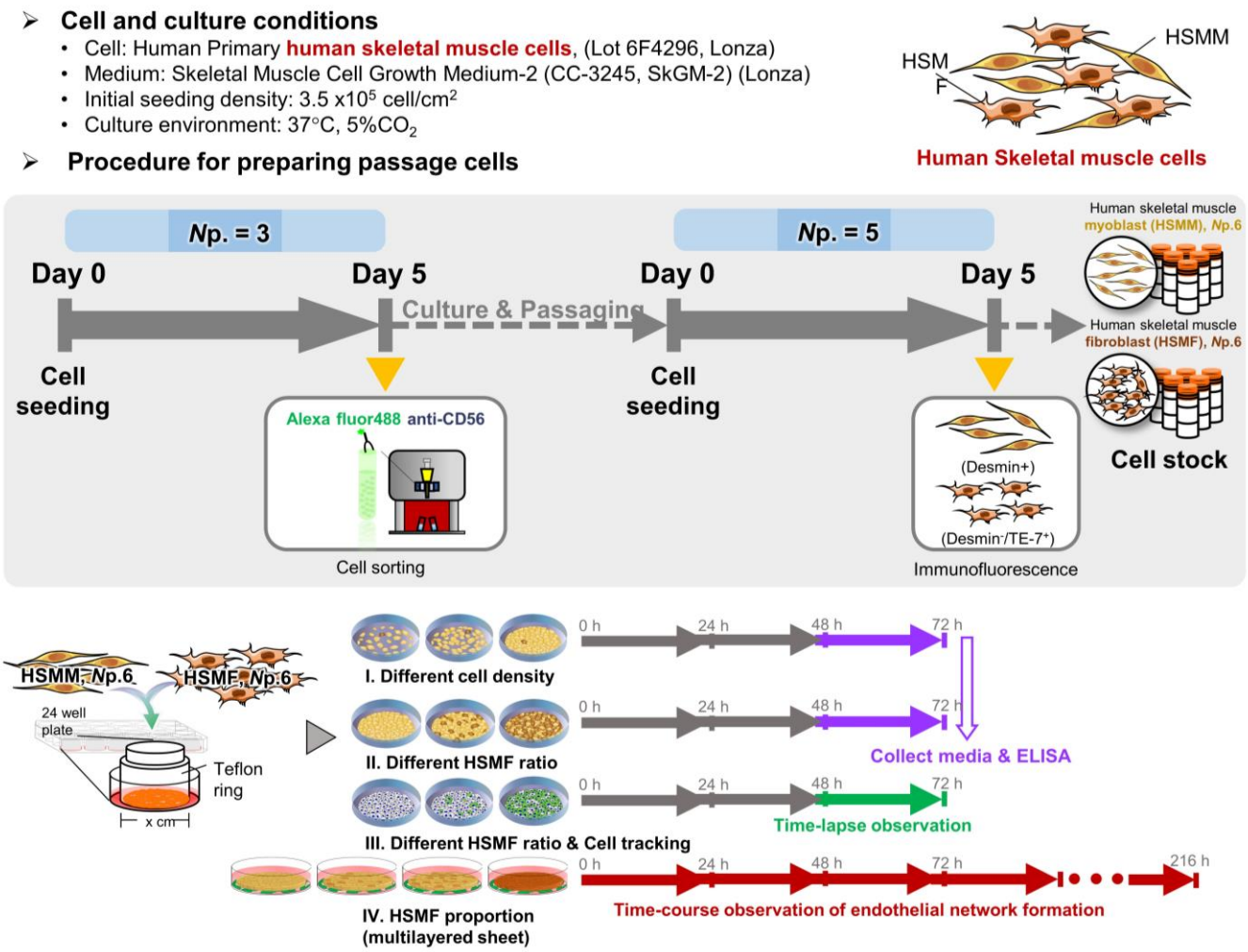

Fig. 2-1 Schematic diagram showing the experimental design of chapter 1

2.2 Materials and methods

2.2.1 Cell culture and preparation

Primary human skeletal muscle cells (Lot. No. 6F4296; Lonza, Walkersville Inc., Walkersville, MD, USA), which contained HSMMs and HSMFs, were used. Skeletal muscle cell culture was performed at 37°C and 5% CO_2 in skeletal cell growth media-2 (SkGM-2; Lonza, Walkersville, MD, USA) formulated by combining SkBM™-2 Basal Medium (Cat. No. CC-3246) with the SkGM™-2 SingleQuots™ kit (Cat. No. CC-3244). Cells were pre-cultured for 5 days in T-225 flasks (Cat. No. 431082, Corning) at an initial density of 3.5×10^3 cell/cm^2 and the medium dept was set at 2 mm throughout the experiments. All cells were harvested until 70-80% confluency.

Green fluorescence protein-expressing human umbilical vein endothelial cells (GFP-HUVECs) (Lot. No. 20100201001; Angio-Proteomie, MA, USA) were maintained in Endothelial Cell Growth Medium-2 (EGM-2; CC-3162, Lonza Walkersville Inc., Walkersville, MD, USA) at 37°C and 5% CO_2. GFP-HUVECs were pre-cultured for three days in T-75 flasks (Cat. No. 430641U, Corning) at an initial density of 3.5×10^3 cell/cm^2 and the medium dept was set at 2 mm throughout the experiments.

2.2.2 Fluorescence-activated cell sorting (FACS)

It has been known that CD56 (also known as neural cell adhesion molecule) is constitutively expressed in myogenic cells, including myoblasts, but not expressed in fibroblasts (Agley et al. 2013). Therefore, CD56 is commonly used as a marker to distinguish between myogenic and non-myogenic cells. In this experiment, CD56 was used to separate myoblast and fibroblast populations from primary human skeletal muscle cells. The original cells at passage No.3 were cultured in SkGM-2 media following the previous method. On day 5, cells were washed three times with PBS, and 1 ml of 0.1% trypsin / 0.02% EDTA solution (Sigma-Aldrich) was treated on the culture area by 1 mL per 45 cm^2 for cell harvesting. Cells were incubated with trypsin for 3 min at 37°C, 5% CO_2, and trypsin inhibitor solution was subsequently added with the equal amount of trypsin-EDTA solution to deactivate trypsin activity. Subsequently, cells were collected into a centrifuge tube and centrifuged at 1000 rpm for 8 min to remove trypsin and trypsin inhibitor solution. After that, the cell pellet was suspended in a buffer consisting of 0.2% BSA (Wako) and 2 mM EDTA in PBS by 1 mL per 1.0×10^7 cells.

The cell suspension was then incubated with Alexa fluor® 488-conjugated anti-CD56 (NCAM) (Cat. No. 2191555, Sony, Sony Biotechnology Inc, San Jose, CA) at 100 μL per 1.0×10^7 cells on ice for 15 minutes. Subsequently, the sample was washed with PBS and centrifuged at 1000 rpm for 5 min to remove the unbound antibody. A buffer consisting of 0.2% BSA in PBS was then added to resuspend the cell pellet, and cell concentration at 5×10^6 cell/mL was prepared. The cell suspension was filtrated using a cell strainer tube (BD Falcon) to obtain a single-cell suspension. The sample was injected into the Fluorescence-activated cell sorter (FACS) (JZAN JR; Bay bioscience Co., Ltd, JP), and the cells

were sorted based on light-scatter and CD56-Alexa fluor 488 intensity. Isotype control was used to determine the level of background surface staining (**Fig. 2-4D**). CD56-positive cells ($CD56^+$) and CD56-negative cells ($CD56^-$) were collected and cultured at an initial seeding density of 3.5×10^3 cells/cm^2 in SkGM-2 medium. The fresh medium was changed every two days. On day 5, cells were harvested for population balance analysis by immunostaining and freezing for cell stock.

2.2.3 Preparation of HSMMs/HSMFs cultured with various initial cell density

In this experiment, sorted HSMMs or HSMFs were cultured in SkGM-2 media for 5 days. After harvesting, the HSMMs and HSMFs were seeded with various initial seeding density (X_0) from 1×10^4 (low density), 8×10^4 (middle density), to 3.5×10^5 (high density) cell/cm^2 inside Teflon rings with the area of 0.95 cm^2 placed on each well of 24-well plates (mono-culture). Cells were cultured as monolayer in SkGM-2 at 37°C in a 5% CO_2, and Teflon rings were then removed after 24 h. The cultured medium was changed with fresh medium every 24 h and collected at 72 h for cytokines measurement.

2.2.4 Preparation of monolayer with various HSMM: HSMF ratio

Sorted HSMMs were mixed with HSMFs were cultured in SkGM-2 media for 5 days. After harvesting, these cells were mixed at the various proportion of 0% to 100% HSMF (HSMF: HSMM ratios of 0:100 to 100:0) and seeded inside Teflon rings with the area of 0.95 cm^2 placed on each well of 24-well plates at X_0 of 3.5×10^5 cells/cm^2. Cells in SkGM-2 media were incubated for 24 h at 37°C in a 5% CO_2 atmosphere to form the monolayer. After 24 h, Teflon rings were removed, and the medium was replaced every 24 h with a fresh medium. At 72 h, the cultured medium was collected for cytokines measurement.

Similarly, sorted HSMFs were stained with 5 μM CellTracker™ Green CMFDA (Cat. No. C7025, ThermoFisher Scientific, USA) in DMEM with no FBS for 20 min at 37°C before mixing with HSMMs to prepare monolayer for cell tracking experiment. Then cells were seeded with initial density at X_0 of 3.5×10^5 cells/cm^2 inside Teflon ring with area 0.95 cm^2 placed on each well of 24-well plates. The

Teflon rings were removed after 24 h, and the cultured medium was replaced with a fresh medium. At 48 h, attached cells were stained with Hoechst 33342 (Cat. No. 4082S, Cell Signaling, USA) according to the manufacturer's instructions for nuclei staining.

2.2.5 Quantitative analysis of HSMM and HSMF migration and cell alignment

Cell tracking and time-lapse observation were used to analyze cell migration and alignment of HSMM and HSMF in monolayers. Monolyeres with various percentages from 0% to 100% HSMF were prepared. According to the previous method, the HSMF was stained with CellTracker™ Green CMFDA, and all cells were nuclei counterstained with Hoechst33240 dye for live-cell imaging. After 48 h of cell culture, images of stained cell nuclei and HSMFs in monolayer were captured every 1 h for 24 h using the IN Cell Analyzer 2000 (GE Healthcare) with the 20x objective lens. The observation system was set to maintain a culture environment at 37°C and 5% CO_2. Original images (1.5 mm x 1.5 mm) of the stained cell with a resolution of 0.74 μm/pixel and 8 bits in grayscale. Images were obtained from random three areas from duplicate samples in 24 well plates. For quantitative analysis, hundred stained nuclear cells from local density in three regions of interest (ROI; 0.8 mm x 0.8 mm) of the duplicated samples were determined. Cells from sequence images were measured position (X, Y) in each time point using Image J software (Manual tracking plugin), and the data was visualized in trajectory plots (**Fig. 2-2A**). Migration velocity ($\vec{v}$) and directional angle (θ and θ') were quantified as shown in **Fig. 2-2B** and **Fig.2-2C**, respectively. A frequency of migration angle of the cell during 48-72 h was plotted in histograms. Cell alignment index was defined as the amount of variation (standard deviation, σ) of migration angle of cells. Thus, a high level of σ value means a higher degree of cell alignment disruption.

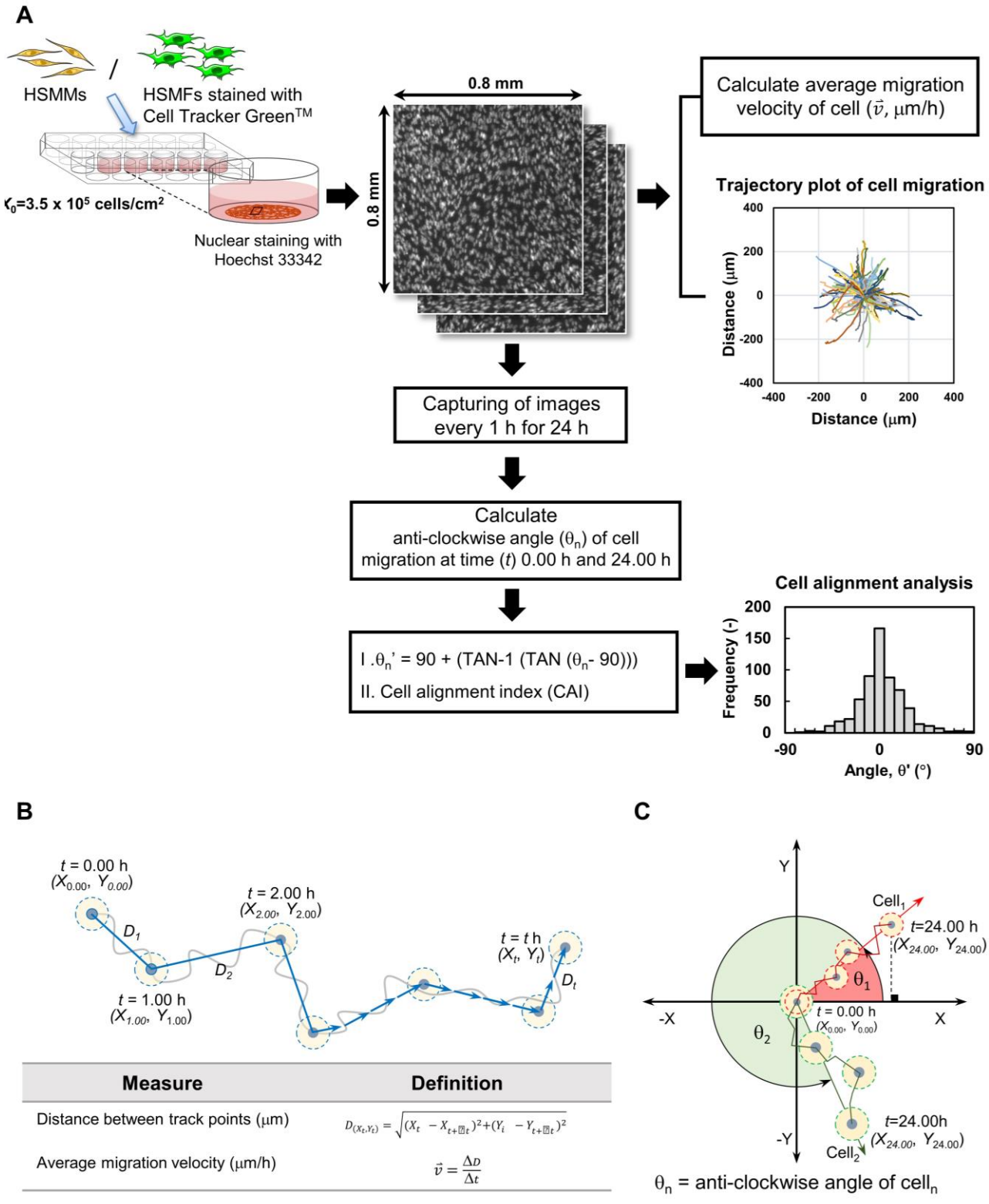

Fig. 2-2 Quantitative analysis of cell migration in monolayer using time-lapse image data analysis. (A) Diagram showing the experimental procedure and data analysis of time-lapse images. The monolayers were prepared skeletal muscle cells with various proportions of human skeletal muscle fibroblast (HSMF) and human skeletal muscle myoblast (HSMM). Cells in monolayers were counterstained with Hoechst 33342. The images of cells in monolayer were captured every 1 h during 48-72 h of incubation.

The positions (X, Y) of the nucleus were measured to evaluate the migration velocity ($\vec{v}$, μm/h), direction angle (θ'), and cell alignment index (CAI) to analyze cell alignment in the monolayer. (B) The position of cells at each time point was measured to calculate the distance of cell migration and average migration velocity. (C) The position of the cell at origin (t = 0.00 h) and the endpoint (t = 24.00 h) were evaluated to analyzed the anti-clockwise angle (θ') of cell migration.

2.2.6 Cytokine productivity measurement

To analyzed the cytokines productivity, cultured media was collected from triplicated samples (*n* = 3) in each condition at 72h to measure the level of VEGF-A, HGF, and FGF-2 level using human VEGF Quantikine ELISA assay (Cat. No. DVE00, R&D Systems Inc., USA), human HGF ELISA Kit (Cat. No. KAC2211, Invitrogen, CA) and human FGF Quantikine ELISA (Cat. No. DFB50, R&D Systems Inc., USA), respectively, according to manufacturer's instructions. The cells in monolayers at 72 h were washed by PBS for 3 times and fixed by 4% paraformaldehyde for 20 min at room temperature. After washing, cells were counterstained by staining with 3μM DAPI in PBS (Cat. No. D1360, ThermoFisher Science, USA) for 30 min at room temperature. Cells were captured using the IN Cell Analyzer 2000 (GE Healthcare) with the 20x objective lens and count to estimate the total cell number in the monolayer. The cytokine productivity was calculated as the amount of cytokine (fg) per cell per hour.

2.2.7 Incubation of 5-layers HSMM sheet with GFP-HUVECs

In this study, five-layered HSMM sheets containing various proportions of HSMFs were fabricated using the gelatin stamping technique (**Fig. 2-3A**) according to the previous method (Nagamori et al. 2013). HSMMs and HSMFs in SkGM-2 media at day 5 were sub-cultured and mixed at various proportion from 0% (no HSMF), 10%, 30% and 40% HSMF (HSMF:HSMM ratios of 0:20, 2:18, 6:14, and 8:12). Cells were stained with CellTracker™ Orange CMTMR Dye in DMEM media with no FBS according to commercially recommended protocol (5 μM for 20 min for live cell imaging). After washing with DMEM media, stained cells were centrifuged at 1,000 rpm, and the pellets were resuspended in DMEM containing 10% FBS. Cells were seeded at 3.5×10^5 cell/cm^2 inside Teflon ring (0.95 cm^2) placed in each well (diameter, 1.9 cm^2) of 24-well UpCell™ plates (CellSeed, Tokyo, Japan) with a temperature-responsive surface, and incubated for 24 h at 37°C in a 5% CO_2 atmosphere to form monolayer sheet. The medium was set to 2 mm in depth throughout the experiments. A gelatin stamp was prepared from a solution of 7.4% (v/v) gelatin by dissolving gelatin powder (G1890-100G; Sigma-Aldrich) in 10 mL

Hank's balanced salt solution (Sigma-Aldrich) and 200 μL of 1N NaOH solution. The gelatin solution was incubated for 30 min at 45 °C and loaded to a mold, and incubated overnight at 4°C. To stacking the cell sheet, gelatin stamps were overlaid onto the monolayer sheet in a well incubated at 37°C, and the plate was then transferred to incubate at 20°C in order to harvest the monolayers. Then, the gelatin stamp was lifted with the monolayer from the bottom surface of the wells and transferred to the next monolayer. These steps were then repeated to harvest monolayer sheets to form a multilayered construct sequentially. The multilayered sheets were transferred to the center of 35-mm culture dishes (ibidi GmbH), which were seeded with GFP-HUVECs seeded at X_0 of 1×10^4 cells/cm^2 and cultured in EGM-2 for 24 in advance at 37 °C in a 5 % CO_2 atmosphere (**Fig. 2-3B**). At the given incubation time (t), triplicate samples were taken for quantitative analysis. The culture medium was replaced with fresh media every day during the incubation period.

A

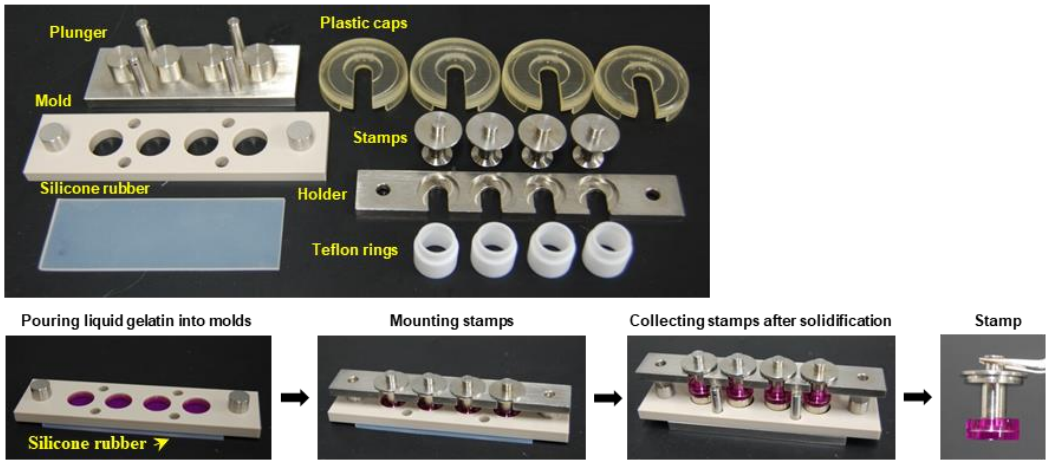

B

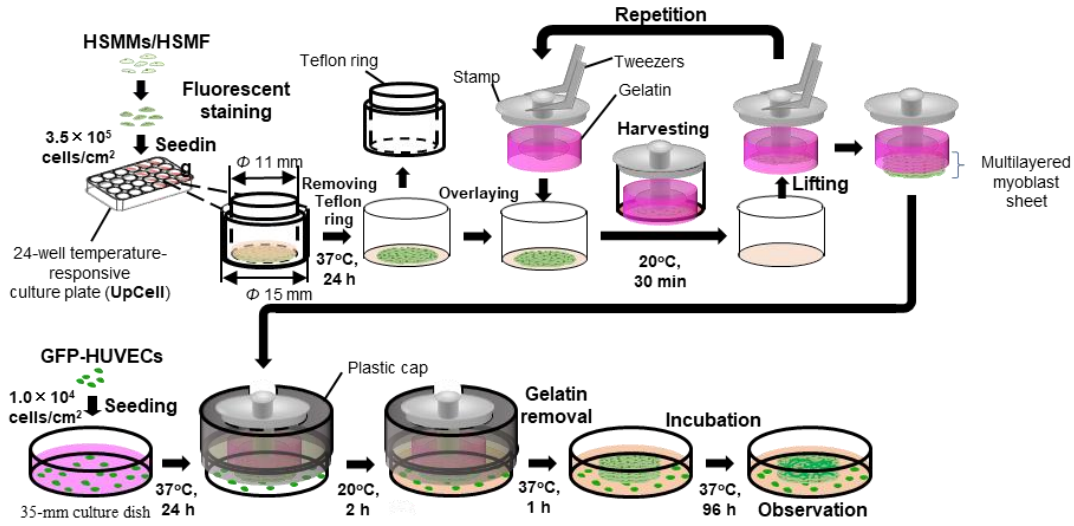

C

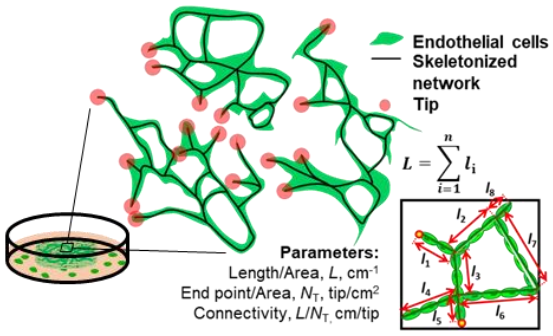

Measure	Local area analysis
Length	$L\ (\mathrm{cm^{-1}}) = \frac{(L\ (\mathrm{pixel}) \div 2) \times a\ (\frac{\mathrm{cm}}{\mathrm{pixel}})}{\mathrm{Area\ (cm^2)}}$
End points	$N_T\ (\mathrm{tip/cm^2}) = \frac{\mathrm{No.\ of\ tip\ (tip)}}{\mathrm{Area\ (cm^2)}}$
Extent of network	$L/N_T\ (\mathrm{cm/tip}) = \frac{L\ (\mathrm{cm^{-1}})}{N_T\ (\frac{\mathrm{tip}}{\mathrm{cm^2}})}$

a is conversion factor to covert pixel to cm

Fig. 2-3 Experimental procedure to prepare multilayer cell sheet. (A) The equipment and (B) method for fabrication of multilayered HSMM sheet and co-incubation with GFP-HUVECs using gelatin stamping. The images were modified from Trung Xuan Ngo's thesis (Xuan 2013). (C) Quantitative analysis parameters for endothelial network formation inside skeletal muscle cell sheet.

2.2.8 Evaluation of GFP-HUVEC network formed inside HSMM sheet

The endothelial cells inside the 5-layered cell sheet were captured every 24 h. The images were then analyzed using a quantitative analysis method similar to a previous study (Nagamori et al. 2013). The image of GFP-HUVECs was captured from 8 positions in each sample using a 10x objective lens of confocal laser scanning microscope (FV-10i, Olympus, Tokyo, Japan. All images were converted to 8-bit grayscale with a size of 256 x 256 pixels, which covered an area of 1.27 mm x1.27 mm using FluoView Ver.4.2a software (Olympus). Next, the images were processed (Image-Pro Plus; Media Cybernetics Inc., Bethesda, MD) using a low-pass filter to remove noise and make a binary image with a certain intensity threshold which was set as the average of the automatic threshold intensity, and the mode intensity. Then, the binary images were subjected to skeletonization, and the secondary noise was removed again with a size threshold to filter out the items with fewer than 16 pixels and the pruning of small branches in the objects. After that, the skeletonized images of the endothelial network were evaluated by measuring the total length of the network per image area (L; cm^{-1}), the number of total tips of the network (N_T; tip/cm^2), and the extent of the HUVEC network (L/N_T; cm/tip). In this measurement, the tips existing at the edge of the image were not counted (**Fig. 2-3C**).

2.2.9 Immunofluorescence staining

To confirm the purity of fibroblast and myoblast, pre-sorted cells and post-sorted cells were seeded at initial density (X_0) of 1×10^4 $cell/cm^2$ in 96 well-plate and cultured in SkGM-2 media. After 24 h incubation, cells were fixed with 4% formaldehyde for 15 min and permeabilized with 0.5% Triton X-100 for 20 min. Next, cells were blocked with 1% BSA for 90 min to prevent non-specific binding. Then cells were probed with a mixture of anti-desmin antibody (Y66) (Cat. No. ab32362, Abcam, USA) and anti-fibroblast (clone TE-7) (Cat. No. CBL271, Millipore, USA) at dilution 1:250 and 1:100, respectively, in 1% w/v BSA at 4°C overnight. After washing, cells were immunolabeled with a mixture of Alexa Fluor® 594 goat anti-rabbit IgG (Cat. No. A11001, Molecular Probes, Life Technologies, USA) and Alexa Fluor® 488 goat anti-mouse IgG (Cat. No. A11012, Molecular Probes, Life Technologies,

USA) at dilution 1:250 in 1% w/v BSA at room temperature for 1 h. After washing with PBS, cells were counterstained with dye 4¢-6-diamidino-2-phenylindole (DAPI) (Cat. No. D1306, Molecular Probes, Life Technologies, USA). For monolayer immunostaining, the samples were washed twice with phosphate-buffered saline (PBS) before fixing with 4% paraformaldehyde in PBS (Wako Pure Chemical Industries, Tokyo, Japan) for 15 min at room temperature. Then, the monolayers were permeabilized with 0.5% Triton X-100 in PBS for 20 min. Non-specific proteins were then blocked for 90 min with Block Ace (Dainippon Sumitomo Pharma Co., Ltd., Osaka, Japan) at room temperature. After that, the cells were incubated with an anti-desmin antibody (Y66) (Cat. No. ab32362, Abcam, USA) at 1:250 dilution prepared in deionized water containing 10% Block Ace at 4°C overnight. Then, the samples were washed twice with Tris-buffered saline (TBS) and immunolabeled with Alexa Fluor® 594 goat anti-rabbit IgG (Cat. No. A11001, Molecular Probes, Life Technologies, USA) at 1:250 dilution prepared in deionized water containing 10% Block Ace at room temperature for 1 h. The F-actin and nuclei were fluorescent stained with Alexa Fluor™ 633 Phalloidin (Cat. No. A22284, Molecular Probes, Life Technologies, USA) and 4¢,6-diamidino2-phenylindole (Cat. No. D1306, Molecular Probes, Life Technologies, USA), respectively. The stained samples were observed by a confocal laser scanning microscope (FV-1000; Olympus, Tokyo, Japan).

2.2.10 Statistical analysis

In this study, all data were presented as mean ± standard deviation. Each experiment was performed on three independent samples (n = 3) for quantitative analysis. The significant differences between groups were statistically evaluated using one-way analysis of variance (ANOVA), and Bonferroni or Least-Significant Different (LSD) was used as a post hoc test (SPSS version 26.0, IBM, USA). The statistical differences were considered when the P-value was less than 0.01.

2.3 Results

2.3.1 Purification of HSMF and HSMM from primary skeletal muscle cells

Fluorescence-activated cell sorting (FACS) is a specialized type of flow cytometry, which provides a sorting mode to separate a heterogeneous mixture of cells into two or more containers, one cell at a time, the specific light scattering and expressing marker on the cell surface. In this experiment, original HSMMs Np.3 (Lot 6F4296), which contain subpopulations of myoblast and fibroblast (**Fig. 2-4A, 2-4B** and **2.4C**), were stained with Alexa 488 conjugated anti-CD56 to allow the separation of myoblast and fibroblast before sorting by FACS. Defining FACS gates is another crucial element of the protocol to ensure isolation of a pure population of these cells. In this experiment, isotype control was used to determine the non-specific background signal level from the staining (**Fig.2.4D**) which the cells were considered as $CD56^-$ cells. The $CD56^+$ cells were defined when the CD56 signal higher than the isotype intensity. In this study, the cell sorting condition was optimized to obtain fibroblast and myoblast with purity higher than 95% and 98%, respectively (**Fig. 2.4C**). The CD56 negative cells ($CD56^-$) were then collected and confirmed the purity of the myoblast and fibroblast population with anti-desmin and anti-fibroblast.

To reliably obtaining the cells with high purity (>95%), sorted cells after five days of culture and unsorted cells were stained with anti-desmin and anti-fibroblast (clone TE-7). Myogenic cells, but not fibroblast, should express desmin (myogenic marker), whereas fibroblast should be positive for fibroblast marker of TE-7 staining. Immunofluorescence staining showed that the unsorted cells were a mixed population of 68% myoblasts and 32% fibroblasts. After sorting, obtained $CD56^+$ cells contain a major population of myoblast with less than 2% non-myogenic cell contamination, whereas the major population of $CD56^-$ cells was fibroblasts mixed with less than 5% myogenic cells. These analyses confirmed that FACS separated myoblasts and fibroblasts with high purity (**Fig. 2-4B** and **2-4C**).

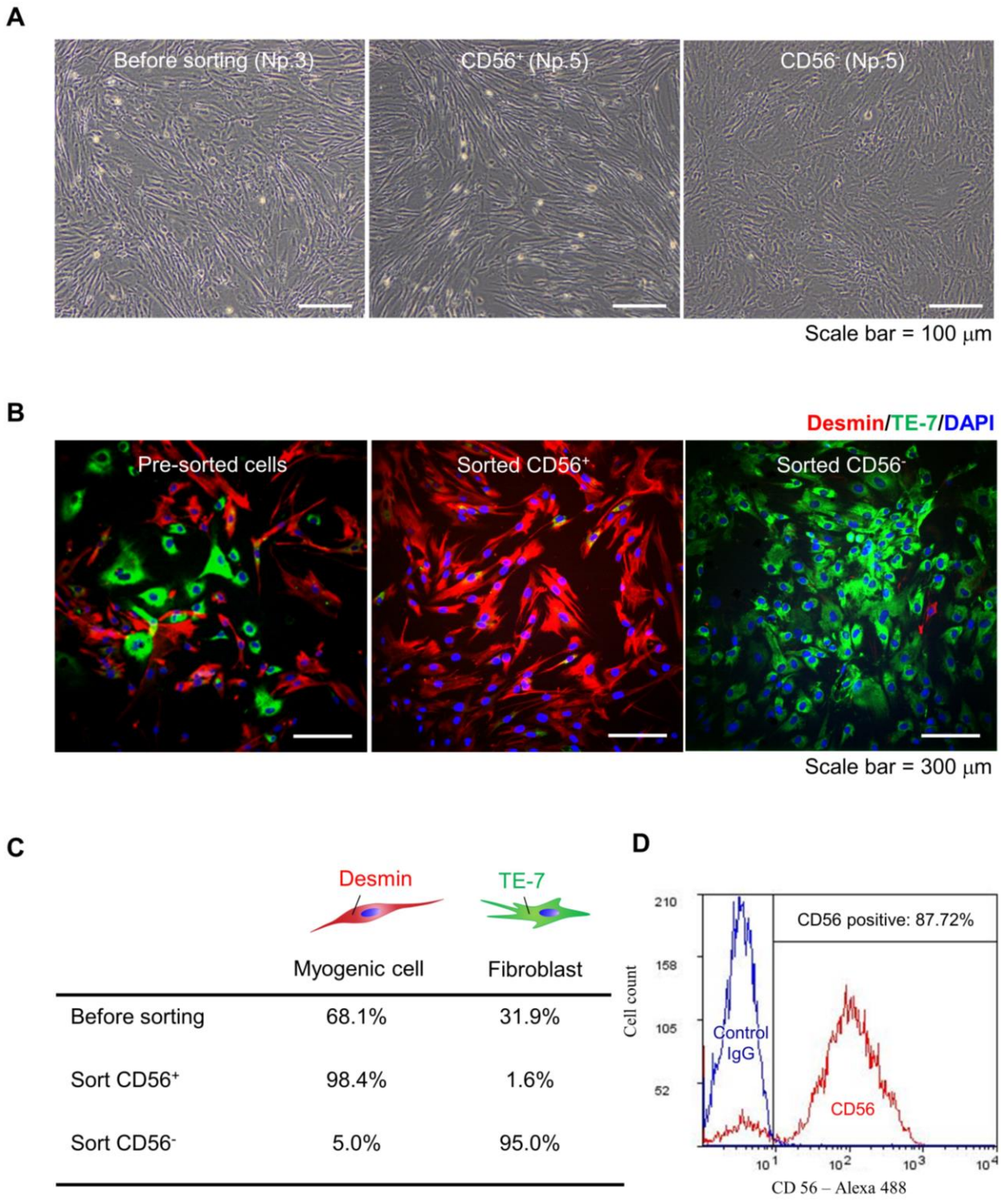

Fig. 2-4 Characterization and quantification of cells during the culturing and sorting processes. (A) Characteristics of pre-sorted and post-sorted cells (CD56+ and CD56− cells) cultured in SkGM-2 media were analyzed under an inverted microscope. Scale bar, 100 μm. Immunostaining of the pre-sorted cells after 5 days of culturing revealed a mixed population of myogenic cells (desmin+) and fibroblasts (desmin−, TE-7+). (B-C) After sorting, the CD56+ cells mainly constituted myogenic cells (desmin+), whereas the CD56− cells mainly constituted fibroblasts. Scale bar: 300 μm. Flow cytometry analysis of

pre-sorted human skeletal muscle myoblasts (HSMM) revealed a mixed population of CD56+ and CD56− cells when compared with the negative control (IgG isotype) (D).

2.3.2 Effect of HSMF proportion (co-culture) on cytokine productivity

Monolayers with various proportions of HSMF from no HSMF to 100% HSMF (HSMF: HSMM ratios from 0:20 to 20:0) were prepared and culture for 72 h. The level VEGF, HGF, and FGF-2 in cultured media from monolayers at 72 h was measured (**Fig. 2-5 (I)**). The VEGF productivity in monolayers derived from mono-cultures of HSMMs and HSMFs was $4.19 \pm 0.10 \times 10^{-2}$ and $4.18 \pm 0.38 \times 10^{-2}$ fg/cell·h, respectively. Interestingly, the VEGF productivity in the monolayer prepared from skeletal muscle cells with 15% (HSMF: HSMM ratio of 3:17) HSMF was approximately 2-fold higher ($8.93 \pm 0.45 \times 10^{-2}$ fg/cell·h) than that in the monolayer derived from mono-cultures of HSMF or HSMM ($P < 0.01$). However, the VEGF productivity reduced when the percentage of HSMF was higher than 15% (**Fig.2-6A**). On the other hand, HGF productivity in the monolayer derived from HSMM mono-culture was negligible ($0.33 \pm 0.33 \times 10^{-2}$ fg/cell·h), while HGF productivity in the monolayer prepared from HSMF mono-culture was high-level at $27.4 \pm 2.27 \times 10^{-2}$ fg/cell·h (**Fig. 2-6B**). The basal levels of VEGF and HGF in culture media without cells used in this experiment were barely detected with 0.11 ± 0.19 and 0.05 ± 0.09 pg/ml, respectively. The levels of FGF-2 were almost undetectable under all conditions (**Fig. 2-6C**). These results suggested that varying the proportions of HSMM and HSMF in the skeletal cell monolayer differentially affected cytokines' production. HGF was secreted only by HSMFs. The VEGF production in the HSMM monolayers can be upregulated by the addition of a small proportion of HSMFs.

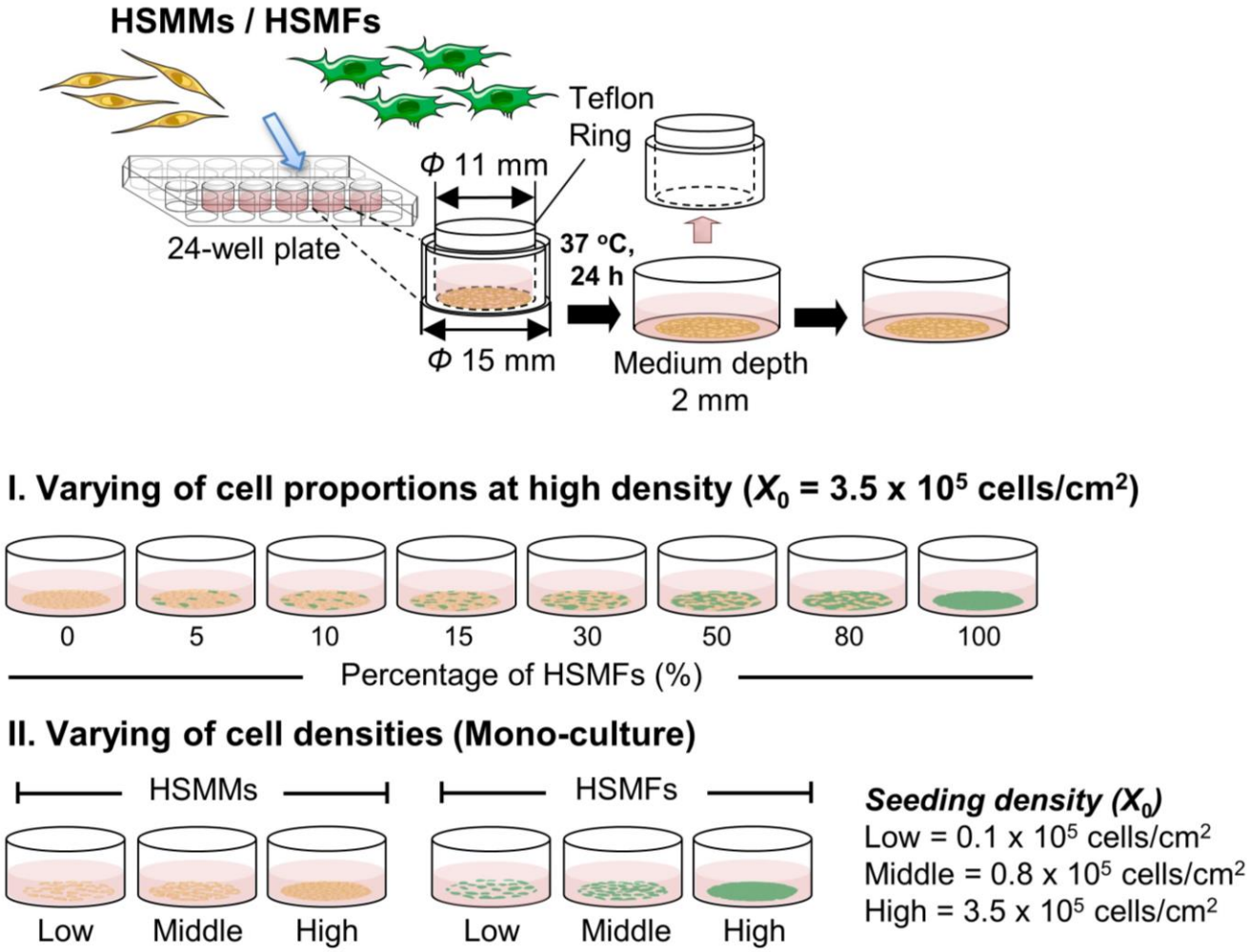

Fig. 2-5 The monolayers were prepared with various proportions of human skeletal muscle fibroblasts (HSMFs) and human skeletal muscle myoblasts (HSMMs) (I) or using various initial seeding densities (X_0) of HSMFs or HSMMs (II).

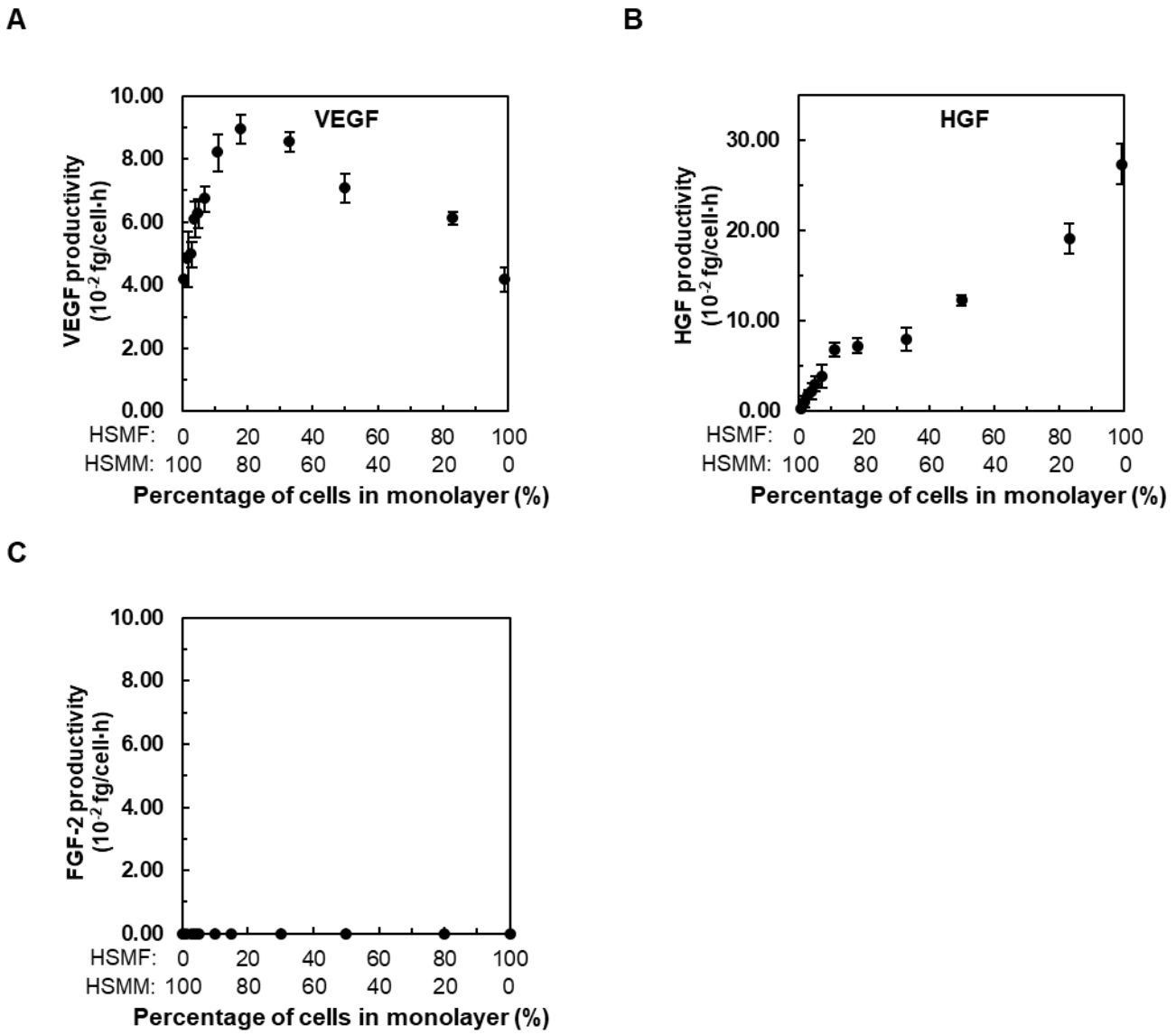

Fig. 2-6 Cytokine productivity in monolayers with various proportions of HSMF and HSMM. The culture medium from monolayers in a high initial seeding density (X_0 = 3.5 x 10^5 cell/cm^2) was collected at 72 h to measure the cytokine levels using enzyme-linked immunosorbent assay (ELISA). (A) Effect of HSMFs and HSMMs proportions in monolayers on vascular endothelial growth factor (VEGF) productivity, (B) hepatocyte growth factor (HGF) productivity, and (C) fibroblast growth factor-2 (FGF-2). Data are expressed as average cytokine productivity ± standard deviation from triplicate samples (n = 3). *P < 0.01; the statistical significance was analyzed using one-way analysis of variance (ANOVA) with Bonferroni post-hoc test.

2.3.3 Effect of cell density (mono-culture) on cytokines productivity in HSMMs and HSMFs

The effect of a minor proportion of HSMFs in the HSMM monolayers on VEGF productivity was investigated by examining the cell-to-cell contact. Here, the VEGF productivity in the HSMMs cultured at low (0.1×10^5 cells/cm^2), medium (0.8×10^5 cells/cm^2), and high (3.5×10^5 cells/cm^2) initial seeding density (X_0) values, which resulted in differing degrees of cell-to-cell contacts, were compared with those of HSMFs (**Fig. 2-5 (II)**). The VEGF productivity derived from the low X_0 value of HSMMs was $20.7 \pm 1.46 \times 10^{-2}$ fg/cell·h. However, the VEGF productivity in the monolayers derived from medium and high X_0 values of HSMMs significantly reduced to $10.3 \pm 0.07 \times 10^{-2}$ ($P < 0.01$) and $5.18 \pm 0.58 \times 10^{-2}$ fg /cell·h ($P < 0.01$), respectively. On the other hand, the productivity of VEGF observed from the HSMF mono-culture varied, which was unrelated to X_0. The VEGF productivities in the monolayer prepared from low, medium, and high X_0 values of HSMFs were $2.18 \pm 1.27 \times 10^{-2}$, $6.90 \pm 0.61 \times 10^{-2}$, and $5.53 \pm 0.60 \times 10^{-2}$ fg/cell·h, respectively (**Fig. 2-7A**). The HGF productivity was high in the monolayer prepared from HSMF mono-cultures at all X_0 values, but the HGF level was almost undetectable in the culture media from HSMM mono-culture. The productivities of HGF in the monolayers prepared from low, medium, and high X_0 values of HSMFs were $22.0 \pm 0.39 \times 10^{-2}$, $21.1 \pm 4.47 \times 10^{-2}$, and $24.3 \pm 4.16 \times 10^{-2}$ fg/cell·h, respectively. In addition, the productivity of HGF was similar in the monolayers prepared from different X_0 values of HSMFs (**Fig. 2-7B**). These results implied that HSMF-mediated myoblast-myoblast contact disruption might promote VEGF production in HSMMs.

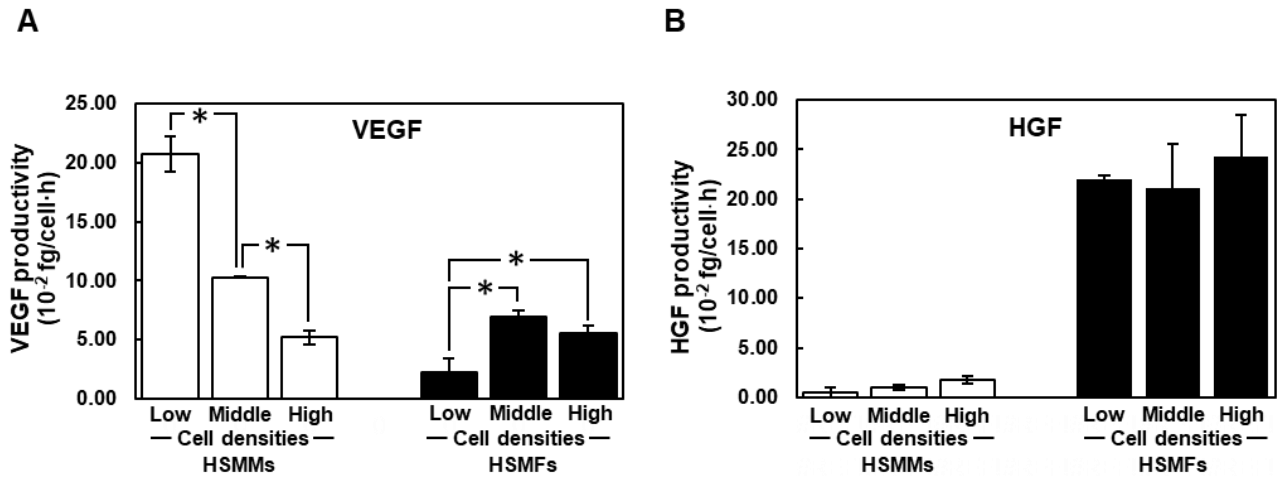

Fig. 2-7 The productivities of VEGF and HGF in HSMMs and HSMFs cultured with various X_0 at 0.1×10^5 (low), 0.8×10^5 (middle) and 3.5×10^5 cells/cm^2 (high) for 72 h. The productivities of (A) vascular endothelial growth factor (VEGF) and (B) hepatocyte growth factor (HGF) in the culture medium were analyzed. Data are expressed as average cytokine productivity ± standard deviation from triplicate samples (n = 3). *P < 0.01; one-way analysis of variance (ANOVA) with Bonferroni post-hoc test.

2.3.4 HSMMs and HSMFs migration and cell alignment in monolayer

Then, the ability of HSMF in the HSMM monolayer to disrupt myoblast-to-myoblast contact was analyzed. Additionally, the time-lapse observation was performed to evaluate the cell interactions and migration of HSMM and HSMF in the monolayer. This study was hypothesized that the migration of HSMFs in the monolayer disrupts the myoblast-to-myoblast contact, which is observed from alteration of the directional migration and alignment of HSMMs. In order to clarify this hypothesis, an HSMM monolayer containing CellTracker Green^{TM}-labeled HSMFs of 2% (HSMM: HSMF ratio of 1:49) observed the individual HSMF and surrounded HSMM migration behaviors. During 48-72 h The nuclei of cells in the monolayer were live-stained with Hoechst 33342 for tracking of cell migration. In the monolayer, the directional migration of HSMMs in the HSMF-free area was compared with that of HSMM in the HSMF-surrounded area (**Fig. 2-8A**). From trajectory plots, the data indicated that HSMMs in the HSMF-surrounded area exhibited multidirectional migration. In contrast, those in the HSMF-free area exhibited unidirectional migration (**Fig. 2-8B**). This result implied that HSMFs are involved in myoblast-to-myoblast contact disruption.

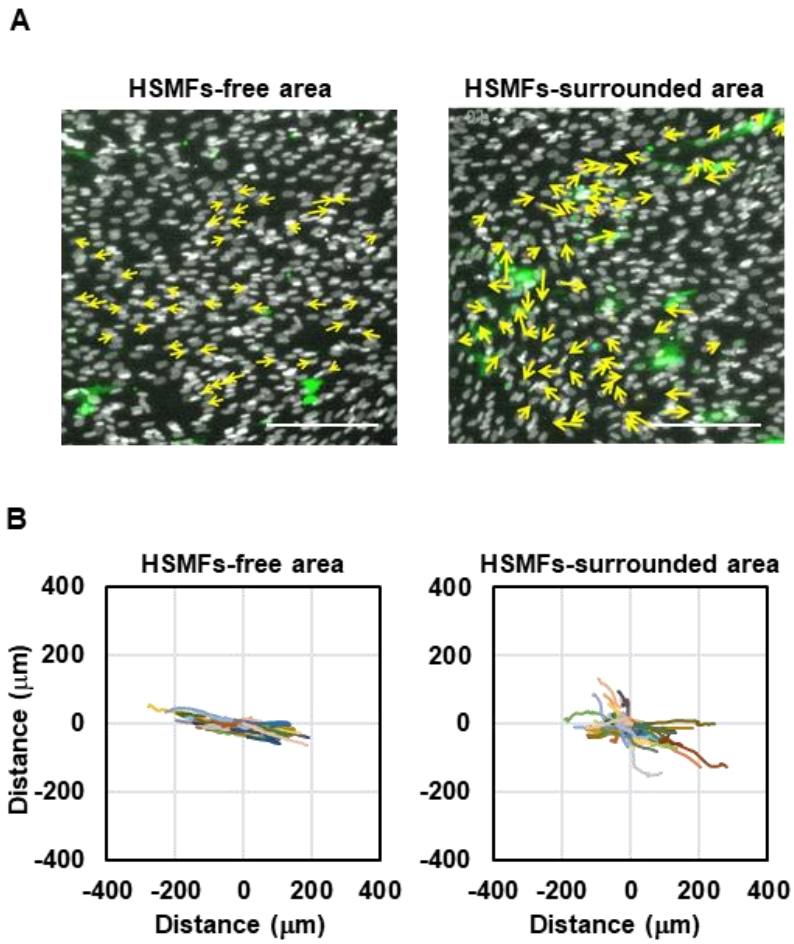

Fig. 2-8 Dynamic behavior of human skeletal muscle myoblast (HSMM) cell migration in the monolayer comprising a small proportion of human skeletal muscle fibroblast (HSMF) population. (A) The HSMM cell monolayer containing 2% HSMF was prepared to observe the migration behaviors of HSMMs in the HSMF-free and HSMF-surrounded areas. The HSMFs were live-stained with CellTracker Green™ to distinguish them from HSMMs. The nuclei of all cells in the monolayer were stained with Hoechst 33342. The images were captured every 1 h during 48-72 h. The yellow arrow defines the direction of cell migration in the local area. Scale bar:200 μm (B) Representative trajectory plots showing directional migration of 100 HSMMs from each area. The direction and distance of cell migration during 24 h of a hundred cell was measured at every position and plotted in the trajectory plot.

To examine the role of HSMF on myoblast-to-myoblast contact disruption in monolayer, cell migration behaviours in the monolayer prepared using HSMMs, and various proportions of HSMFs were observed using an inverted microscope. The HSMM monolayer without HSMFs showed uniform cell alignment. In comparison, the cell alignment was deficient in some areas of the monolayer consisting of a small proportion of HSMFs. Furthermore, monolayers with the various proportions of HSMFs were prepared, and cell migration behaviors, as well as alignment, were analyzed. The result demonstrated that the cell alignment was completely dysregulated in the monolayer comprising a high proportion of HSMFs (**Fig. 2-9**).

The HSMFs showed active migration in the monolayer comprising low proportions of HSMF (5 to 15% HSMF). Additionally, HSMFs showed a wide range of migration velocity, which higher than that of HSMMs ($P < 0.01$). However, the migration velocity of HSMFs decreased when the proportion of HSMFs increased in the monolayer (**Fig. 2-10**).

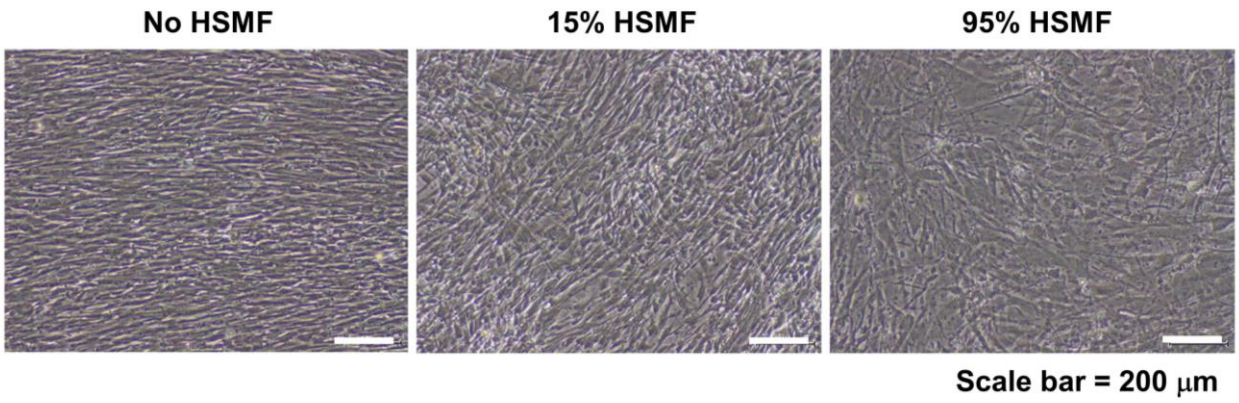

Fig. 2-9 Analysis of cell alignment in the monolayer. The monolayers prepared using skeletal cells with various proportions of human skeletal muscle fibroblast (HSMF) and human skeletal muscle myoblast (HSMM) (0, 15, and 95% HSMF) were analyzed under a 10X objective lens of an inverted microscope.

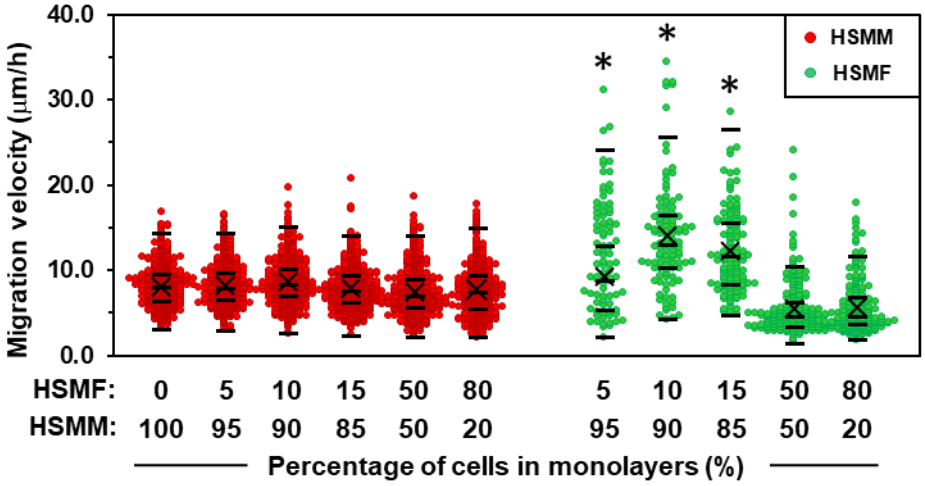

Fig. 2-10 The migration velocity of HSMMs and HSMFs in the monolayer with varying proportions of HSMFs (5 to 15% HSMF). *$P < 0.01$; Statistical significance was analyzed using one-way analysis of variance (ANOVA) followed by Least-Significant Different (LSD) post-hoc test.

The trajectory plot of HSMM migration in the monolayer containing no HSMFs exhibited unidirectional migration, while the number of HSMMs showing multidirectional migration increased with a rising HSMF proportion (**Fig. 2-11A**). In comparison, HSMFs exhibited multidirectional migration in monolayers, especially in monolayers containing 5%, 10%, and 15% (**Fig. 2-11B**). These results suggested that cell migration behaviours depend on the proportion of HSMM and HSMF. The random active migration of HSMFs disturbed the directional migration of HSMMs, suggesting the myoblast-to-myoblast contact disruption by active HSMF migration.

To quantitate the level of cell alignment disruption, the nucleus of HSMMs from three areas per sample was tracked for 24 h and calculated the migration angle (θ') as a robust metric to judge overall alignment (**Fig. 2-2A and Fig. 2-2C**). The θ' of HSMM migration in the monolayers comprising various HSMF proportions was plotted in a histogram (**Fig. 2-12**). In monolayer with no HSMF, the histogram showed a unimodal peak of θ' from HSMM migration suggesting well alignment of cell in the monolayer. In contrast, the multimodal peaks were observed with a rise HSMF proportion from 5%. The degree of HSMM alignment between conditions was enhanced. Then, the variation of θ' as the standard deviation (σ) values was comparatively analyzed to quantitate the level of cell alignment disruption in monolayer with various HSMF proportions (**Fig. 2-13**). Higher σ values mean an increase in the degree of myoblast alignment disruption. The σ value of HSMM monolayer without HSMF was 25.67 ± 4.67, while the skeletal muscle cell monolayer with HSMF proportion of 5, 10, 15, 50, and 80% were 31.19 ± 9.52, 37.57 ± 3.27, 44.41 ± 5.70 (maximum σ value), 42.30 ± 3.43 and 43.73 ± 2.42, respectively. The fluorescent staining of F-actin and desmin was performed to confirm the alignment disorder in HSMM monolayer containing 15% HSMF compared to the monolayer with no HSMF, in which well alignment was observed (**Fig. 2-14**). These results indicate that the HSMFs inhibited the myoblast-to-myoblast contact and consequently disrupt the myoblast alignment.

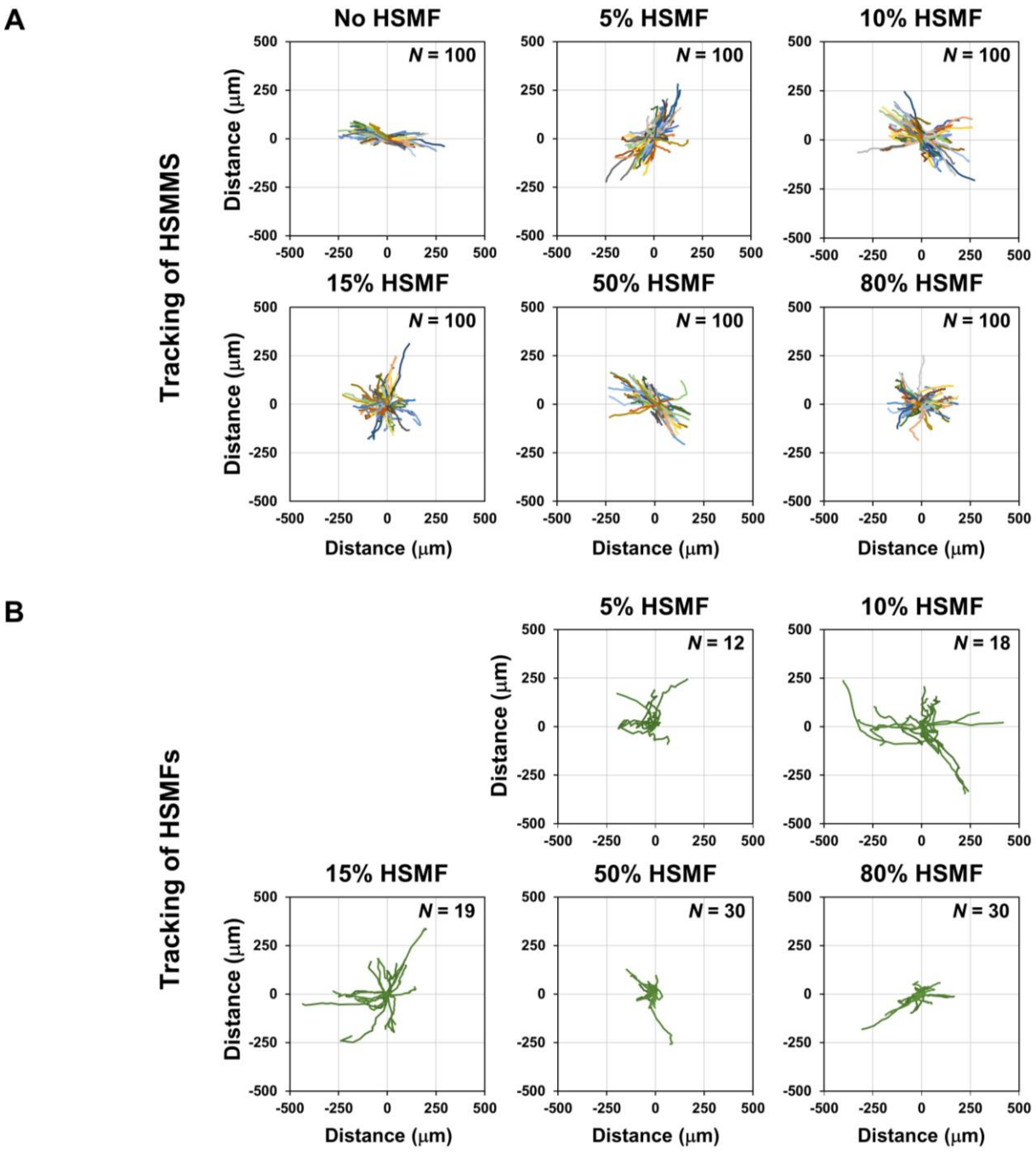

Fig. 2-11 Migration behaviors of human skeletal muscle myoblasts (HSMMs) and human skeletal muscle fibroblasts (HSMFs) in a monolayer sheet comprising various proportions of HSMF. (A) The trajectory plot shows the direction and distance of HSMM migration in the monolayer containing various proportions of HSMFs during 48-72 h of incubation. Representative images show data obtained from a hundred HSMM from each local area. (B) Trajectory plot represents the HSMF migration in monolayer comprising various proportions of HSMFs during 48-72 h of incubation.

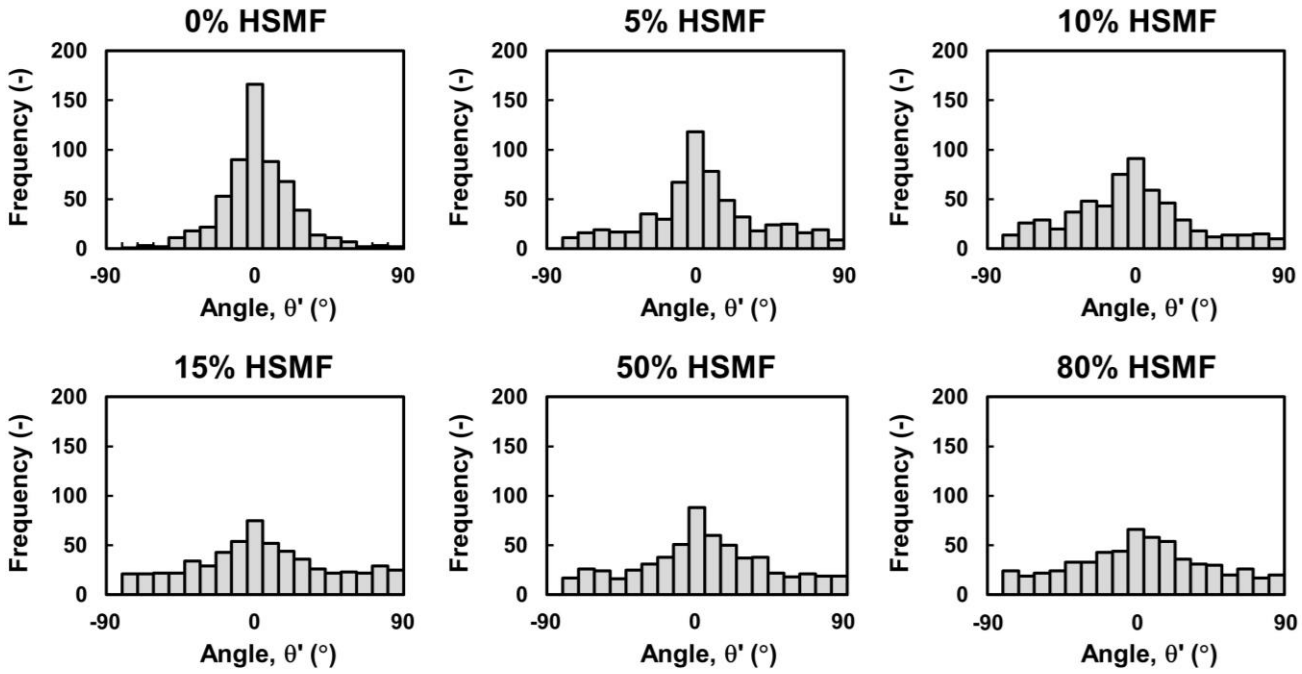

Fig. 2-12 Histograms show quantitative analysis of human skeletal muscle myoblast (HSMM) alignment at high density in the monolayer comprising various proportions of human skeletal muscle fibroblasts (HSMFs). HSMMs were co-cultured with various proportions of HSMFs to prepared monolayers at an initial seeding density (X_0) of 3.5×10^5 cells/cm^2. All nuclei in the monolayer were stained with Hoechst 33342 before observation for cell tracking. The positions of the cell (X, Y) at the initial (t = 0 h) and ending (t = 24 h) time points were measured to calculate the migration angle (θ') and were plotted in a histogram. Data were obtained from six hundred HSMM from six random areas from duplicated samples were analyzed (n = 600).

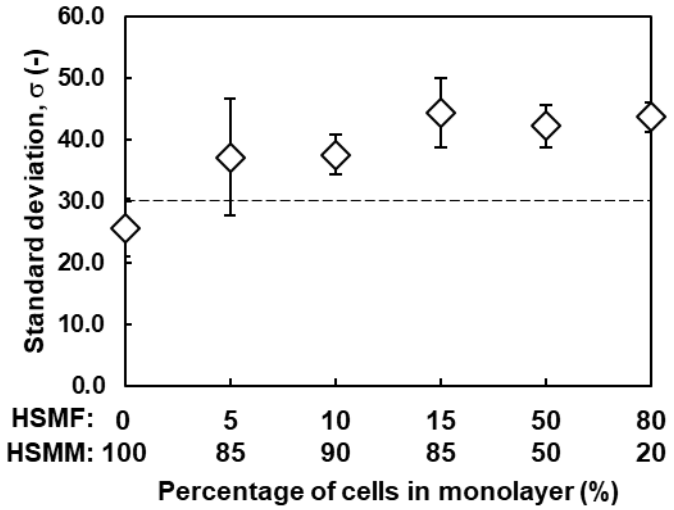

Fig. 2-13 Quantitative analysis of myoblast alignment disruption. Cell alignment was quantitated by measuring the direction angle of cell migration. Data were obtained from 600 human skeletal muscle myoblasts (HSMMs). The standard deviation (σ) values were used as a metric of variation index of direction migration and were compared among different conditions. A high σ value indicated multidirectional migration and high myoblast alignment disruption.

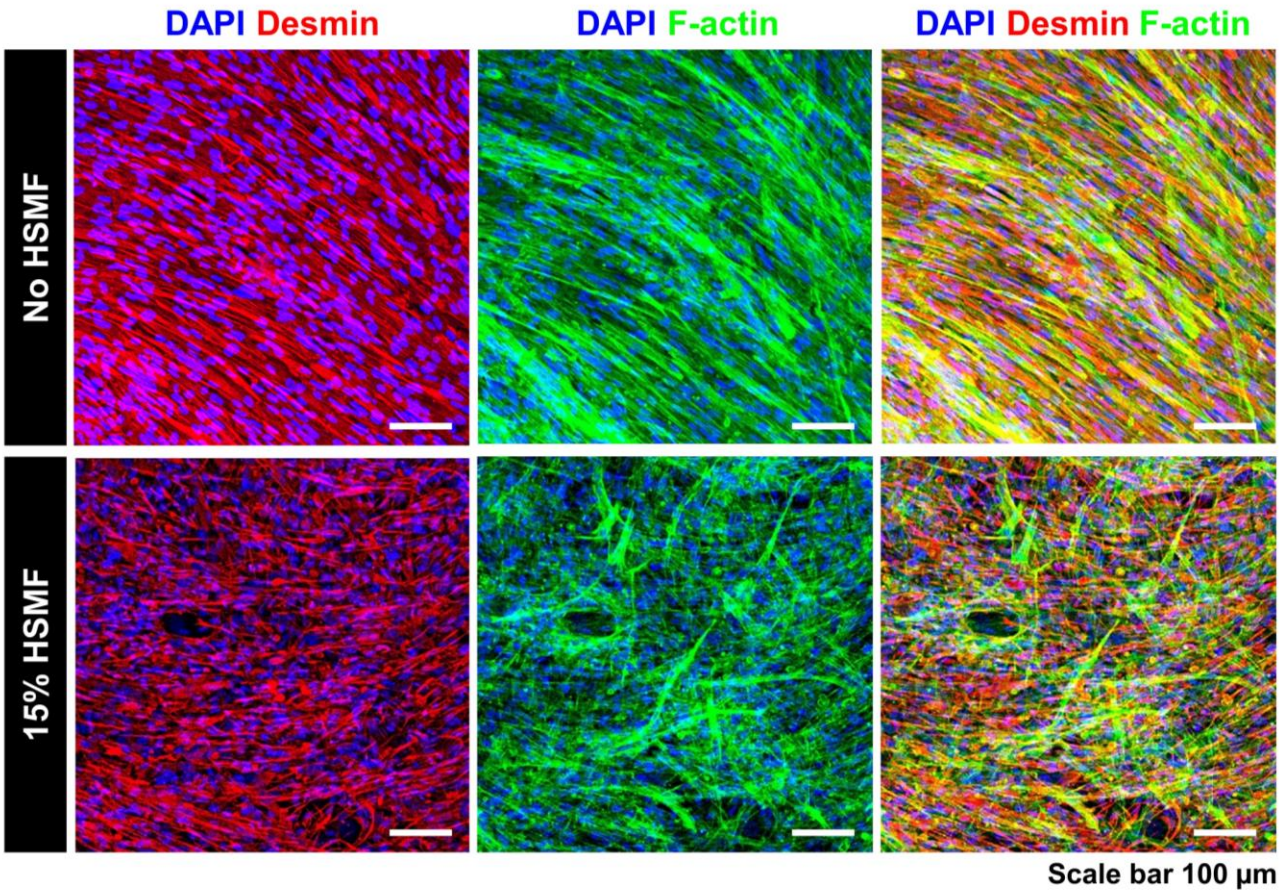

Fig. 2-14 Fluorescent staining images of desmin (red) and F-actin (green) structures towards nuclei (blue) in human skeletal muscle myoblast (HSMM) monolayers containing with or without 15% human skeletal muscle fibroblast (HSMF).

2.3.5 Effect of HSMF on GFP-HUVECs network formation inside the HSMM sheet

During angiogenesis, endothelial cells from the existing vessel must be activated from stimuli for migration, connection, and branching (De Smet et al. 2009). In this experiment, the efficiency of human skeletal muscle cell sheets with various HSMF proportions to promote angiogenesis was evaluated using *in vitro* angiogenesis assay mimicking the transplantation area *in vivo* (Nagamori et al. 2013). In this model, GFP-HUVECs were co-incubated under the 5-layered skeletal muscle cell sheets mimicking *in vivo* angiogenesis after transplantation, and GFP-HUVECs were captured every 24 h for time-course analysis (**Fig. 2-15**). The images of GFP-HUVECs inside the cell sheet were quantitatively analyzed endothelial network, which three parameters, total network length (L), the total number of endpoints (N_T), and extent of the network (L/N_T), were determined (**Fig. 2-3C**).

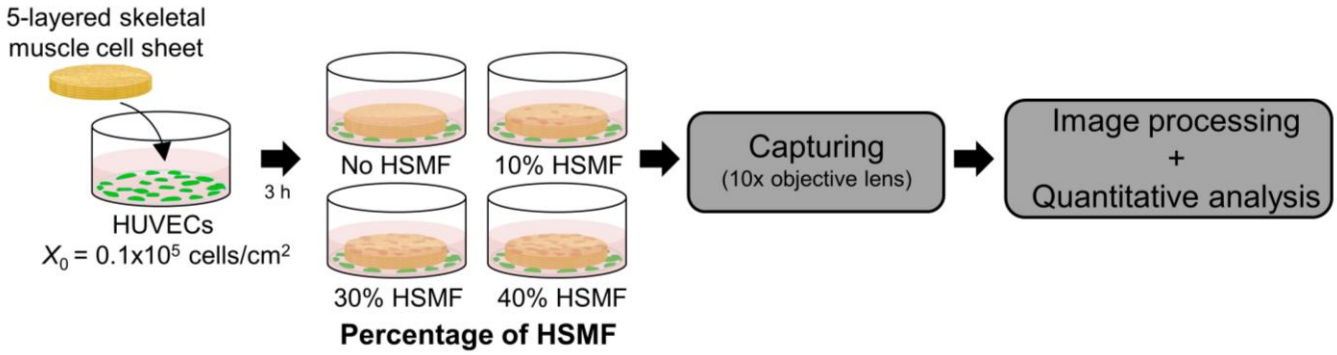

Fig. 2-15 Schematic drawing shows the experimental design to evaluate the effect of HSMF proportion on endothelial network formation. Five-layered HSMM sheets containing various proportions of HSMFs were prepared and co-cultured with green fluorescent protein-tagged HUVECs (GFP-HUVECs) and observed for 216 h.

The morphology of fabricated skeletal muscle cell sheets prepared by this method is shown in **(Fig. 2-16).** The GFP-HUVECs were observed for 216 h to estimate the growth and network formation. At t=0h, GFP-HUVECs were initially localized at the bottom of the skeletal muscle cell sheet and vertically migrated into the inner portion of the sheet to generate a flat network inside the sheet after several days of co-incubation (**Fig. 2-17**). The network formation of GFP-HUVECs in the 5-layered cell

sheets was analyzed according to L, N_T, and L/N_T parameters (**Fig. 2-3C**). The X_0 value of GFP-HUVECs was confirmed at $0.16 \pm 0.01 \times 10^5$ cells/cm^2. As shown in **Fig. 2-18**, the GFP-HUVECs exhibited single and round shapes at the initial incubation time ($t = 0$). However, it was observed that some GFP-HUVECs with early elongation were detected in the cell sheets with HSMF proportions of 30% and 40%. The endothelial network formation was quantitated using L, N_T, and L/N_T parameters, as shown in **Fig. 2-19**. The GFP-HUVECs became elongated and were connected with each other in the cell sheets containing HSMFs resulting in increasing of L and decreasing of N_T. In contrast, the GFP-HUVECs exhibited poor connection with each other in HSMM sheets without HSMFs, which L and L/N_T were much lower than that with HSMFs. The cell sheet prepared from skeletal muscle cells containing 30% HSMFs exhibited the early maturation of endothelial network formation, where the maximum values of L (111.3 ± 4.71 cm^{-1}) and L/N_T (0.05 ± 0.01 cm/tip) were found at 48 h, compared with those observed at 24 h and other conditions. At this time point, a maximum L/N_T value of 0.034 ± 0.02 cm/tip in the skeletal muscle cell sheet with 10% HSMF was observed. This value was larger than that of other time points under this condition. Although L/N_T decreased in other conditions at 96 h, the elongation and smooth connection of GFP-HUVECs in skeletal muscle cells with 40% HSMF was observed with the maximum L and L/N_T values of 115.76 ± 5.59 cm^{-1} and 0.07 ± 0.01 cm/tip, respectively. These results indicated that different proportions of HSMFs in skeletal muscle cell sheets affect angiogenesis after transplantation in an *in vitro* angiogenesis assay.

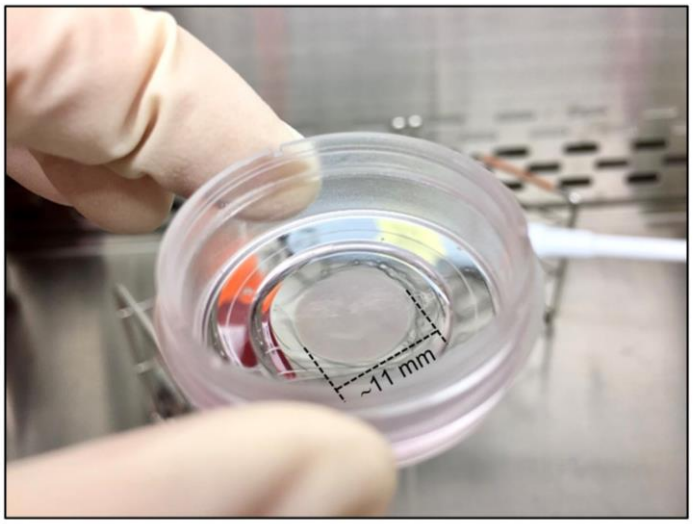

Fig. 2-16 morphology of multilayered HSMM sheet after transferring to the center of a 35 mm culture dish, seeded with GFP-HUVECs (X_0 of 0.1 × 10^5 cells/cm^2) in EGM-2 at 37°C and 5 % CO_2 for 24 h.

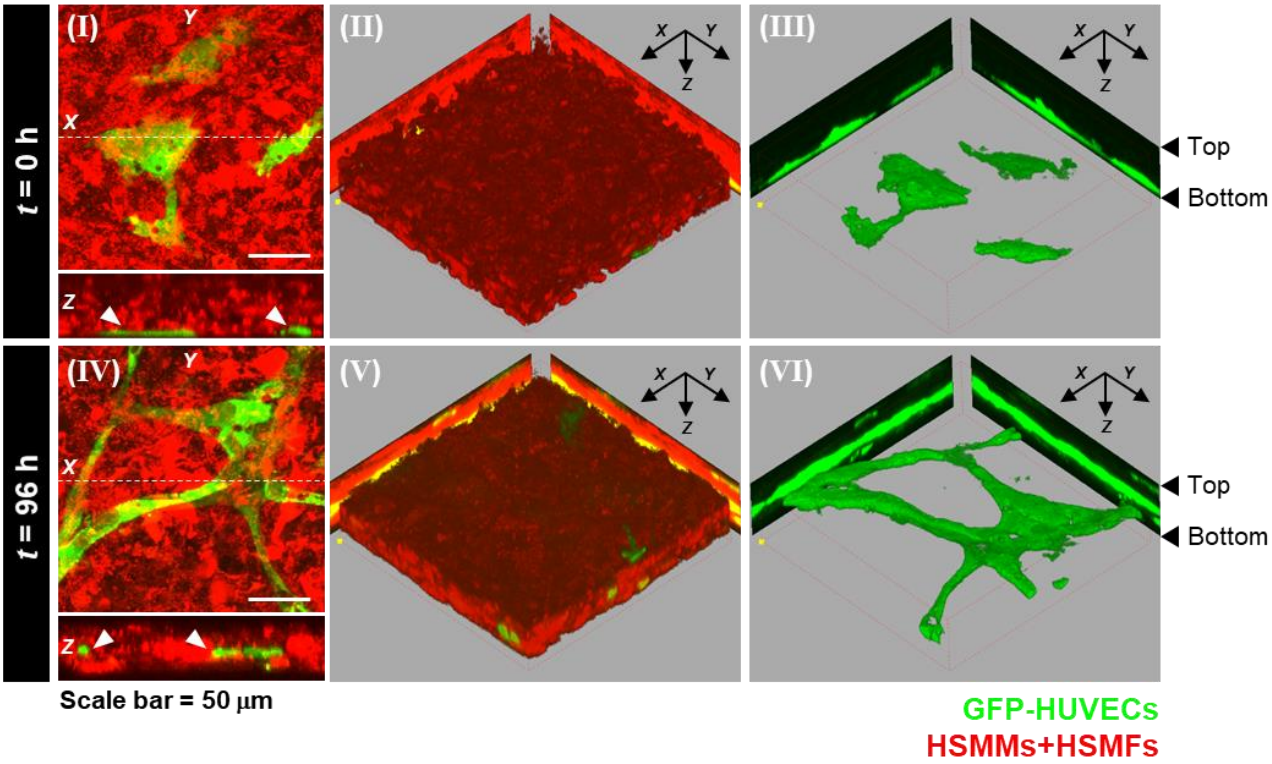

Fig. 2-17 Characterization of endothelial network formation inside multilayered skeletal muscle cell sheet. The stacking images of GFP-HUVECs (green) in a multilayered skeletal cell sheet (red) were captured at t = 0 h (I) and t = 96 h (II) by confocal laser scanning microscope using a 60X objective lens.

The 3D images were generated to show the 3D structure of the cell sheet (II and V) and HUVECs network structure (III and VI) inside.

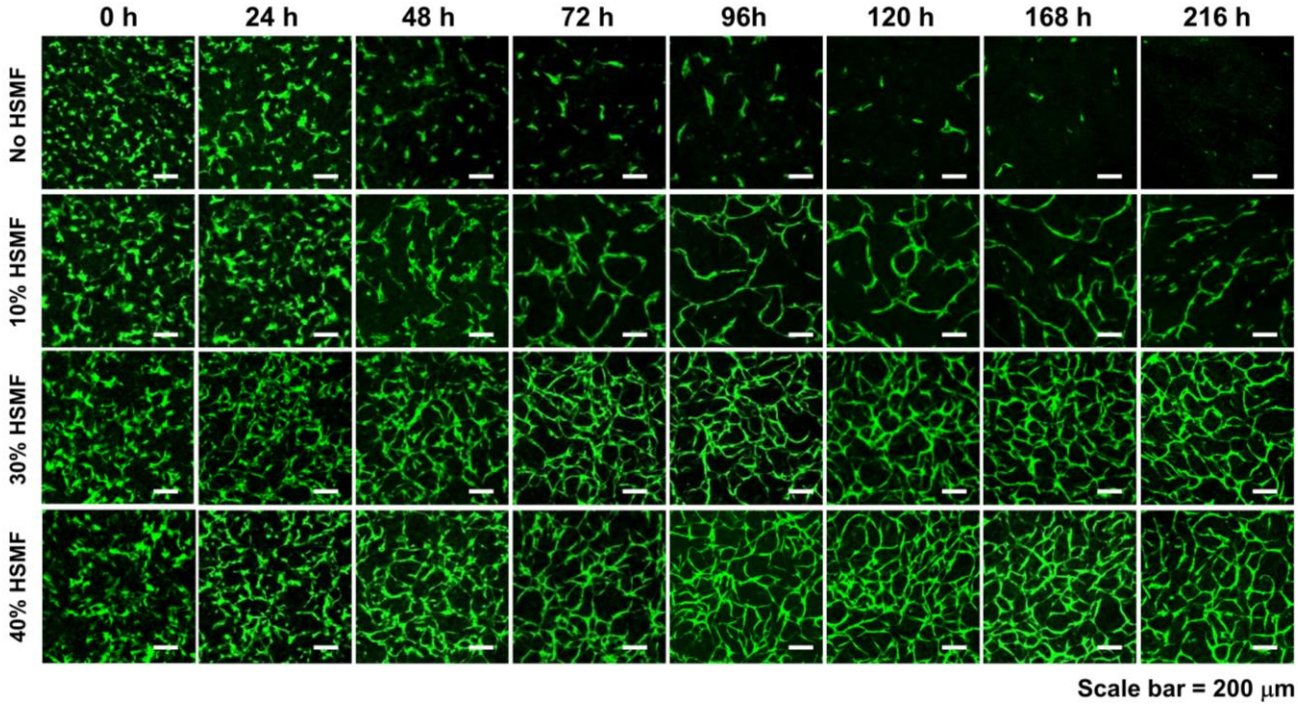

Fig. 2-18 Representative image of human umbilical vein endothelial cell (HUVEC) network formation in the five-layered human skeletal muscle myoblast (HSMM) sheet comprising various proportions of human skeletal muscle fibroblast (HSMF). Scale bar: 200 μm.

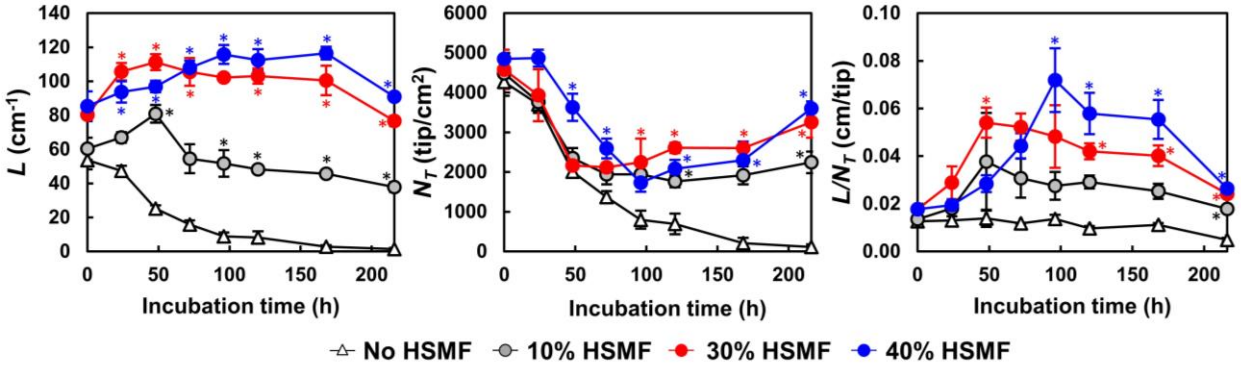

Fig. 2-19 Quantitative analysis of HUVEC network formation in multilayered human skeletal muscle cell sheets comprising various proportions of HSMF. Three parameters, including total length (L, cm^{-1});, total tip number (N_T, tip/cm^2), the extent of network formation (L/N_T, cm/tip) were measured for several

hours. The error bars express the standard deviation (SD) (n = 3). *P < 0.01; Statistical significance was analyzed using one-way analysis of variance (ANOVA with Bonferroni post-hoc test.

2.4 Discussion

Transplantation of skeletal muscle myoblasts for the treatment of myocardial infarction was first demonstrated by Menasché and colleagues (Menasche et al. 2003). Later, several studies have reported safety, feasibility, and improved cardiac performance with skeletal muscle myoblast transplantation (Siminiak et al. 2004; Dib et al. 2005; Gavira et al. 2006). In addition, the myoblasts are prepared as cell sheets, which increases the efficiency of cell transplantation and the induction of therapeutic potential (Hata et al. 2006). Transplantation of skeletal muscle myoblast has been demonstrated for safety and therapeutic efficiency and showed no severe arrhythmia or ventricular extrasystole frequency alterations (Sawa et al. 2015). Although skeletal muscle myoblast sheets have shown their therapeutic effect possibly through the various paracrine production (Pouzet et al. 2001), however, the effect of skeletal muscle cells consisting of different proportions of myoblasts and fibroblasts on angiogenic cytokine production and angiogenesis is not yet understood. This study focused on the regulation of cytokine production by specific cell types in human skeletal muscle cell sheets. Monolayers with different densities (monoculture) and proportions (co-culture) of HSMMs and HSMFs were prepared. VEGF production was observed in the monocultures of HSMMs and HSMFs, with low productivity. However, a low proportion of HSMFs in the HSMM monolayer resulted in increased VEGF productivity, with maximum productivity observed in the monolayer of skeletal cells with 15% HSMFs (**Fig. 2-6A**). The production of HGF was observed in the HSMF mono-culture only (**Fig. 2-6B**), whereas that of FGF-2 was almost undetectable in the mono-cultures of both cell types (**Fig. 2-6C**). Previous studies in primary human retinal pigment epithelial (RPE) cells have shown that VEGF expression is strongly upregulated at the edges of the scratched RPE layers after the physical disruption of RPE cell-to-cell interactions. This enhanced VEGF expression was correlated with the delocalization of ZO-1, an essential molecule for intercellular signal transduction in cells (Farjood et al. 2017). Therefore, this study investigated the role of cell-to-cell contact disruption in increasing VEGF production in the monolayers derived from the co-culture of HSMM and HSMF.

The degree of cell-to-cell contact was then evaluated by culturing the purified HSMMs and HSMFs at various X_0 values. At a high X_0 value (3.5×10^5 cells/cm^2), the cells were in contact with the neighboring cells. In the culture at a low X_0 value (0.1×10^5 cells/cm^2), the cells decreased in their contact with the neighboring cells. This study showed that VEGF productivity in the HSMM monolayer was inversely proportional to the cell density (**Fig. 2-7A**). In contrast, the productivity of other cytokines in the HSMM monolayer was not associated with cell density. Moreover, the productivity of the cytokines in the HSMFs was not dependent on the cell density (**Fig. 2-7B**). Therefore, these data suggested that myoblast-to-myoblast contact may regulate VEGF production in HSMMs. Furthermore, the effect of HSMF in the HSMM monolayer on the disruption of myoblast-to-myoblast contact was examined using cell tracking and time-lapse analysis to investigate the migration behavior. The free HSMFs showed active migration and affected the direction of HSMMs migration without affecting the migration velocity of HSMMs. (**Fig. 2-8A** and **Fig. 2-8B**). It has been suggested that HSMF migration in the monolayer disrupts myoblast-myoblast contact, which alters the directional migration and alignment of HSMMs. The role of HSMF in HSMM alignment was assessed by measuring the directional angle of cell migration, expressed as cell alignment index value (σ), in the HSMM monolayers with different proportions of HSMF. At low proportions in the HSMM monolayer, the HSMFs showed active multidirectional migration. However, at high proportions in the monolayer of human skeletal muscle cells with 50% and 80% HSMF, the HSMFs showed inactive migration and aggregation. (**Fig. 2-10**). In the mono-culture of HSMM as a monolayer, HSMMs exhibited unidirectional migration (**Fig. 2-11A**). Nevertheless, the presence of HSMFs increased the multidirectional migration of HSMMs (**Fig. 2-11B**). Moreover, the alignment disorder in the monolayer with a small proportion of HSMF was confirmed by F-actin staining, as shown in **Fig. 2-14**. Thus, the cell alignment index values (σ) in the co-culture monolayer were higher than those in the mono-culture HSMM monolayer (**Fig. 2-13**). These results support the hypothesis that fibroblasts, which increase VEGF productivity in the HSMM monolayer, exhibit active migration and consequently disrupt myoblast-to-myoblast contact. These results suggest

that HSMFs regulate cytokine secretion and that cytokine productivity depends on the proportion of HSMFs in the human skeletal muscle sheets.

The effect of HSMFs in the human skeletal muscle sheets on therapeutic efficiency after transplantation was evaluated using an *in vitro* angiogenesis assay. Five-layered HSMM sheets with different proportions of HSMFs were prepared and co-cultured with GFP-HUVECs (**Fig. 2-15**). Although the GFP-HUVECs in the human skeletal muscle cell sheet without HSMFshowed elongation at an early time point, the endothelial network connection was poor at a later time. In the presence of HSMFs, the GFP-HUVEC network formation in HSMM sheets was enhanced. However, the growth of the GFP-HUVEC network was dependent on the proportion of HSMF and the levels of VEGF and HGF (**Fig. 2-18** and **Fig. 2-19**). Various cytokines are involved in inducing angiogenesis. A previous study in the animal model showed that treatment of scaffolds releasing VEGF alone could increase the growth of blood vessels; however, the obtained vessel was fragile and exhibited vascular leakage. In the combination of triple cytokines, VEGF, HGF, and angiopoietin-1, the blood vessel growth was enhanced, and the integrity was improved (Saif et al. 2010). In the present study, GFP-HUVECs in the skeletal muscle cell sheets with 10% HSMF initially showed network formation, which decreased significantly over time. In contrast, GFP-HUVECs exhibited higher connectivity in the sheets prepared from skeletal cells containing 30 and 40% HSMF than in the cell sheets prepared from skeletal cells containing 10% HSMF. HGF levels under these conditions may be sufficient to promote a strong connection among GFP-HUVECs when the VEGF productivity was similar. In addition, HGF and VEGF levels may influence the timing of network maturation. The GFP-HUVEC network maturation in the skeletal muscle cell sheet comprising 30% HSMF was observed at 48 h with the maximum value of L/N_T, whereas maturation of endothelial network in the skeletal muscle cell sheets prepared from skeletal cells with 40% HSMF was observed at 96 h. The GFP-HUVEC network at 96 h was more stable than that at 48 h. The late maturation of the HUVEC network may be due to low VEGF productivity, and the network's stability may be due to the high productivity of HGF.

Although serum VEGF and HGF levels are elevated in myocardial infarction patients (Kubota et al. 2004; Seko et al. 2004; Atluri et al. 2008; Huang et al. 2020) (**Table 1**), it is noteworthy that the amount of these cytokines secreted by the 5-layered HSMM sheets co-cultured with HSMFs was much higher (**Table 2**), indicating the ability of the 5-layered HSMM sheets to induce the angiogenesis at the injured site.

Table 1. Angiogenic growth factor level from previous studies

Growth factors	Subjects/cells	Conditions	Sample	Detection method	Detected concentration	References
VEGF	Human (*n*=17)	Myocardial infarction	Blood serum	ELISA	685.6±150.3 pg/ml	(Seko et al. 2004)
VEGF	Human (*n*=17)	Healthy	Blood serum	ELISA	173.7±33.6 pg/ml	
HGF	Human (*n*=17)	Myocardial infarction	Blood serum	ELISA	3,638±1,285 pg/ml	
HGF	Human (*n*=17)	Healthy	Blood serum	ELISA	59±13 pg/ml	
VEGF	Human (*n*=44)	Myocardial infarction	Blood serum	Cytometric Bead Array	53.8 ± 42.7 pg/ml	(Atluri et al. 2008)
VEGF	Human (*n*=25)	Healthy	Blood serum	Cytometric Bead Array	36.3 ± 8.9 pg/ml	
VEGF	Human (*n*=248)	Coronary artery disease	Blood serum	ELISA	645.57 pg/ml	(Huang et al. 2020)
VEGF	Human (*n*=48)	Healthy	Blood serum	ELISA	160.93 pg/mL	
HGF	Human (*n*=12)	Ischemic heart diseases	Plasma	ELISA	12.0 ± 1.8 ng/ml	(Kubota et al. 2004)
			Pericardial fluid	ELISA	**0.26 ± 0.04 ng/mL**	
FGF	Human (*n*=12)	Ischemic heart diseases	Plasma	ELISA	243.5 ± 50.9 pg/ml	
			Pericardial fluid	ELISA	**49.6 ± 7.8 pg/mL**	
VEGF	Human (*n*=12)	Ischemic heart diseases	Plasma	ELISA	47.2 ± 17.6 pg/ml	
			Pericardial fluid	ELISA	**24.5 ± 3.6 pg/mL**	
VEGF	Cardiomyocyte cell line (AP16 cell)	Normoxia	Culture media	ELISA	~ 1000 pg/ml (> $1x10^6$ cells)	(Casals et al. 2009)
		Hypoxia	Culture media	ELISA	~ 2000 pg/ml (> $1x10^6$ cells)	

Table 2. Angiogenic growth factor productivity in 5-layer HSMM sheet in cultured media of *the present study*

Cytokines	Conditions	Cytokine concentration (pg/ml)	Cytokine productivity (pg/sheet·day)
VEGF	No fibroblast	928.1 ± 92.9	1484.9 ± 148.7
	10% fibroblast	2850.6 ± 181.1	4560.8 ± 289.7
	30% fibroblast	2154.8 ± 26.2	3447.6 ± 41.9
	40% fibroblast	2572.3 ± 33.3	4115.7 ± 53.2
HGF	No fibroblast	93.4 ± 33.4	149.5 ± 53.5
	10% fibroblast	1607.4 ± 291.4	2871.8 ± 466.2
	30% fibroblast	2855.4 ± 19.4	4568.7 ± 31.0
	40% fibroblast	3450.4 ± 291.7	5520.7 ± 466.8

In this study, the effect of ECM protein deposition on the skeletal muscle cell sheet with different proportions of HSMFs was not evaluated. Therefore, the effects of ECM on promoting HUVEC network formation and supporting network stability cannot be excluded. Furthermore, the skeletal muscle cell sheets prepared from HSMF higher than 50% were unable to evaluate since the sheets containing a high proportion of HSMFs were fragile and self-contracted during preparation. It is possible that the self-contracted sheet was attributed from the aggregation of HSMFs at high proportions (**Fig. 2-10** and **Fig. 2-11B**) due to the strong connection between HSMFs.

2.5 Summary

In summary, this chapter demonstrated that different ratios of HSMM and HSMF differentially affect cytokine balance and angiogenesis, as shown in **Fig. 2-20**. Fibroblast is the crucial mediator to maintain cytokine balance in skeletal muscle cell sheet through high secretion levels of HGF and stimulate HSMM, possibly by disruption of myoblast-to-myoblast contact. The co-culture of HSMF and HSMM at an appropriate ratio (30% or 40%) promotes angiogenesis and cytokine production. These findings can be applied in the tissue engineering field to improve the therapeutic efficiency of human skeletal muscle sheets or engineered tissues for transplantation and highlight the role of fibroblasts in the regulation of VEGF secretion from adjacent tissue.

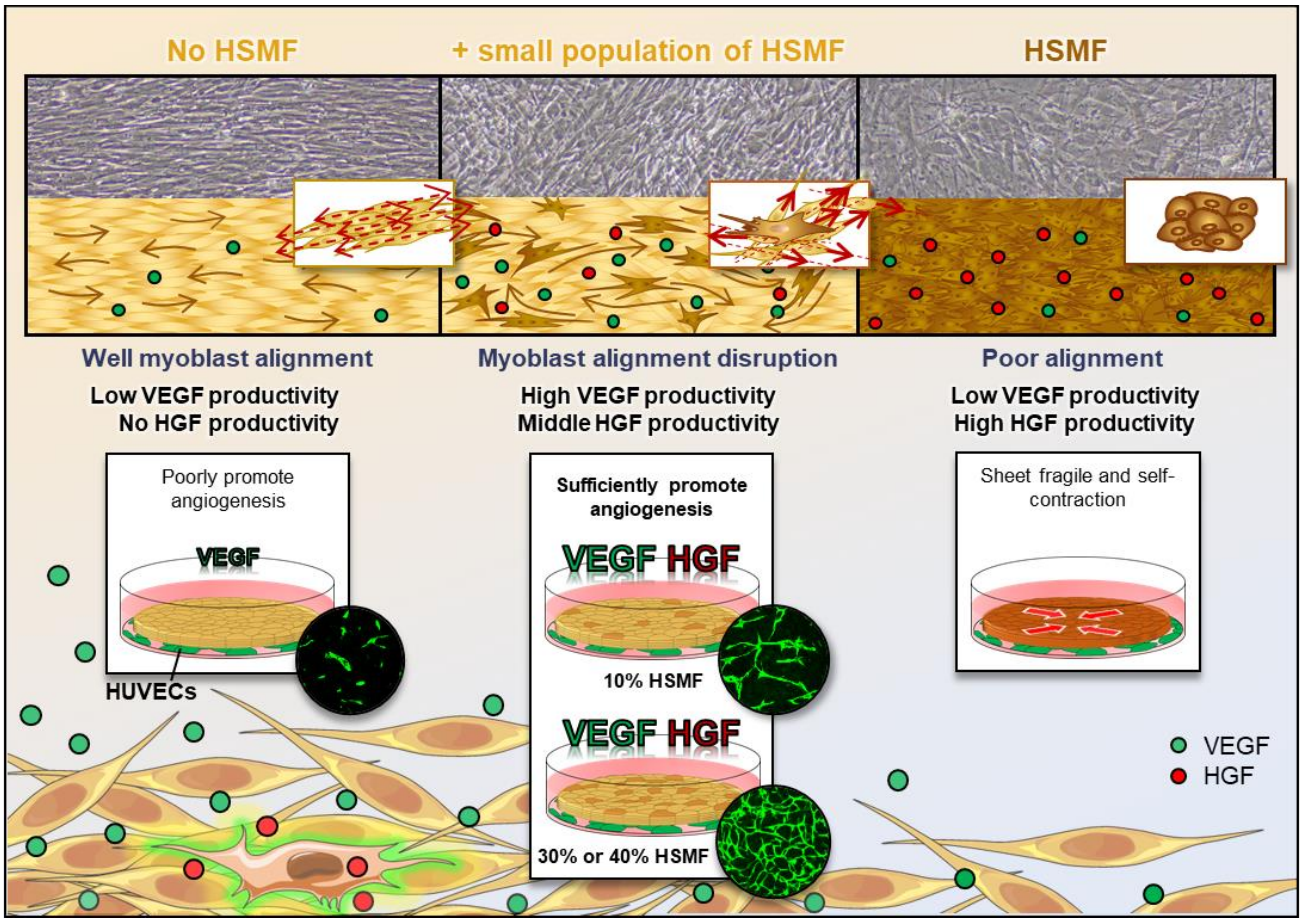

Fig. 2-20 Schematic drawing shows the effect of human skeletal muscle fibroblasts (HSMFs) co-cultured in skeletal muscle cell sheets on angiogenic cytokine balance and angiogenesis.

Chapter 3

Effect of exogenous FGF-2 on endothelial functions in 5-layered skeletal muscle cell sheet

3.1 Introduction

The growth of blood vessels from the pre-existing vasculature, called angiogenesis, is a fundamental process related to tissue development, regeneration, and restoration (Gianni-Barrera et al. 2020). This process is essential for the pre-vascularization of engineered tissue constructs and restoration of blood supply to the ischemic areas after transplantation (Mastrullo et al. 2020). The biological process of angiogenesis is highly dynamic with endothelial cell proliferation, migration, connection, and formation of a primitive vascular structure that undergoes maturation and remodeling (Betz et al. 2016). These processes require the incorporation of multiple stimuli, including cytokines and extracellular matrix components (Mongiat et al. 2016; Potente et al. 2017), which may originate from cells of the host tissue following tissue injury (Laschke et al. 2009) or tissue constructs with protein delivery systems or different cell types (Richardson et al. 2001; Laschke et al. 2008; Schumann et al. 2009).

Vascular endothelial growth factor (VEGF) and fibroblast growth factors (FGFs) are positive angiogenesis stimuli that exert directly or indirectly. VEGF plays a vital role in directly regulating the proliferation, migration, and survival of endothelial cells during angiogenesis (Olsson et al. 2006). VEGF binds to its receptor (VEGFR) on the endothelial cell surface and stimulates VEGF signaling (Distler et al. 2003; Shibuya 2011; Imoukhuede et al. 2012). In addition to VEGF, FGFs are potent mitogens critical in regulating various cellular processes, including angiogenesis. FGFs act directly by binding to specific surface receptors (FGFRs) and indirectly by upregulating the expression of other angiogenic proteins such as VEGF or VEGFR (Yun et al. 2010; Murakami et al. 2011). Fibroblast growth factor-2 (FGF-2), also known as basic FGF (bFGF), is the most potent cellular regulator in various tissues among the 23 members of the FGF family (Yun et al. 2010). It acts as a cardioprotective agent (Detillieux et al. 2003)

and mediates angiogenic stimuli that regulate the proliferation, migration, organization, and tubular-like structure formation of endothelial cells (Javerzat et al. 2002; Presta et al. 2005). These multiple functions make FGF-2 an attractive candidate for incorporating engineered tissue constructs (Yun et al. 2012; Zhang et al. 2018; Piard et al. 2019; Benington et al. 2020). Previous studies have demonstrated the treatment of ischemic diseases through FGF-2 delivery to target tissues. However, *in vivo* injection of free FGF-2 solution results in rapid diffusional loss and enzymatic degradation, resulting in decreased functional biological activity. Therefore, various studies have developed delivery systems to target FGF-2 to different tissues by adsorption and controllable release of FGF-2-encapsulated materials. A wide range of biomaterials, including synthetic or natural polymers and engineered tissues, have been studied as candidate materials to carry FGF-2 and elicit their therapeutic efficacy *in vitro* and *in vivo* (Rinsch et al. 2001; Bhang et al. 2009; Chu et al. 2011; She et al. 2012).

Cell sheet engineering is a crucial tissue engineering technique that requires no scaffold (Yang et al. 2005). This technology has been established for several diseases and trauma treatment. For myocardial infarction treatment, skeletal muscle myoblast has been developed for autologous transplantation (Sawa et al. 2015). Although the secretion of angiogenic cytokines, including VEGF, hepatocyte growth factor (HGF), and FGF-2 from skeletal muscle myoblast sheets, has been hypothesized as the main reason promoting angiogenesis and recovery of ischemic tissues, the precise function of FGF-2 in angiogenesis in human skeletal muscle cell sheets for transplantation is still unknown.

The previous chapter has been shown that the secreted FGF-2 was undetectable in culture media of human skeletal muscle fibroblasts (HSMFs) and myoblasts (HSMMs). Furthermore, the role of FGF-2 to promote endothelial functions in the human skeletal muscle cell sheet has not been elucidated yet. The aim of the current study is to investigate whether the angiogenesis effect induced by FGF-2 is strengthened after the cell sheet implantation. We fabricated multilayered skeletal muscle sheets comprising myoblasts and fibroblasts co-incubated with green fluorescent protein-expressing human umbilical vein endothelial cells (GFP-HUVECs). Exogenous FGF-2 treatment was performed, and *in vitro* angiogenesis was measured by quantification of the endothelial network. The time-lapse

observation was carried out to monitor the dynamic endothelial behavior during network formation (**Fig. 3-1**).

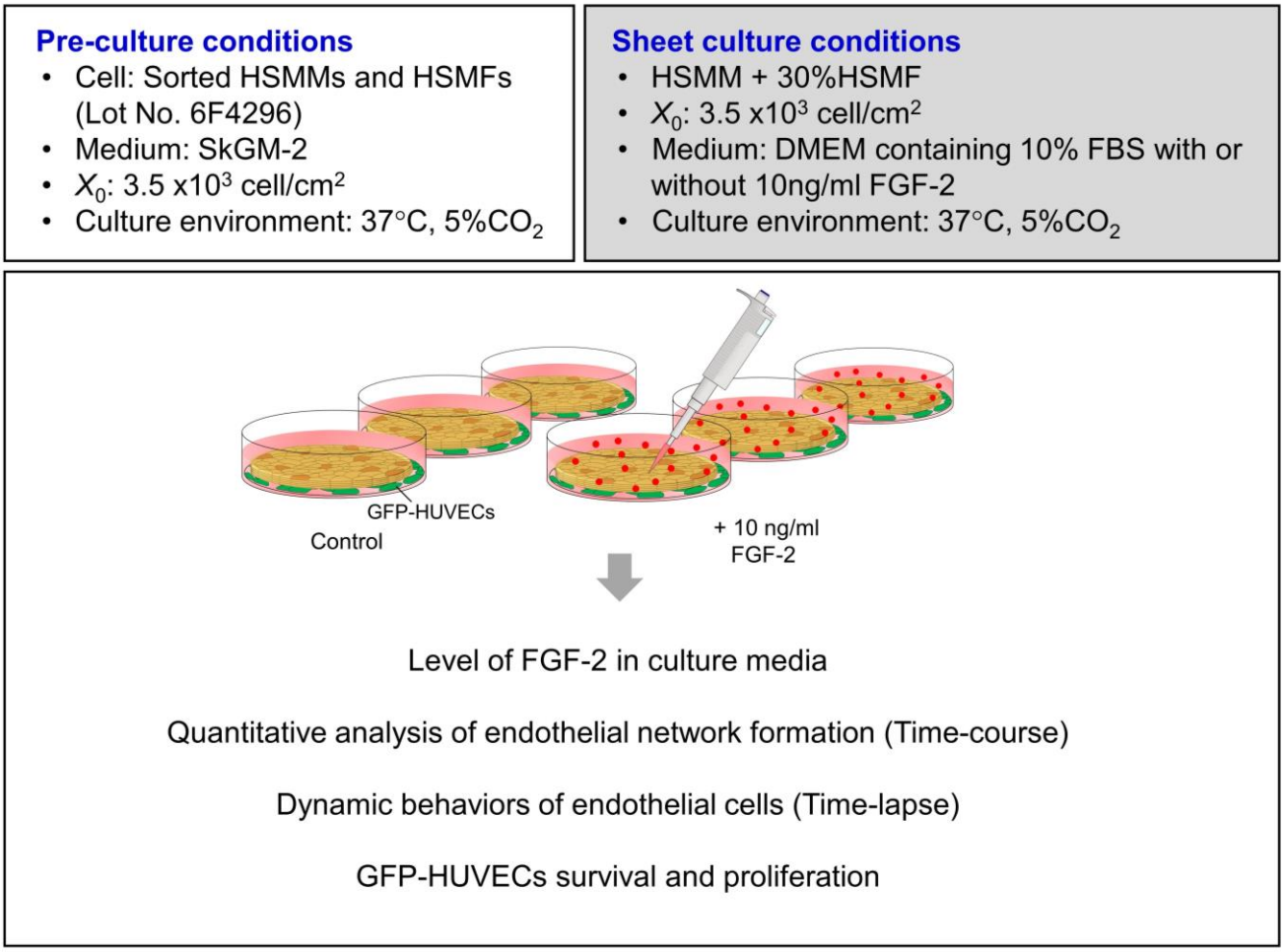

Fig. 3-1 Schematic diagram showing the experimental design of chapter 2.

3.2 Materials and methods

3.2.1 Cells culture and culture conditions

In the present study, human skeletal muscle cells (Lot. No. 6F4296; Lonza, Walkersville Inc., Walkersville, MD, USA), including human skeletal muscle myoblasts (HSMMs) and fibroblasts (HSMFs), and GFP-HUVECs (Lot. No. 20100201001; Angio-Proteomie, MA, USA) were used. Subcultures of sorted HSMM and HSMF cells were conducted at 37°C in and 5% CO_2 in skeletal cell growth media-2 (SkGM-2; Lonza, Walkersville, MD, USA) formulated by combining SkBM™-2 Basal

Medium (Cat. No. CC-3246) with the SkGM™-2 SingleQuots™ kit (Cat. No. CC-3244). Cells were pre-cultured for 5 days in T-225 flasks (Cat. No. 431082, Corning) at an initial density of 3.5×10^3 cell/cm^2 and the medium dept was set at 2 mm throughout the experiments. All cells were harvested until 70-80% confluency. The medium was set to 2 mm in depth throughout the experiment.

Green fluorescence protein-expressing human umbilical vein endothelial cells (Lot. No. 20100201001; Angio-Proteomie, MA, USA) were sub-cultured at 37°C and 5% CO_2 in Endothelial Cell Growth Medium-2 (EGM-2; CC-3162, Lonza Walkersville Inc., Walkersville, MD, USA). GFP-HUVECs were pre-cultured for 3 days in T-75 flasks (Cat. No. 430641U, Corning) at an initial density of 3.5×10^3 cell/cm^2 and the medium dept was set at 2 mm throughout the experiments.

3.2.2 Incubation of 5-layers HSMM sheet with GFP-HUVECs

A five-layered HSMM sheet containing 30% of HSMFs was fabricated according to the previous method. Briefly, HSMMs and HSMFs cultured in SkGM-2 media at day 5 were harvested and mixed at 30% HSMF (HSMF: HSMM ratio of 3:7). Cells were stained with CellTracker™ Orange CMTMR Dye in DMEM media with no FBS according to the commercially recommended protocol (5 μM for 20 min for live cell imaging). After washing with DMEM media, stained cells were centrifuged at 1,000 rpm, and the pellets were resuspended in DMEM containing 10% FBS. Cells were seeded at 3.5×10^5 cell/cm^2 inside Teflon ring (0.95 cm^2) placed in each well (diameter, 1.9 cm^2) of 24-well UpCell™ plates (CellSeed, Tokyo, Japan) with a temperature-responsive surface and incubated for 24 h at 37°C in a 5% CO_2 atmosphere to form monolayer sheet. The medium was set to 2 mm in depth throughout the experiments. A gelatin stamp was prepared from a solution of 7.4% (v/v) gelatin by dissolving gelatin powder (G1890-100G; Sigma-Aldrich) in 10 mL Hank's balanced salt solution (Sigma-Aldrich) and 200 μL of 1N NaOH solution and incubated at 45 °C for 30 min. Then, the gelatin solution was loaded to a mold and incubated overnight at 4°C. To stacking the cell sheet, gelatin stamps were overlaid onto the monolayer sheet in a well incubated at 37°C, and the plate was then transferred to incubate at 20°C. This step was then repeated to harvest monolayer sheets to form a multilayered construct sequentially. The

multilayered sheets were then transferred to the center of 35-mm culture dishes (ibidi GmbH) seeded with GFP-HUVECs at X_0 of 1×10^4 cells/cm^2 for 24 h in EGM-2 at 37 °C in a 5 % CO_2 atmosphere. At the given incubation time (t), triplicate samples were taken for quantitative analysis. The five-layered skeletal cell sheets were then cultured in Dulbecco's modified Eagle's medium (DMEM; Sigma-Aldrich, St. Louis, MO, USA) containing 10% fetal bovine serum (FBS); Invitrogen, Grand Island, NY, USA) and antibiotics (100 U/cm^3 streptomycin, and 0.25 mg/cm^3 penicillin G, 0.1 mg/cm^3 amphotericin B; Invitrogen) with or without 10 ng/mL FGF-2 (Cat. No. RCHEOT002; Reprocell, USA). During the incubation period, the medium was replaced with a fresh medium every day. The sampling time (*t*), triplicate samples were used for quantitative analysis.

3.2.3 Evaluation of GFP-HUVEC network formed inside HSMM sheet

GFP-HUVECs in five-layered skeletal muscle cell sheets were observed at 0, 24, 48, 72, and 96 h of incubation to elucidate its morphology. Endothelial network formation from random areas was analyzed following a previous protocol (Nagamori et al. 2013). Briefly, the images GFP-HUVECs inside the cell sheet from eight positions were captured using a 10× objective lens of a confocal laser scanning microscope (FV-10i, Olympus, Tokyo, Japan). Images were converted to an 8-bit grayscale with 256 × 256 pixels covering an area of 1.27 mm × 1.27 mm. All images were processed (Image-Pro Plus; Media Cybernetics Inc., Bethesda, MD) to make a skeletonized structure of endothelial network using a low-pass filter for primary noise removal and binarization at fixed threshold intensity of automatic threshold intensity and the mode intensity. Then, the binary images of the endothelial network were subjected to skeletonization and secondary noise removal with a size threshold to remove items smaller than 16 pixels. Furthermore, the small branches were pruned in the objects. The processed skeletonized images were then measured the total length of the network per image area (L; cm^{-1}), the number of total tips of the network (N_T; tip/cm^2), and extension of the endothelial network (L/N_T; cm/tip). The network tips at the edge of the image were not excluded for counting (**Fig. 2-3**).

Furthermore, the five-layered cell sheets were captured using a fluorescence microscope (IN CELL Analyzer 2000, GE Healthcare) under a 2× objective lens with 2048 × 2048 pixels. Nine images

were captured and tiled with 50% overlapping covering an area of 15.3 mm × 15.3 mm. Skeletal muscle cells were stained with 5μM CellTracker™ Orange CMTMR Dye in DMEM media with no FBS and incubated at 37° for 20 min. Then, the cell sheets were captured for masking to define the sheet boundary. Image processing was performed using Image-Pro Plus software (Media Cybernetics Inc., Bethesda, MD, USA). The images of sheet morphology were converted to 12-bit grayscale to obtain a color quality for masking binary images. The image was adjusted using a low-pass filter of Image-Pro Plus software for noise removal and binarization at fixed threshold intensity (average of the mode intensity and the automatic threshold intensity). The cell sheet boundary was then selected, and the sheet area was filled with white background. Images were modified to 8 bits to reduce their size. Similarly, images of HUVECs were captured, tilled, and changed to 8-bit grayscale. The masking was overlaid on the network image, and outside endothelial cells were then subtracted to obtain the image of endothelial cells inside the sheet as a region of interest (ROI). Subsequently, the GFP-HUVECs images were processed using a low-pass filter for noise removal. The binary images of endothelial cells were subjected to skeletonization and secondary noise removal with a size threshold to eliminate items smaller than 11 pixels. The pruning of small branches was processed in the objects (**Fig. 3-2**). The total length of the network per sheet (L; cm/sheet) and the number of total tips of the network per sheet (N_T; tip/sheet) were measured to calculate the extent of network formation in the cell sheet (L/N_T; cm/tip) (**Fig. 3-3**). In addition, the length of each network in the sheet and the number of networks (N_N) longer than 0.2 and 0.4 cm were measured to classify networks as short ($L < 0.2$ cm), medium ($0.2 \text{ cm} \leq L < 0.4$ cm), and long ($L \geq 0.4$ cm) (**Fig. 3-2**).

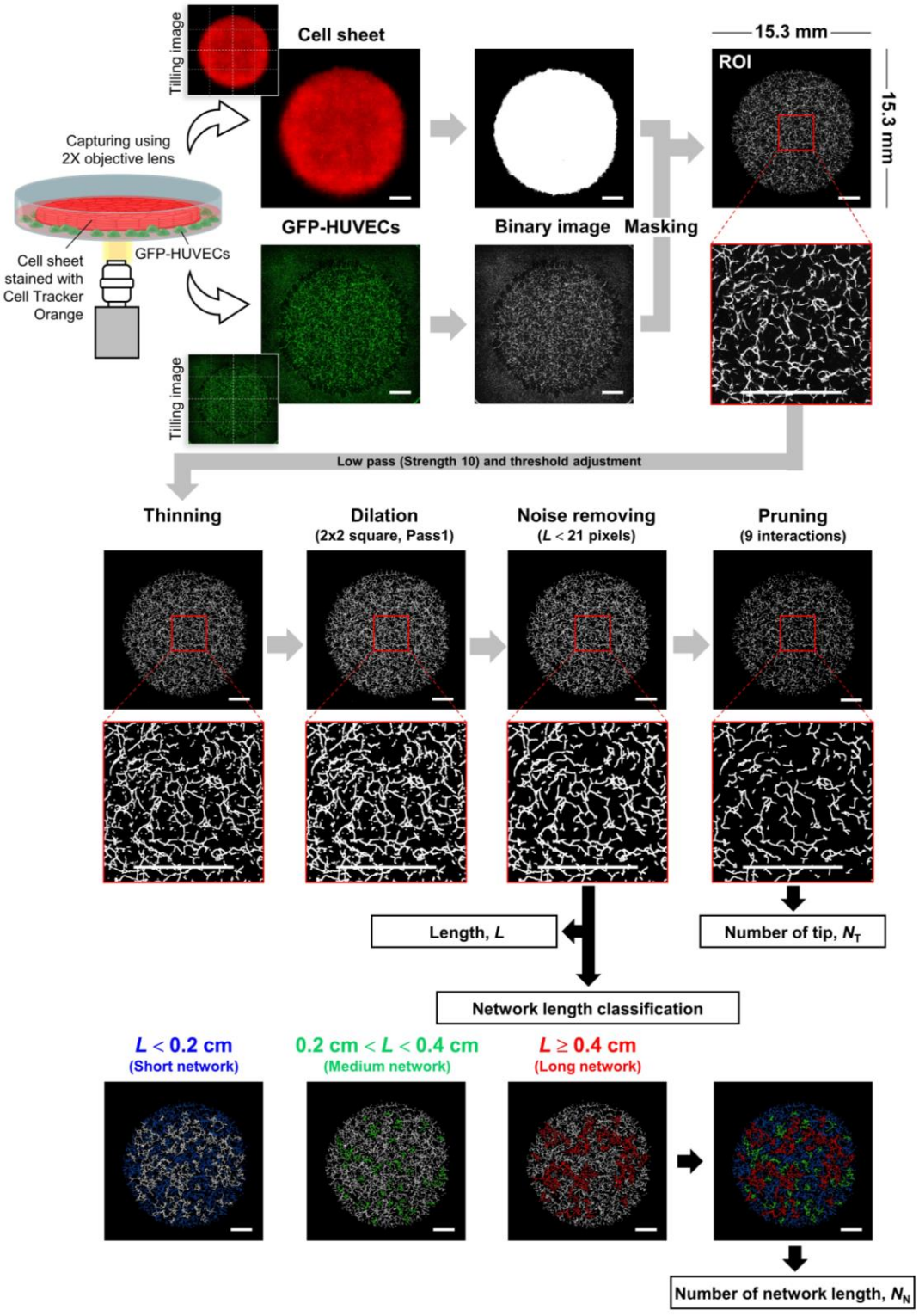

Fig. 3-2 Quantitative analysis of GFP-HUVEC network formation inside a five-layered human skeletal muscle cell sheet. Image processing procedure to quantify endothelial network formation from the whole sheet area. The image was captured using a 2× objective lens of a fluorescence microscope. Tilled images were converted to binary images and dilated to make skeletonized objects and noise removal. Scale bar: 2 mm.

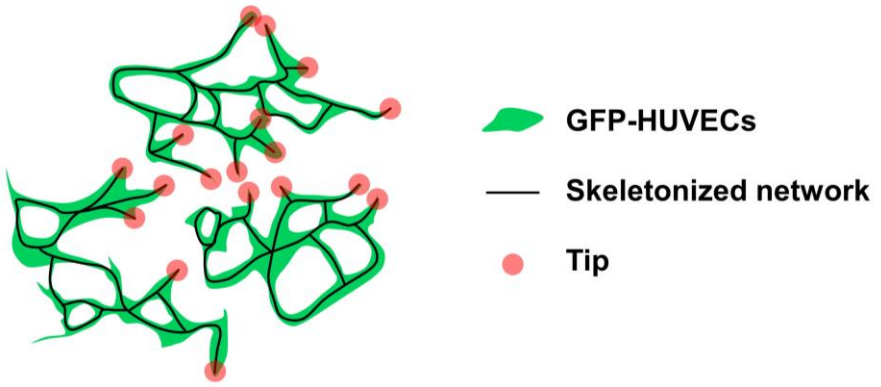

Measure	Definition	
	Local area analysis	Whole sheet analysis
Length	$\boldsymbol{L}\ (\mathrm{cm^{-1}}) = \frac{(L\ (\mathrm{pixel}) \div 2) \times a\ (\frac{\mathrm{cm}}{\mathrm{pixel}})}{\mathrm{Area}\ (\mathrm{cm^2})}$	$\boldsymbol{L}\ (\mathrm{cm/sheet}) = (L\ (\mathrm{pixel}) \div 2) \times a\ (\frac{\mathrm{cm}}{\mathrm{pixel}})$
End points	$\boldsymbol{N_T}\ (\mathrm{tip/cm^2}) = \frac{\mathrm{No.\ of\ tip\ (tip)}}{\mathrm{Area}\ (\mathrm{cm^2})}$	$\boldsymbol{N_T}\ (\mathrm{tip/sheet}) = \mathrm{No.\ of\ tip\ per\ sheet\ (tip/sheet)}$
Extent of network	$\boldsymbol{L/N_T}\ (\mathrm{cm/tip}) = \frac{L\ (\mathrm{cm^{-1}})}{N_T\ (\frac{\mathrm{tip}}{\mathrm{cm^2}})}$	$\boldsymbol{L/N_T}\ (\mathrm{cm/tip}) = \frac{L\ (\mathrm{cm/sheet})}{N_T\ (\frac{\mathrm{tip}}{sheet})}$

a is conversion factor to covert pixel to cm

Fig. 3-3 Quantitative analysis of endothelial network formation in five-layered skeletal muscle cell sheets. The length of the network per sheet (L) and the number of endpoints (N_T) were measured from the skeletonized network and used to calculate the extent of the GFP-HUVEC network (L/N_T). In this study, the endothelial network from local areas and whole-cell sheet areas were evaluated.

3.2.4 Time-lapse observation of GFP-HUVECs

For time-lapse observation, skeletal muscle cell sheets co-incubated with GFP-HUVECs were captured every 1 h during 48-96 h of co-incubation to understand the dynamic behavior of GFP-HUVECs using a confocal laser scanning microscope (FV-10i, Olympus, Tokyo, JP) under a 10× objective lens covering an area of 1.27 mm × 127 mm. The sequence images were processed using FluoView 4.2 software (Olympus, Tokyo, Japan). The numbers of endothelial connection and disconnection events per area were counted.

3.2.5 GFP-HUVECs culture and FGF-2 treatment

To investigate the effect of FGF-2 on endothelial survival and proliferation, GFP-HUVECs were sub-cultured for 3 days and harvested for seeding at X_0 of 1×10^4 cell/cm^2. After 24 h, GFP-HUVECs were cultured in DMEM media containing 10% FBS with or without 10 ng/ml FGF-2 for 96 h. Fresh medium was replaced every day, and cells were captured every 24 h by a confocal laser scanning microscope (FV10i, Olympus, JP) using a 10× objective lens.

2.5 3.2.6 Measurement of FGF-2 level

The level of FGF-2 in cultured media was measured using the human FGF Quantikine ELISA (Cat. No. DFB50, R&D Systems Inc., USA). The *E*. coli-expressed recombinant human FGF-2 provided from the ELISA kits was used to establish the standard curve. The baseline levels of FGF-2 in cultured media without cells were measured.

3.2.7 Statistical analysis

All values in this study are expressed as the mean ± standard deviation (SD). Each experiment was performed using triplicate samples (n = 3). Normally distributed data with equal variances were evaluated by an independent sample t-test when two groups were compared. To analyze data with more than two groups, a one-way analysis of variance (ANOVA) followed by the Bonferroni test was

performed. All statistical analyses were evaluated using SPSS software (version 26.0, IBM, USA). Differences were considered statistically significant when the value of P was less than 0.05.

3.3 Results

3.3.1 Endogenous production of FGF-2 in the five-layered skeletal muscle cell sheet

In this study, a five-layered skeletal muscle cell sheet comprising HSMF and HSMM co-incubated with GFP-HUVECs was cultured in DMEM containing 10% FBS. We first measured the basal level of FGF-2 in the cultured media without cells and that endogenously produced from five-layered skeletal muscle cell sheets and found that it was undetectable from both conditions. These data demonstrate that the endogenous production of FGF-2 by skeletal muscle cell sheet was deficient.

3.3.2 Effect of exogenous FGF-2 treatment on endothelial network formation

In this study, the efficiency of HUVEC network formation in skeletal muscle cell sheets was analyzed using an *in vitro* angiogenesis assay imitated from the area of *in vivo* transplantation (Nagamori et al. 2013). The five-layered skeletal muscle cell sheets co-incubated with GFP-HUVECs were treated with 10 ng/mL FGF-2 in DMEM containing 10% FBS. Quantitative analysis of endothelial network formation in the skeletal muscle cell sheets was performed. Cell sheets cultured in media without exogenous FGF-2 were used as controls. The density of GFP-HUVECs at 24 h after seeding was confirmed to be $1.24 \pm 0.50 \times 10^4$ cells/cm^2. Endothelial networks were examined using a fluorescence microscope every 24 h from 0 to 96 h using 10× and 2× objective lenses for the analysis of the local and whole areas. As shown in **Fig. 3-4A**, most GFP-HUVECs in five-layered skeletal muscle cell sheets were single and had a round shape at the beginning of the incubation period (t = 0). Quantitative analysis of endothelial network formation revealed a low value of L and L/N_T but a high value of N_T. GFP-HUVECs became elongated and connected after 24 h under both conditions, resulting in an increase in L and L/N_T values and a decrease in the N_T value. After FGF-2 treatment, the L value steadily increased and was significantly different as compared to that of the control sample at 96 h. In contrast, L in the control

condition gradually increased and then leveled off. The local analysis revealed no significant differences in the connectivity expressed by L/N_T value between FGF-2 and control treatment (**Fig. 3-4B**).

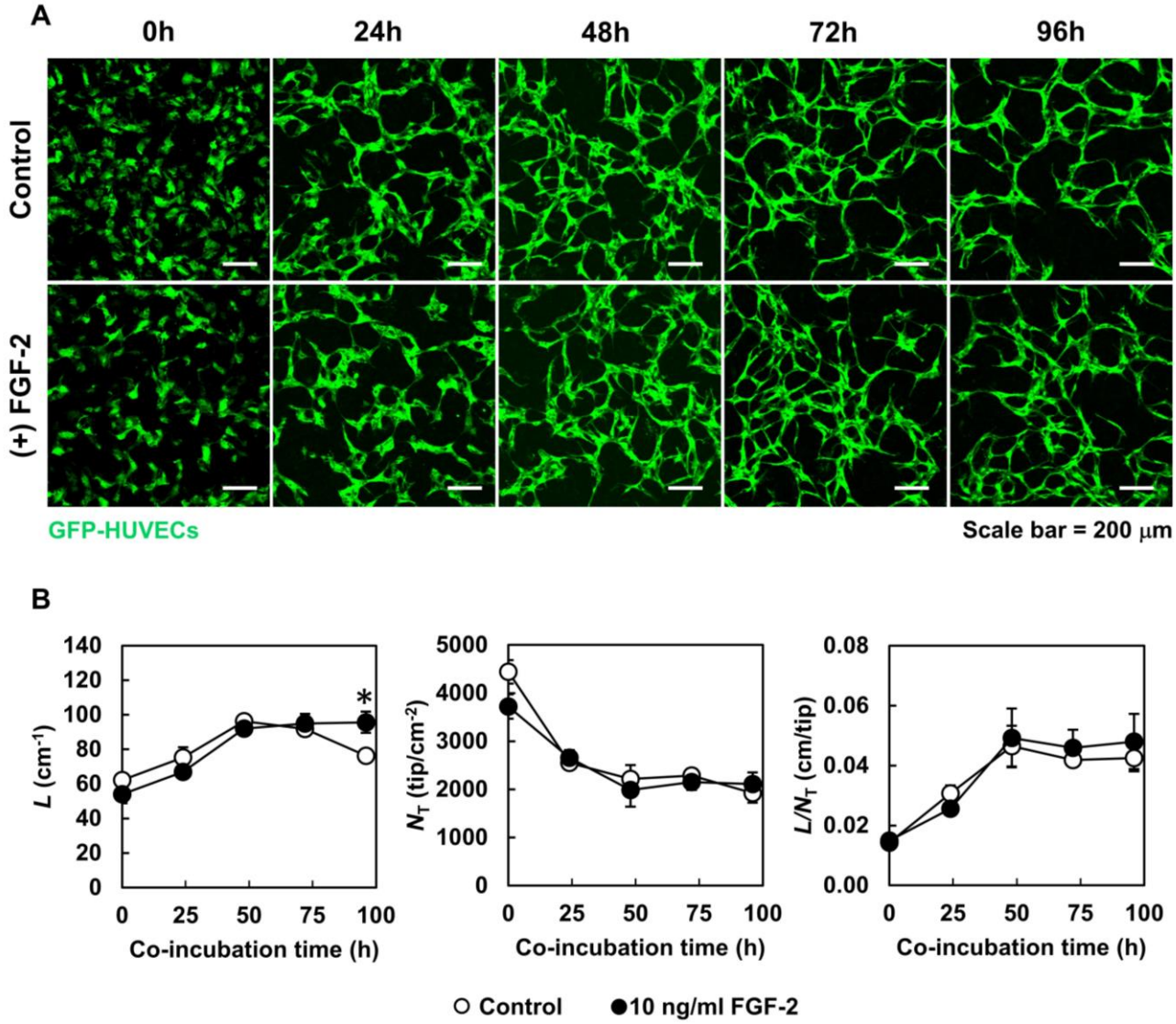

Fig. 3-4 GFP-HUVECs from the local area inside five-layered human skeletal muscle cell sheets treated with or without 10 ng/mL FGF-2. (A) Images of GFP-HUVEC morphology were captured using a 10× objective lens of a confocal laser scanning microscope. Scale bar: 200 μm. (B) The length of the network per sheet (L; cm^{-1}), number of network (N_T; tips/cm^2), and extent of the GFP-HUVEC network (L/N_T; cm/tips) were evaluated from eight random areas in each sample. Three samples were measured (n = 3). Data are expressed as average ± SD. *P < 0.05; independent sample t-test.

Evaluation of the endothelial network from the local area was unable to well understand the total endothelial network with long length in a sheet since the endothelial cells were captured from the small areas in the cell sheet. Therefore, an analysis method to evaluate the total endothelial network formation in the sheet was established. The network formation of GFP-HUVECs in the five-layered HSMM sheets was quantitated based on the total network length per sheet (*L;* cm/sheet), the number of total tips of network per sheet (N_T; tip/sheet), and the extent of the network (L/N_T; cm/tip). The quantitative analysis of endothelial network formation revealed low *L* and L/N_T values but high N_T values at the initial time (**Fig. 3-5**), similar to that observed in local network analysis. After 24 h, GFP-HUVECs became more elongated and connected under both conditions, resulting in an increase in *L* and L/N_T values and a decrease in the N_T value. In the control group, *L* and L/N_T values increased but leveled off after prolonged culture. In contrast, *L* and L/N_T values steadily increased and remained constant after treatment with 10 ng/mL FGF-2. The endothelial habitat inside the skeletal muscle cell sheet was observed; the endothelial cells migrated from the culture surface to form a network and remained inside the five-layered skeletal muscle cell sheet under both conditions after 96 h (**Fig. 3-6**).

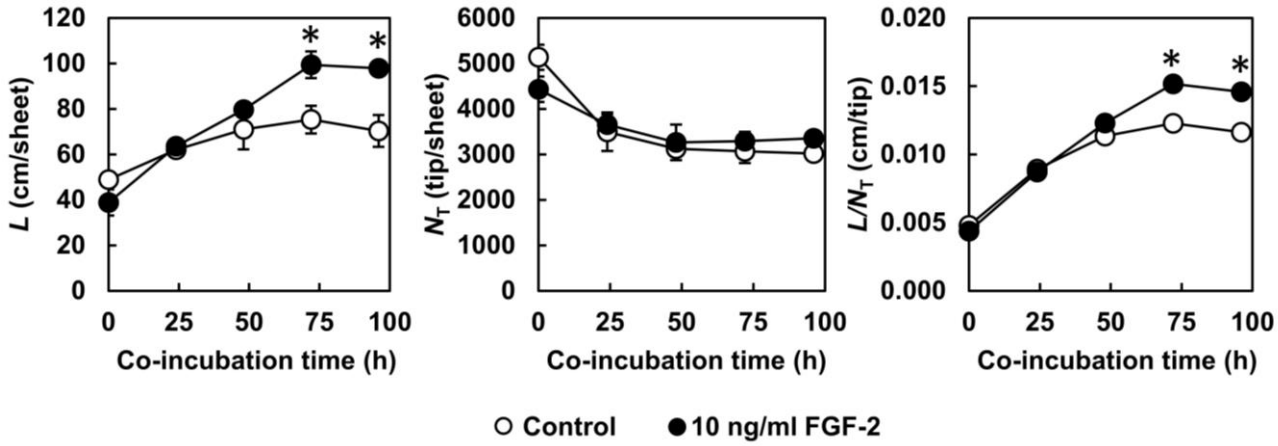

Fig. 3-5 GFP-HUVECs from the whole area of cell sheets were captured using a fluorescence microscope and 2× objective lens. All images were tilled and processed for endothelial network quantitation. The length of the network per sheet (*L*; cm/sheet), number of the network (N_T; tip/sheet), and extent of the

GFP-HUVEC network (L/N_T; cm/tip) were evaluated. Three samples were measured (n = 3). Data are expressed as average ± SD. *P < 0.05; independent sample t-test.

To evaluate the ability of FGF-2 to promote the extension of the endothelial network, we determined the number of endothelial networks longer than 0.2 and 0.4 cm for the medium and long endothelial networks. A network length of less than 0.2 cm was considered as a short network (**Fig. 3-7A**). The total length and number of medium and long endothelial networks were significantly higher in the skeletal muscle cell sheet treated with 10 ng/mL FGF-2 than in the control group at 72 h (**Fig. 3-7B** and **3-7C**). Together, these results suggest that FGF-2 treatment could promote endothelial network formation and increase the number of extended networks in five-layered skeletal muscle cell sheets.

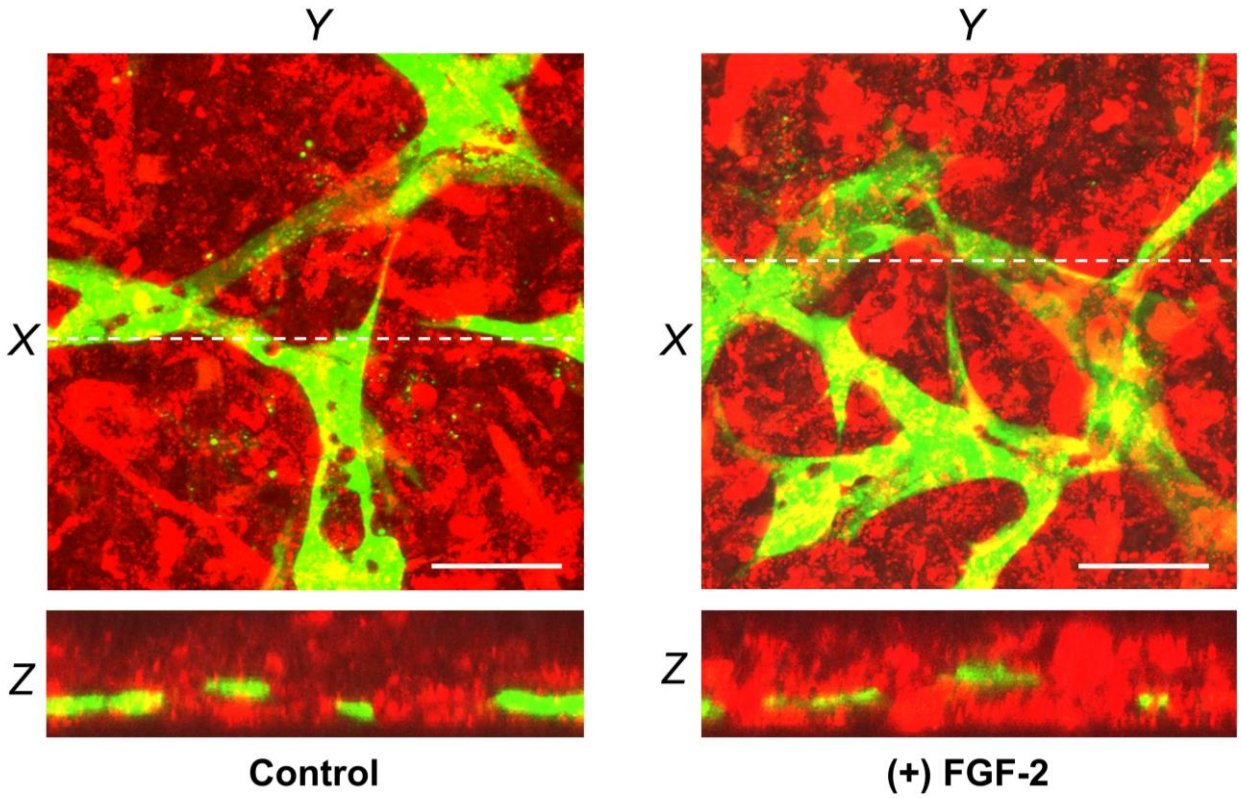

Fig. 3-6 Stacking images were captured at t = 96 h by confocal laser scanning microscopy using a 60× objective lens. The 3D images were generated to show the 3D structure of cell skeletal muscle cell sheets (red) and GFP-HUVEC (green) network formation in the presence or absence of 10 ng/mL FGF-2. Scale bar: 50 μm.

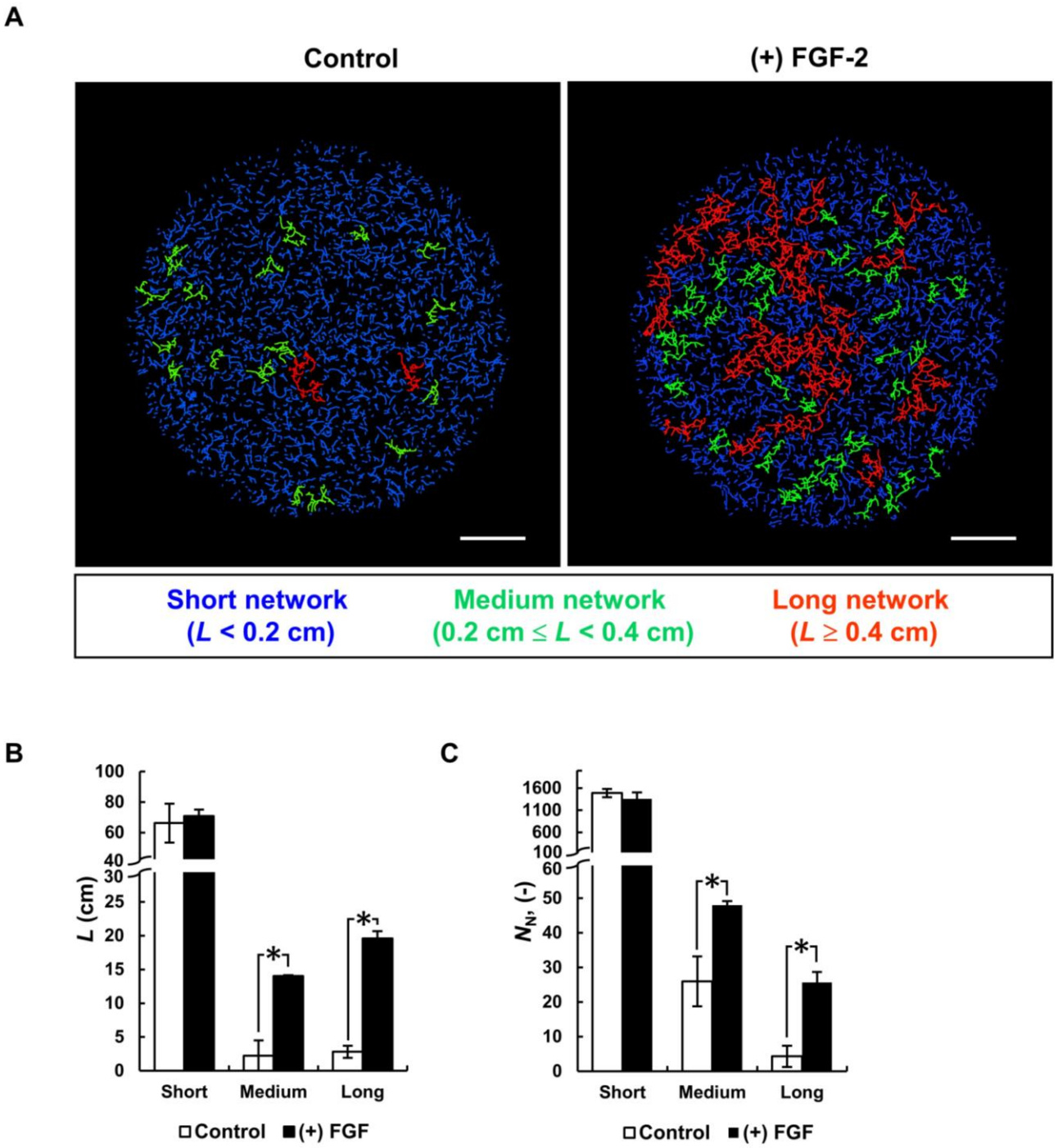

Fig. 3-7 Evaluation of extended GFP-HUVEC network in five-layered skeletal muscle cell sheets. (A) Skeletonized images of endothelial networks in skeletal muscle sheets treated with or without 10 ng/mL FGF-2; networks were grouped as short (blue), medium (green), and long networks (red). Scale bar: 2 mm. (B) The total length and number of networks in the cell sheet from each group were compared. Three samples were measured (n = 3). Data presents with ± SD.

3.3.3 Dynamic behavior of GFP-HUVECs in five-layered skeletal muscle cell sheets treated with FGF-2

The dynamic behavior of GFP-HUVECs in five-layered skeletal muscle cell sheets was monitored to clarify the precise role of FGF-2 in endothelial network formation. GFP-HUVECs in five-layered skeletal muscle cell sheets treated with 10 ng/mL FGF-2 were compared with those in untreated control sheets. Time-lapse observation revealed endothelial network formation inside the cell sheet after 48 h of incubation under both conditions. The GFP-HUVECs in cell sheets dynamically migrated, connected, and disconnected during endothelial network formation (**MOV. 2-1** and **MOV.2-2**). To evaluate whether FGF-2 plays any role in maintaining stabilized endothelial connection and preventing endothelial disconnection, we determined the frequency of connection (red arrow) and disconnection (white arrow) of endothelial cells in these sheets after FGF-2 and control treatment. Endothelial network formation is the dynamic process of connection and disconnection of endothelial cells. The high frequency of connection and low frequency of disconnection should stabilize the endothelial network. In control with not FGF-2, the endothelial network in the skeletal muscle cell sheet was decayed, showing a higher frequency of disconnection (white arrow) compared to one with FGF-2 treatment (**Fig. 3-8A** and **3-8B**). Although the frequency of new GFP-HUVECs connection was not higher in FGF-2 (**Fig. 3-9A**), the frequency of GFP-HUVEC disconnection resulting in network degradation in the five-layered skeletal muscle cell sheet treated with 10 ng/mL FGF-2 was lower than that in the control group (**Fig. 3-9B**). These data imply that FGF-2 plays a role in preventing endothelial disconnection during network formation in five-layered skeletal muscle cell sheets.

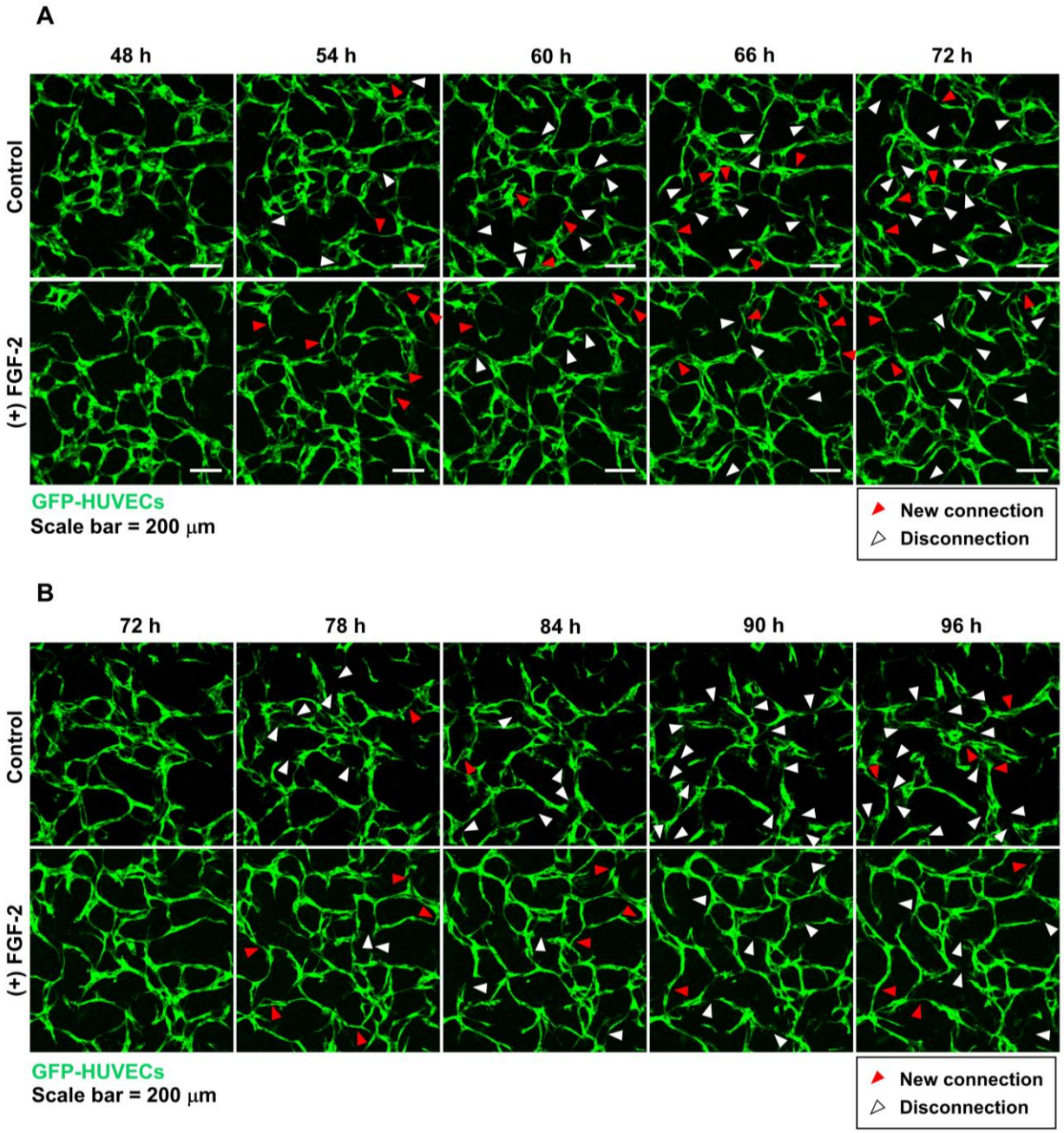

Fig. 3-8 Dynamic GFP-HUVEC network formation in five-layered skeletal muscle cell sheets treated with or without 10 ng/mL FGF-2. Time-lapse observation of GFP-HUVEC behavior in layered skeletal muscle cell sheet. The GFP-HUVECs (green) in the sheet were captured every 1 h by a confocal laser scanning microscope using a 60× objective lens during 48-72 h (A) and 72-96 h (B). Endothelial network formation is the dynamic process of endothelial connection (red arrow) and disconnection (white arrow). Less frequency of disconnection stabilized endothelial network formation in the cell sheet. Scale bar: 200 μm.

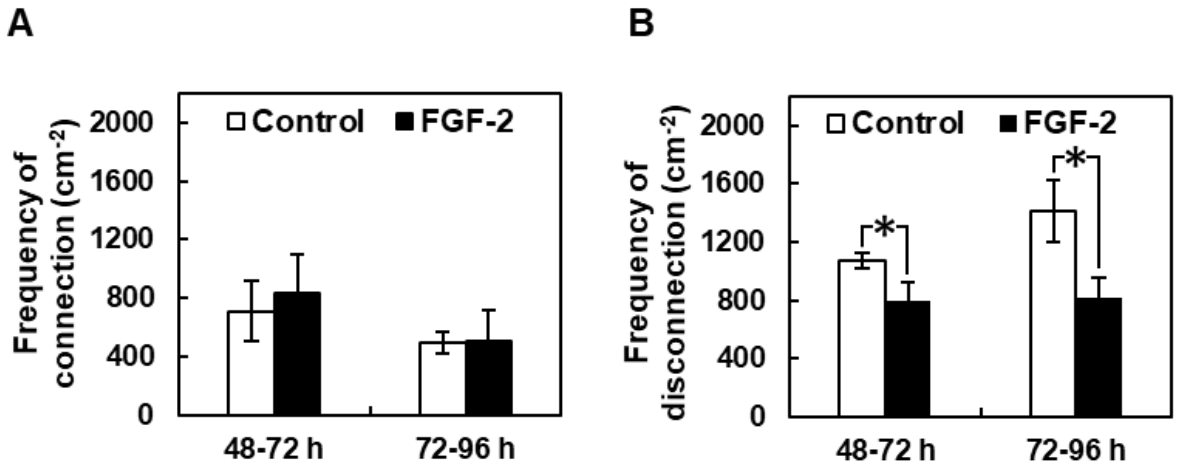

Fig. 3-9 The events of endothelial connection and disconnection during 48-72 h (A) and 72-96 h (B) were counted and expressed as the number of GFP-HUVEC connection and disconnection per area (cm^{-2}).

3.3.4 Effect of FGF-2 on endothelial behavior outside the five-layered skeletal muscle cell sheet

In this model, GFP-HUVECs were seeded in 35 mm culture dishes 24 h before the transfer of the five-layered skeletal muscle cell sheets into the center of culture dishes. This model allows monitoring of GFP-HUVECs inside as well as outside of the sheets. GFP-HUVECs outside the cell sheet were round in shape at 0 h, similar to those inside the sheet. The density of GFP-HUVECs outside the sheet did not differ between conditions with or without FGF-2. After prolonged incubation, only inside, but not outside, GFP-HUVECs formed endothelial networks under both conditions. This result indicates the requirement of interaction between cell sheets and endothelial cells to promote endothelial network formation. The number of GFP-HUVECs outside the cell sheet increased after prolonged culture and was higher in the FGF-2 treatment group than in the control group at 72 h (**Fig. 3-10**). Many outer GFP-HUVECs was lost in the control group, possibly owing to cell death and detachment under FGF-2 deficiency. To confirm the requirement of FGF-2 for survival, the GFP-HUVECs were cultured with or without 10 ng/mL FGF-2 (**Fig. 3-11**). The results showed that GFP-HUVECs could grow well and attach to the culture surface in the presence of FGF-2. In contrast, GFP-HUVECs were undetached in the control group owing to FGF-2 deficiency. These observations indicate the critical role of FGF-2 in maintaining GFP-HUVEC survival and attachment.

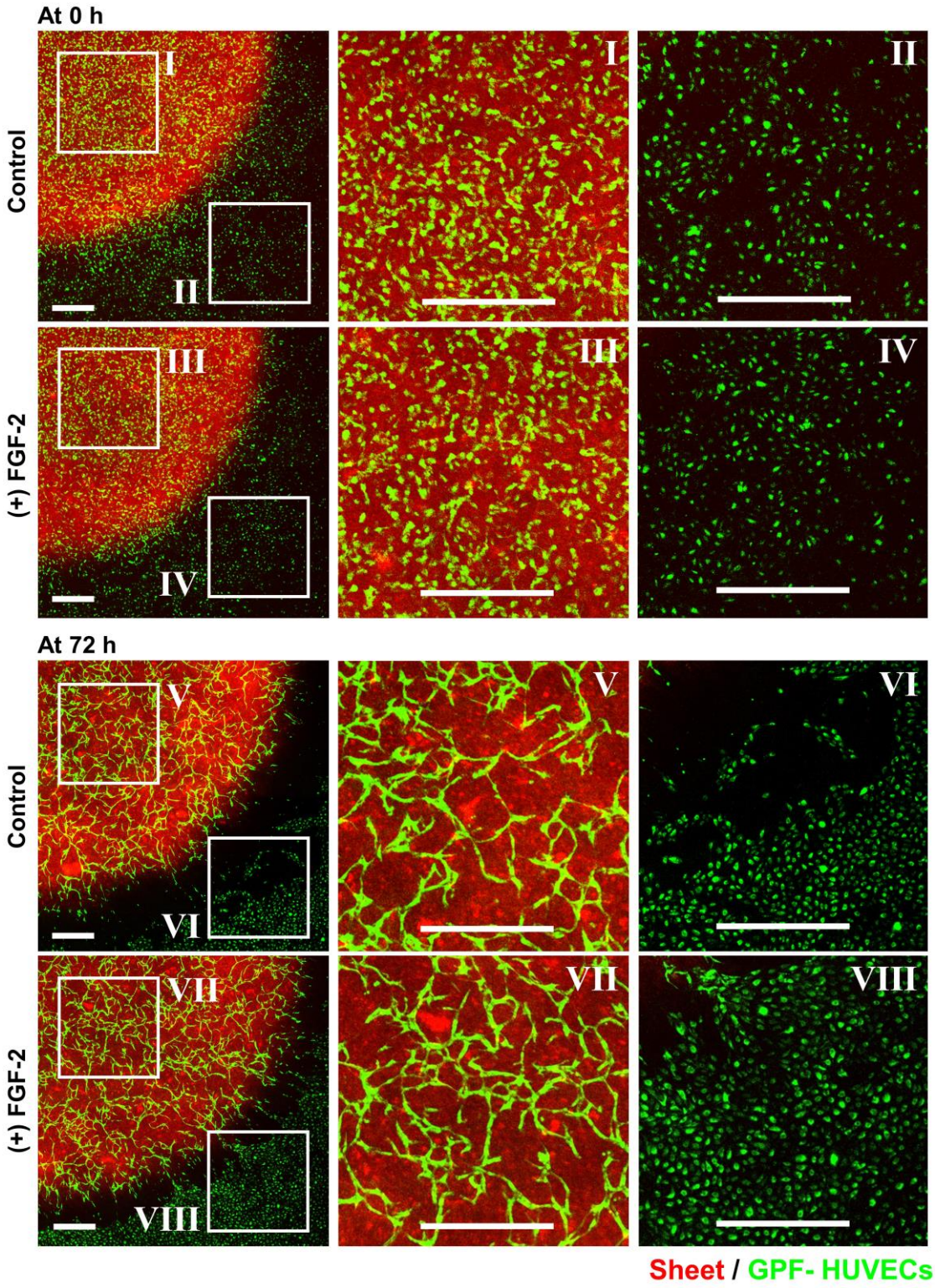

Fig. 3-10 Effect of FGF-2 on GFP-HUVEC growth outside five-layered skeletal muscle myoblast sheets after culture for 72 h. The skeletal muscle myoblast sheet (red) was stained with Cell tracker dye, co-incubated on GFP-HUVEC (green), and cultured in a medium containing 10 ng/mL FGF-2. The sheets cultured in medium without FGF-2 were used as controls. Samples were captured by a fluorescence microscope using a 2× objective lens. Scale bar: 2 mm.

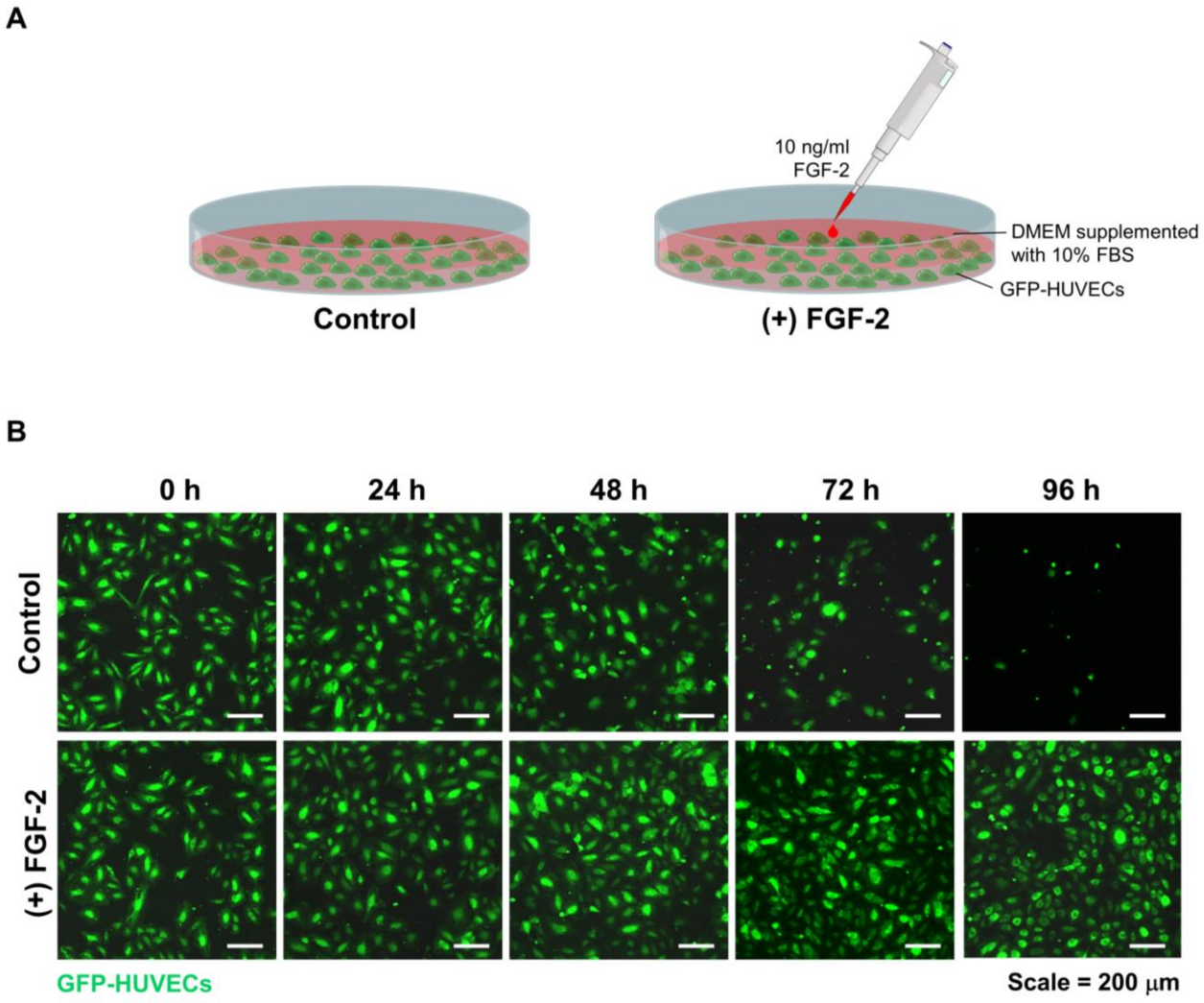

Fig. 3-11 Culture of GFP-HUVECs in DMEM supplemented with FBS with or without 10 ng/mL FGF-2. (A) GFP-HUVECs (green) were seeded at an initial seeding density of 1×10^4 cell/cm^2. Cells were treated with or without 10 ng/mL FGF-2 for 72 h. (B) Cells were captured every 24 h by a confocal laser scanning microscope using a 10× objective lens. Scale bar: 200 μm.

3.4 Discussion

Although the process of angiogenesis has been primarily studied both *in vivo* and *in vitro*, investigation of this process *in vitro* is challenging owing to the need for the development of rapid vascularization of tissue-engineered constructs to treat ischemic conditions (Adams et al. 2007; Tahergorabi et al. 2012; Gianni-Barrera et al. 2020). Numerous soluble growth factors, including VEGF, FGFs, and HGF, have been reported to stringently regulate angiogenesis progression involving the development of structural blood vessels for vascularized tissue or grafting (Montesano et al. 1986; Xin et al. 2001; Matkar et al. 2017). Cell sheet technology using skeletal muscle cells was developed for autologous transplantation to treat myocardial infarction (Durrani et al. 2010; Terajima et al. 2014). To understand the angiogenic properties of skeletal muscle cells, we evaluated the productivity of growth factors, including VEGF, HGF, and FGF-2, in five-layered skeletal muscle cell sheets. We have shown that skeletal myoblast sheets containing some fibroblasts can secrete high VEGF and HGF levels, consequently promoting endothelial function to form a network (Thummarati et al. 2020). However, the production of FGF-2 and its precise role in angiogenesis in skeletal muscle cell sheets are still unclear.

In the present study, an *in vitro* angiogenesis system based on a multilayered skeletal muscle cell sheet containing HSMM and HSMF co-incubated with GFP-HUVECs was used to mimic the *in vivo* angiogenesis process after transplantation. The evaluation method was adapted from a previous study (Nagamori et al. 2013) to quantitate endothelial network formation inside the five-layered skeletal muscle cell sheet. We first measured the basal FGF-2 level in culture media and the endogenous production of FGF-2 from skeletal muscle sheets. We demonstrated that the level of FGF-2 secreted from the five-layered skeletal muscle myoblast sheet in cultured media was undetectable, suggesting no endogenous production of FGF-2 from the skeletal muscle cell sheet. The level of FGF-2 secreted from the cell sheet in cultured media was undetectable and much lower than the therapeutic concentration (>1 ng/ml) necessary to promote endothelial function for angiogenesis, as previously reported (Montesano et al. 1986; Fafeur et al. 1990; Zubilewicz et al. 2001; Kano et al. 2005). To investigate whether FGF-2 is required to promote endothelial function, exogenous FGF-2 was added to the skeletal muscle cell sheet

co-incubated with GFP-HUVECs, and endothelial network formation was evaluated. First, the endothelial network formation both in the local and whole areas of the sheet during 96 h was quantified by measuring total endothelial network length (L) to observe elongation and connection of all endothelial cells and the number of the endpoint of the network per sheet (N_T). These two factors were then used to calculate the extension of the endothelial network in the cell sheet (L/N_T). At the initial time, endothelial cells from both conditions were round with no elongation and/or connection (**Fig. 3-4A**). Therefore, the L and L/N_T values were low, but the N_T was high. After 24 h, the endothelial cells became more elongated, and some were connected to neighboring cells. Therefore, L and L/N_T increased and the number of tips reduced, resulting in a decrease in N_T value. Although L and L/N_T increased after the maturation of the endothelial network after 48 h of incubation, no differences were observed in these values between FGF-2 and control treatment groups (**Fig. 3-4B**). However, after 48 h, the L and L/N_T values failed to increase in the absence of FGF-2 and tended to reduce after prolonged culture (up to 96 h). On the other hand, these values continuously increased after FGF-2 treatment. These data suggest that FGF-2 could support and maintain the endothelial network in five-layered skeletal muscle cell sheets after prolonged culture and endothelial network maturation (**Fig. 3-5**).

Endothelial elongation with a stable connection should not increase the total length of the endothelial network and the number of extended networks in the sheet. We measured the length of networks in the sheet and counted the number of extended networks longer than 0.2 or 0.4 cm at 72 h. The number of extended networks increased in skeletal muscle cell sheets following FGF-2 treatment, suggesting its role in endothelial elongation and connection (**Fig. 3-7A** and **Fig. 3-7B**). The increase in the number of extended networks may result from the stabilized endothelial connection after FGF-2 treatment. To test this hypothesis, the time-lapse observation was performed to monitor dynamic endothelial interaction inside the skeletal muscle cell sheet. We found that endothelial network formation is a dynamic process wherein endothelial cells are connected and disconnected (**Fig. 3-8**). However, FGF-2 treatment prevented endothelial connection and stabilized network formation as compared to the control treatment without FGF-2 (**Fig. 3-9**). The mechanism by which the FGF-2 stabilizes endothelial

network formation in the skeletal muscle cell sheet has not yet been elucidated in this study. Previous studies demonstrated that vascular elongation and stabilization are involved in endothelial cell-to-cell adhesion molecules (Sauteur et al. 2014; Cao et al. 2017). Numerous transmembrane adhesive proteins are commonly associated with endothelial cell-to-cell adhesion include; vascular endothelial (VE) and neural (N) cadherin, occludin, claudins, and the junctional adhesion molecules (JAMs) (Lampugnani 2012). These molecules hold the endothelial cells together and anchor to the actin cytoskeleton and signaling molecules, consequently stabilize junctions and transfer cell signaling to mediate cellular functions (Dejana et al. 1999). Accordingly, we hypothesized that FGF-2 might enhance the expression and/or localization of these adhesive molecules in GFP-HUVECs inside the skeletal muscle cell sheets, leading to the stabilization of endothelial network formation.

Additionally, FGF-2 has been reported to promote angiogenesis indirectly by influencing other growth factors and chemokines such as VEGF, HGF, platelet-Derived Growth Factor (PDGF), and transforming growth factor (TGF) (Kano et al. 2005; Bai et al. 2014), contributing to vascular maturation. Our previous study has demonstrated that the skeletal muscle cell sheet containing HSMF secreted both VEGF and HGF (Thummarati et al. 2020). Therefore, exogenous FGF-2 and cell sheet secreted growth factors might synergistically enhance the endothelial network inside the sheet. These hypotheses need to be elucidated in the future.

The effects of FGF-2 on endothelial cells on the culture surface outside the skeletal muscle cell sheet was observed. This study demonstrated that FGF-2 treatment promoted the proliferation of endothelial cells outside the cell sheet, as previously reported (Garmy-Susini et al. 2004; Sahni et al. 2004; Romo et al. 2011). In the presence of FGF-2 in the culture medium, endothelial cells outside the skeletal muscle cell sheet could not form endothelial networks, unlike those inside the sheet. It has previously shown that skeletal muscle cell sheets comprising fewer fibroblasts secrete high concentrations of VEGF and HGF in the culture media. Thus, only soluble factors, including VEGF, HGF, and FGF-2 in culture media, were insufficient to facilitate network formation by endothelial cells; instead, endothelial cells require other cells to promote the network formation (**Fig. 3-10** and **Fig. 3-11**).

Extracellular matrix proteins such as collagen I are driving factors of endothelial cells during angiogenesis and mediate disruption of vascular endothelial-cadherin, resulting in a pre-capillary cord formation *in vitro* (Sottile 2004; Davis et al. 2005). Furthermore, other studies have demonstrated that the interaction between endothelial and other cells affects the expression of other angiogenic factors (Heydarkhan-Hagvall et al. 2003). Skeletal muscle sheets may provide VEGF and HGF and extracellular matrix proteins and interact with endothelial cells inside the sheet to promote network formation.

3.5 Summary

In conclusion, this is the first time to demonstrate that angiogenesis was enhanced in skeletal muscle cell sheets by the addition of 10 ng/mL FGF-2, as evident from the extension of endothelial network length through stable endothelial connection (**Fig. 3-12**). From a future perspective, coculture with other cells such as human mesenchymal stem cells (hMSCs) in skeletal muscle cell sheets to produce FGF-2 is required to improve therapeutic efficiency (Leuning et al. 2018).

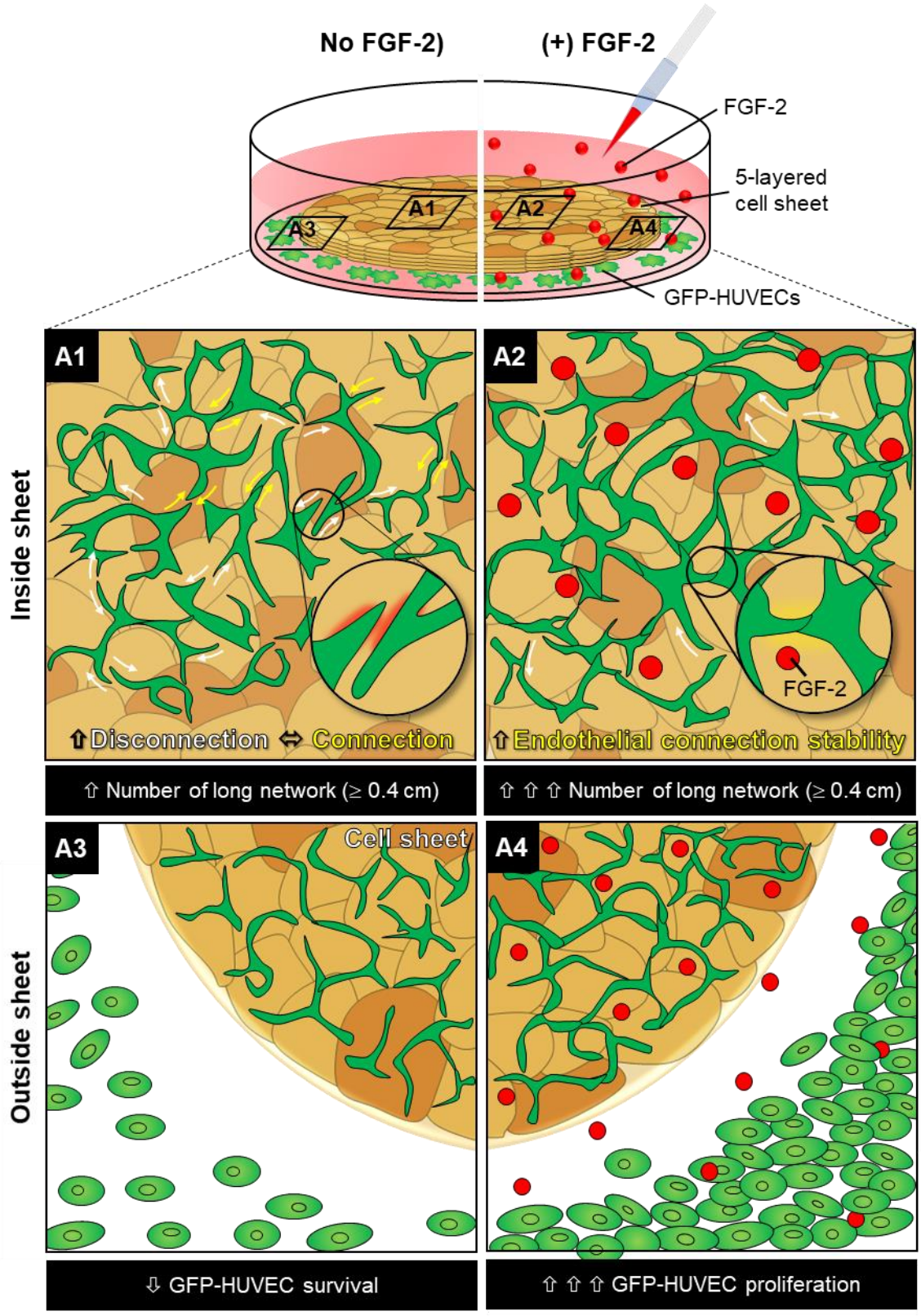

Fig. 3-12 Schematic representation of the effect of FGF-2 on GFP-HUVEC behavior in skeletal muscle cell sheets.

Chapter 4

Conclusion remarks

4.1 Research conclusion

This research provides new insights into the angiogenic potential enhancing of the human skeletal muscle cell sheet. The first study using a co-culture system of HSMMs and HSMFs shows that the different proportions of these cells affected the productivity of angiogenic growth factors, VEGF, and HGF. According to the present evidence, HSMMs and HSMMs can produce VEGF, but only HSMFs in the co-culture system can secrete HGF with high productivity. However, the FGF-2 level was undetectable from the culture media of two cell types, possibly from the FGF-2 synthesis or secretion insufficiency. The HSMF with a small proportion in the co-culture enables the enhancement of the production of VEGF in HSMM (**Fig. 4-1A**), which is potentially mediated through inhibition of active HSMM migration that results in the loss of myoblast-to-myoblast contact and cell alignment (**Fig. 4-1B**). However, the molecular mechanism under this phenomenon has not been elucidated in the current study. Besides, multilayer skeletal muscle cell sheets containing a suitable HSMF proportion (30 to 40%) co-cultured in GFP-HUVECs were shown to drastically enhance endothelial network formation by increasing endothelial network length and connectivity (**Fig. 4-1A**). Therefore, HSMFs and HSMMs co-culture should be controlled at a suitable proportion to maintain the balance of these cytokines and angiogenic potential. These findings highlight the crucial role of HSMF, which is the super stimuli to promote angiogenetic potential in the human skeletal muscle cell sheets.

Next, this research investigated the role of FGF-2 in endothelial network formation in the human skeletal muscle cell sheet lacking endogenous FGF-2. The endothelial network was formed with a high network length and connectivity in five-layered cell sheets comprising HSMMs and HSMFs at the initial culture, despite no FGF-2 in culture media. Therefore, additional FGF-2 might not be essential to initiate endothelial network connection. However, exogenous FGF-2 treatment was shown to stabilize the

endothelial network after prolonged culture, in which the high network length, connectivity, and numbers of the long and medium networks were shown. FGF-2 retarded endothelial network disconnection in the skeletal muscle cell sheet for the precise functions. Moreover, the FGF-2 also promoted attachment and survival of the endothelial cells observed outside the cell sheet (**Fig. 4-1 C**). This study provides knowledge about FGF-2 to increase the stable endothelial network in the human skeletal muscle cell sheet.

To sum up, these findings provide cellular regulators in the human skeletal muscle cell sheet to improve the angiogenic potential for transplantation and establish models of biological research.

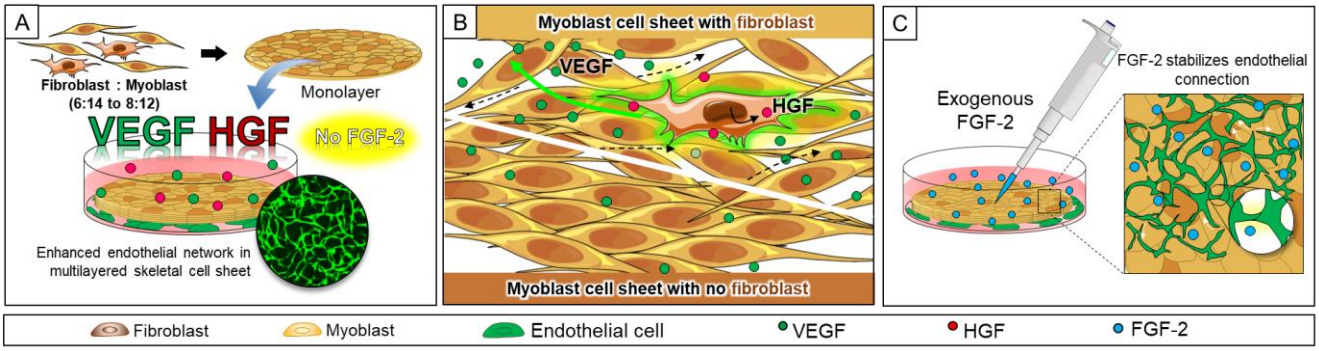

Fig. 4-1 Schematic diagram showing the concepts of angiogenic growth factor production and angiogenesis in skeletal muscle cell sheet. (A) Five-layered human skeletal muscle cell sheet containing 30% or 40% maintained VEGF and HGF production and enhanced endothelial network formation. (B) A small proportion of skeletal muscle fibroblast (HSMF) on cell alignment and VEGF productivity. (C) Exogenous FGF-2 treatment promoted endothelial encounter and connection in five-layered skeletal muscle cell sheet with low endogenous FGF-2 production.

4.2 Future perspectives

Several experiments have been demonstrated in this research to provide new insights into skeletal muscle cell sheet engineering; however, many perspectives are listed for further studies to strengthen this research field (**Fig. 4.2**).

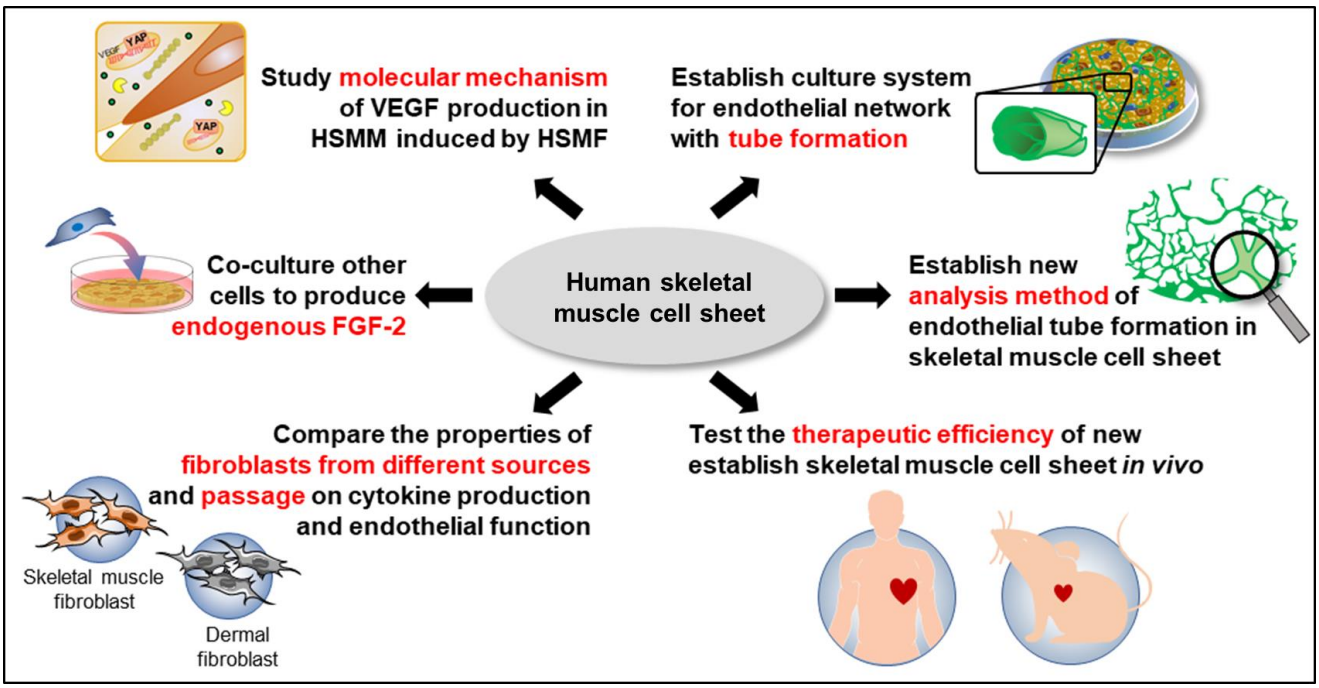

Fig. 4-2 Future perspective to extend this research towards tissue engineering and biological research application.

4.2.1 Molecular mechanism of VEGF section induced by myoblast-to-myoblast contact

From the present study, the effect of HSMF proportion on cytokine productivity showed that VEGF productivity was enhanced in monolayers comprising a small proportion of HSMF but maintained at a low level of monocultures. Furthermore, the time-lapse observation of cell migration in monolayer implied that myoblast-to-myoblast contact disrupted by a small proportion of HSMF might promote VEGF production in HSMM (**Fig. 2-7** to **2-11**). However, the molecular mechanism to explain this phenomenon has not been clarified. In the future, the VEGF expressing related molecules and Myo-to-Myo adhesion proteins should be identified in HSMM monolayers comprising with or without a small

proportion of HSMF to proposed the molecular mechanism under this phenomena. It was hypothesized that the disruption of myoblasts-to-myoblast contact might transduce the intracellular signal to promote VEGF expression and secretion via mechanosensory such as YAP (Robinson et al. 2009; Schlegelmilch et al. 2011; Ahmad et al. 2015) (**Fig. 4-2**). To prove this hypothesis, immunostaining of YAP, cadherin, and β-catenin, the mechanical sensing molecules of cell-to-cell contact, and gene expression profile are expected to demonstrate using skeletal muscle cell monolayers with or without a small proportion of HSMF.

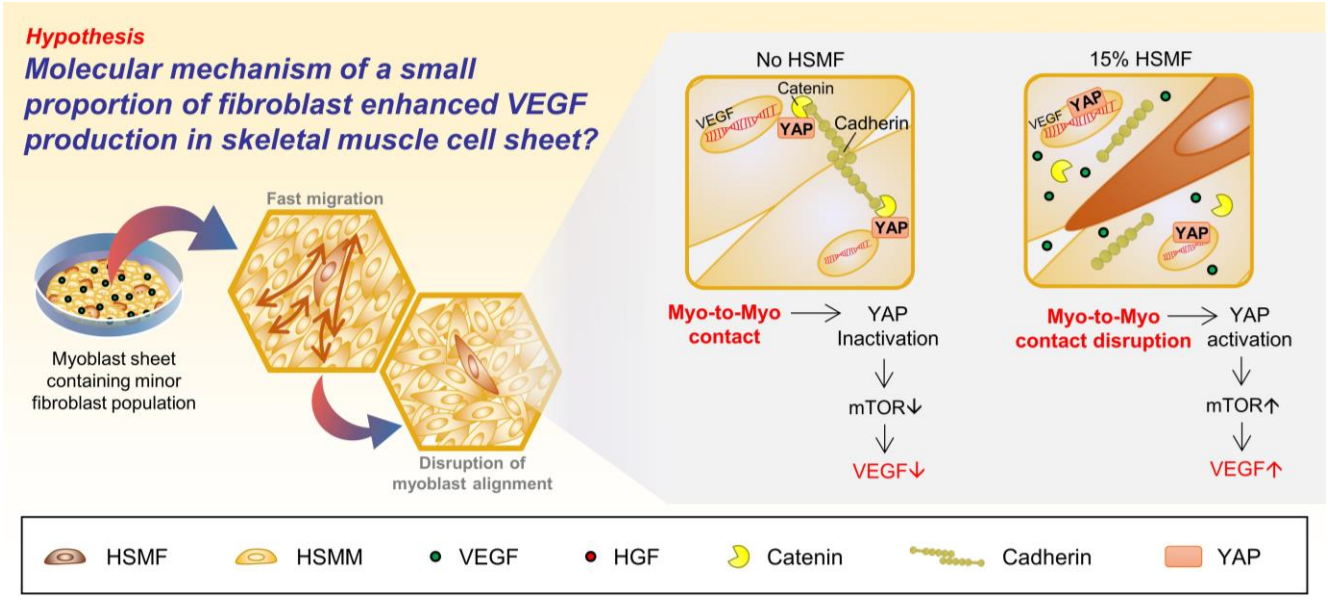

Fig. 4-2 Hypothesis of molecular mechanism to promote VEGF production in human skeletal muscle myoblast (HSMM) induced by human skeletal muscle fibroblast (HSMF)

4.2.2 Effect of human mesenchymal stem cells co-culturing in multilayered skeletal muscle cell sheet in FGF-2 production and endothelial network stability

FGF-2 has a role in maintaining endothelial network formation in skeletal muscle cell sheets. However, the level of FGF-2 in culture media from HSMM and HSMF was undetectable. These cells may be insufficient to synthesize or secrete FGF-2. Therefore, co-culture skeletal muscle cell sheets with other cells such as human mesenchymal stem cells (hMSCs) to produce FGF-2, which could promote

the stabilized endothelial network and transplantation's therapeutic efficiency. Moreover, it would be interesting to establish a pre-vascularized cell sheet with lumen formation in a multilayered skeletal muscle cell sheet and a new quantitative method of lumen formation (**Fig. 4-3**).

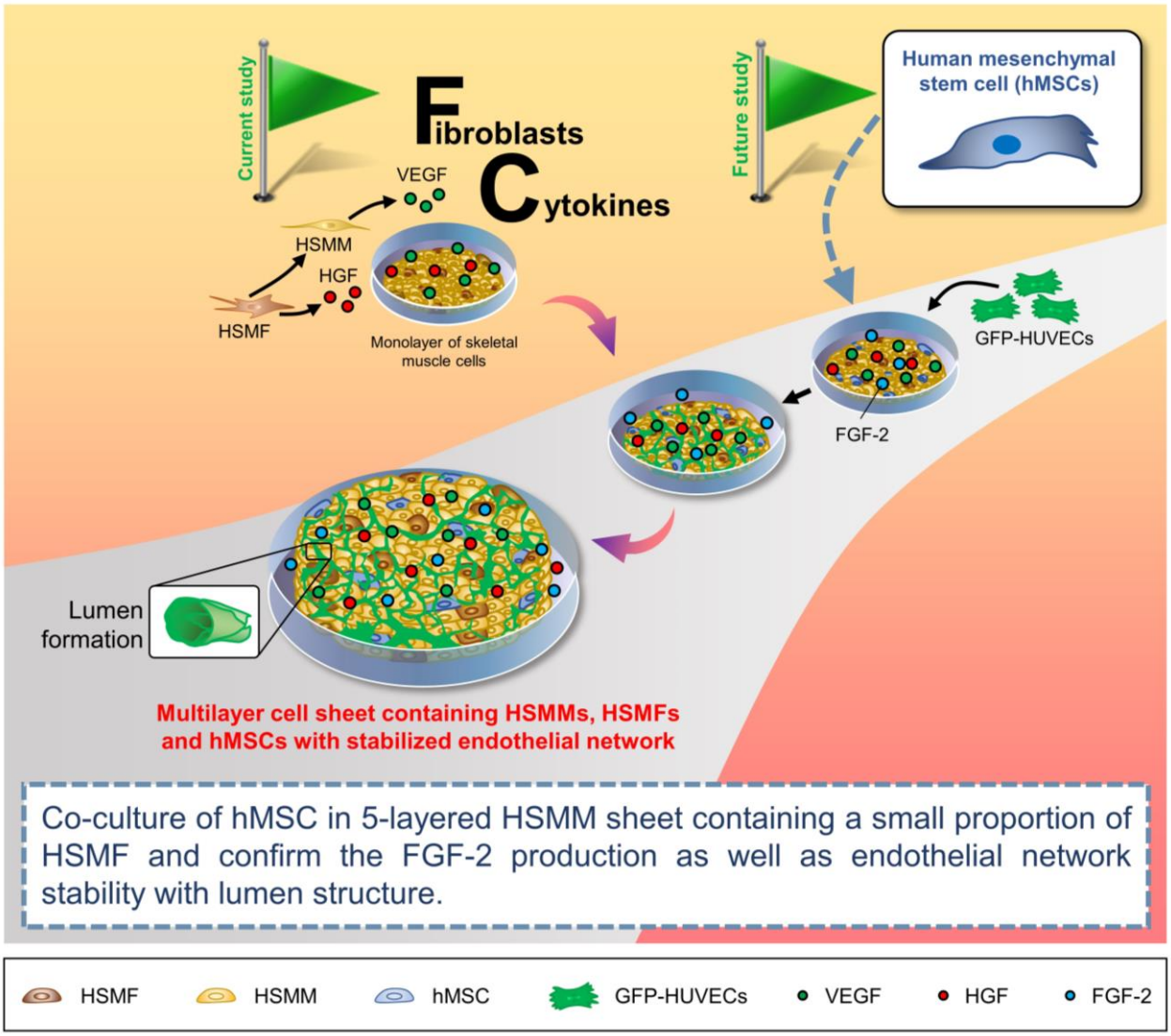

Fig. 4-3 Schematic drawing of a co-culturing system to fabricate multilayered skeletal muscle sheet with stabilized endothelial network and lumen formations

4.2.3 Study on effects of fibroblasts from different sources on cytokine production and endothelial function

Fibroblasts are the most abundant connective tissue cells, with diverse structures depending on their location and activity. Fibroblasts derived from different tissue may provide differences in cell properties such as extracellular matrix production, growth factor secretion, and morphology (Ichim et al. 2018). In this research, the origin of fibroblasts used to study is human skeletal muscle; however, fibroblast from other sources has not been compared. To increase the flexibility of cell sources, the fibroblasts from other sources such as dermal fibroblast are interesting for skeletal muscle myoblast sheet fabrication, and the angiogenic properties should be analyzed. Furthermore, the passage number of cells is an important consideration when designing an experiment in all cell culture laboratories. Especially, the passage is a crucial descriptor for primary cells. For cell sheet engineering using fibroblast, it is interesting to investigate the effect of fibroblasts passage number on angiogenic cytokines and angiogenesis to clarify the passage number range (**Fig. 4.4**).

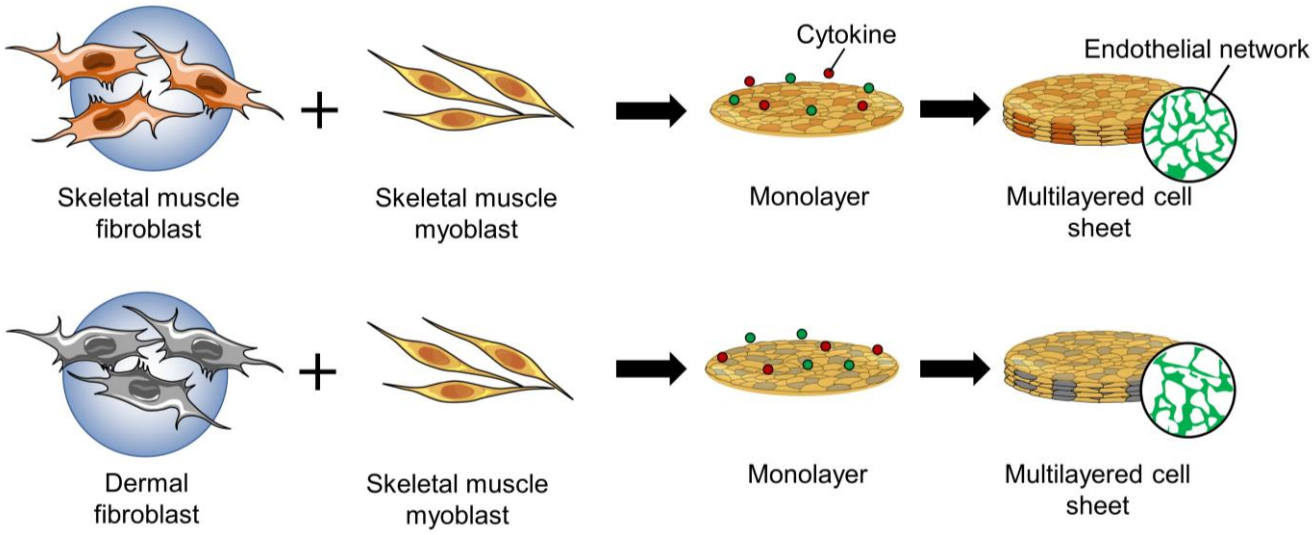

Fig. 4.4 Effect of different sources of fibroblast on angiogenic properties of the skeletal muscle cell sheet

4.2.4 Measuring of angiogenic growth factors and extracellular matrix protein deposition in the multilayered skeletal muscle cell sheet

Angiogenesis is multiple steps that require numerous factors to modulate the angiogenic reaction. However, this study measured only three major cytokines, including VEGF, HGF, and FGF-2. Other angiogenic growth factors and stimuli such as platelet-derived growth factor-1 (PDGF-1) (Sanz-Nogues et al. 2016), stromal cell-derived factor 1 (SDF-1) (Ferrara et al. 2005), angiopoietins (ANGs), and extracellular matrix (ECM) proteins (Davis et al. 2005) have been studied to promote angiogenesis from other research literature. However, these cytokines were not demonstrated in the present study of the human skeletal muscle cell sheet. It is recommended to investigate these stimuli to complete the angiogenic stimuli profile secreted by skeletal muscle cell sheets (**Fig. 4-5**).

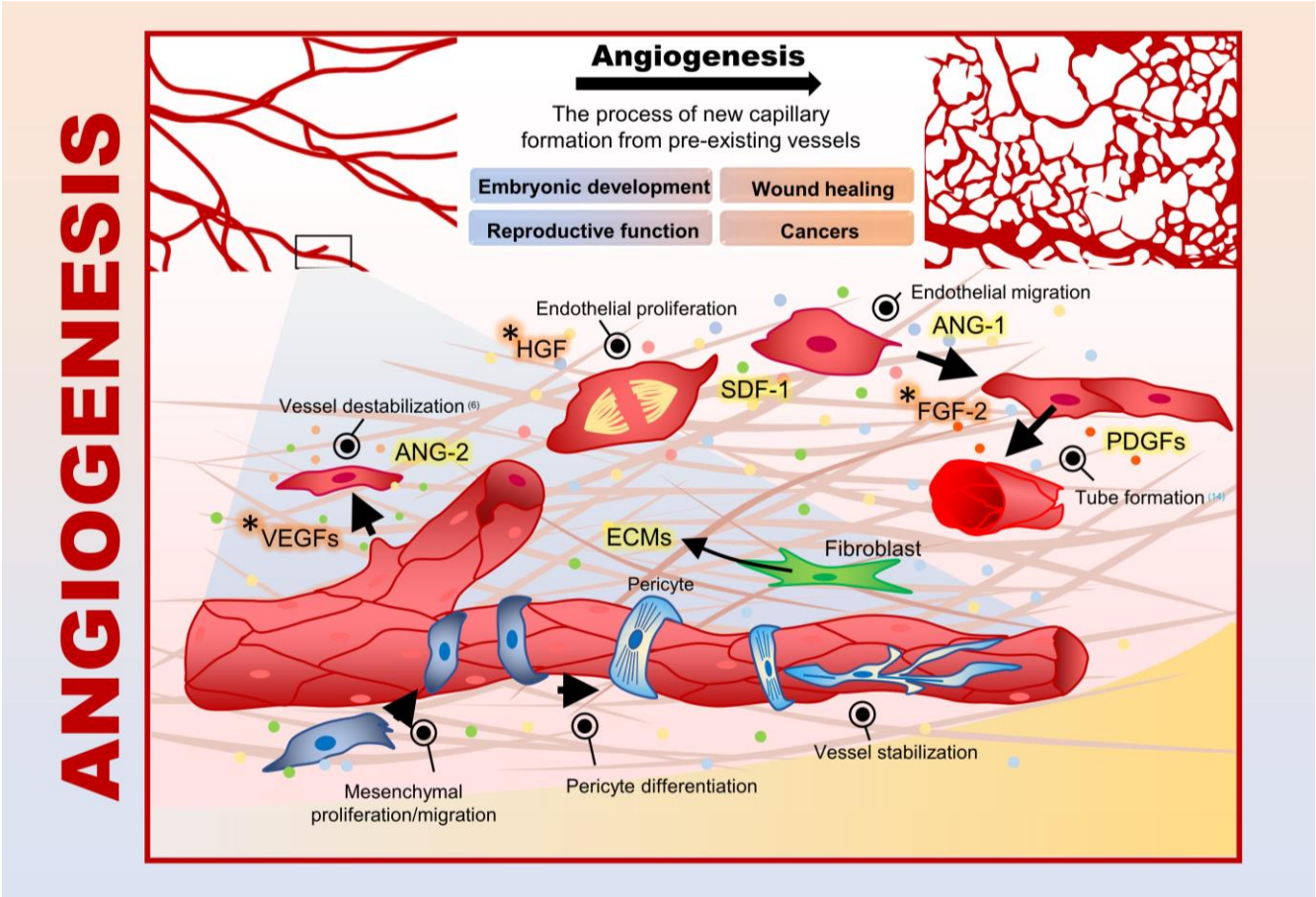

Fig. 4-5 Overview of the angiogenic process and its associated stimuli. (* The growth factors which were elucidated in skeletal muscle cell sheet in this research.)

4.2.5 Testing safety and therapeutic efficiency of skeletal muscle cell sheet *in vivo*

This research provided a new strategy to fabricate skeletal muscle cell sheets by optimizing cell proportion to enhance endothelial network formation. For pharmacological developments, after skeletal muscle cells sheet have been established by new tissue engineering strategies *in vitro*, it is essential to test the viability, safety, and efficacy of engineered tissues in an animal model before clinical application (**Fig. 4-6**).

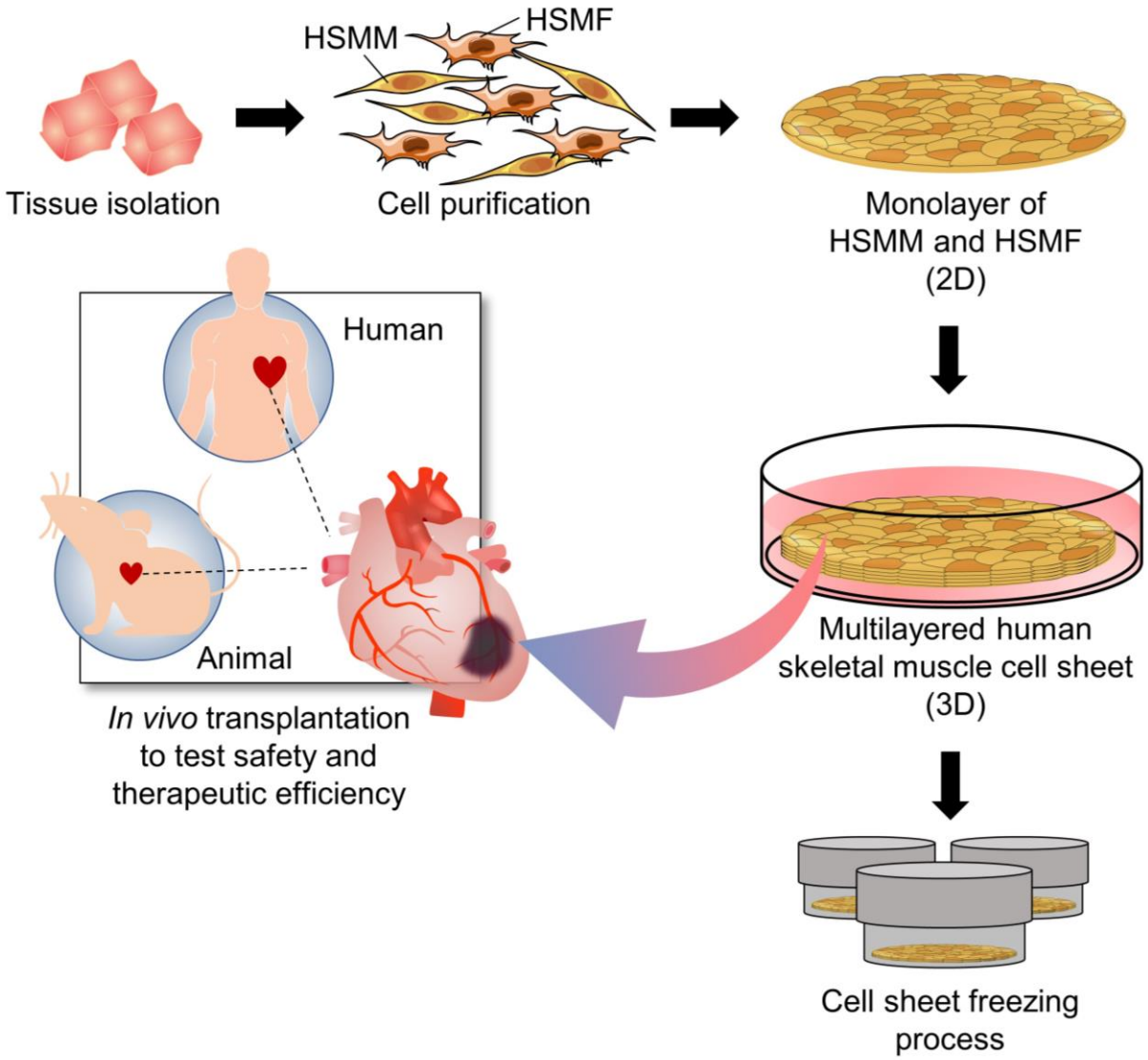

Fig. 4-6 Fabrication of multilayered skeletal muscle cell sheet and testing the safety and therapeutic efficiency by *in vivo*

Nomenclature

(x_i, y_i)	Centroid of cells	[-]
θ	Directional angle	[degree, °]
L/N_T	Extent of endothelial network	[cm/tip]
X_0	Initial density of cell seeding	[cells/cm2]
L	Length of endothelial network	[cm^{-1} or cm/sheet]
D	Migration distance	[μm]
t	Observation time	[h]
σ	Standard deviation	[-]
N_T	Tip number of endothelial network	[tip/cm^2 or tip/sheet]
v	Velocity of cell migration	[μm/h]

Abbreviations

2D	Two-dimensional
3D	Three-dimensional
ANGs	Angiopoietins
bFGF	Basic fibroblast growth factor
BSA	Bovine serum albumin
CAI	Cell alignment index
CD	Cluster of differentiation
cm	Centimeter
CMFDA	Chloromethylfluorescein diacetate
CLSM	Confocal laser scanning microscope
DMEM	Dulbecco’s modified Eagle’s medium
ECM	Extracellular matrix
EGM-2	Endothelial growth medium-2
FGF-2	Fibroblast growth factor
FGFR	Fibroblast growth factor receptor
GFP-HUVEC	Green fluorescence protein human umbilical vein endothelial cell
HSMM	Human skeletal muscle myoblast

HSMF	Human skeletal muscle fibroblast
HGF	Hepatocyte growth factor
μm	Micrometer
mm	Millimeter
ml	Milliliter
NCAM	Neural cell adhesion molecule
ng	Nanogram
PFA	Paraformaldehyde
pg	Picogram
PDGF-1	platelet-derived growth factor-1
SD	Standard deviation
SkGM-2	Skeletal muscle cell growth medium-2
SDF-1	Stromal cell-derived factor 1
VEGF	Vascular growth factor
VEGFR	Vascular endothelial growth factor receptor

References

Book: Institute of Medicine (US) Committee on Social Security Cardiovascular Disability Criteria (2010). Cardiovascular Disability: Updating the Social Security Listings. Washington (DC).

Adams, R. H. and K. Alitalo (2007). Molecular regulation of angiogenesis and lymphangiogenesis. *Nat Rev Mol Cell Biol*. 8; 6, 464-478. doi: 10.1038/nrm2183

Agley, C. C., A. M. Rowlerson, C. P. Velloso, N. R. Lazarus and S. D. Harridge (2013). Human skeletal muscle fibroblasts, but not myogenic cells, readily undergo adipogenic differentiation. *J Cell Sci*. 126; Pt 24, 5610-5625. doi: 10.1242/jcs.132563

Ahmad, S., P. W. Hewett, T. Fujisawa, S. Sissaoui, M. Cai, G. Gueron, et al. (2015). Carbon monoxide inhibits sprouting angiogenesis and vascular endothelial growth factor receptor-2 phosphorylation. *Thromb Haemost*. 113; 2, 329-337. doi: 10.1160/TH14-01-0002

Anderson, C. R., A. M. Ponce and R. J. Price (2004). Immunohistochemical identification of an extracellular matrix scaffold that microguides capillary sprouting in vivo. *J Histochem Cytochem*. 52; 8, 1063-1072. doi: 10.1369/jhc.4A6250.2004

Andree, B., H. Ichanti, S. Kalies, A. Heisterkamp, S. Strauss, P. M. Vogt, et al. (2019). Formation of three-dimensional tubular endothelial cell networks under defined serum-free cell culture conditions in human collagen hydrogels. *Sci Rep*. 9; 1, 5437. doi: 10.1038/s41598-019-41985-6

Atluri, P. and Y. J. Woo (2008). Pro-angiogenic cytokines as cardiovascular therapeutics: assessing the potential. *BioDrugs*. 22; 4, 209-222. doi: 10.2165/00063030-200822040-00001

Bai, Y., Y. Leng, G. Yin, X. Pu, Z. Huang, X. Liao, et al. (2014). Effects of combinations of BMP-2 with FGF-2 and/or VEGF on HUVECs angiogenesis in vitro and CAM angiogenesis in vivo. *Cell Tissue Res*. 356; 1, 109-121. doi: 10.1007/s00441-013-1781-9

Baudin, B., A. Bruneel, N. Bosselut and M. Vaubourdolle (2007). A protocol for isolation and culture of human umbilical vein endothelial cells. *Nat Protoc*. 2; 3, 481-485. doi: 10.1038/nprot.2007.54

Benington, L., G. Rajan, C. Locher and L. Y. Lim (2020). Fibroblast Growth Factor 2-A Review of Stabilisation Approaches for Clinical Applications. *Pharmaceutics*. 12; 6, doi: 10.3390/pharmaceutics12060508

Betz, C., A. Lenard, H. G. Belting and M. Affolter (2016). Cell behaviors and dynamics during angiogenesis. *Development*. 143; 13, 2249-2260. doi: 10.1242/dev.135616

Bhang, S. H., S. W. Cho, J. M. Lim, J. M. Kang, T. J. Lee, H. S. Yang, et al. (2009). Locally delivered growth factor enhances the angiogenic efficacy of adipose-derived stromal cells transplanted to ischemic limbs. *Stem Cells*. 27; 8, 1976-1986. doi: 10.1002/stem.115

Boehler, R. M., J. G. Graham and L. D. Shea (2011). Tissue engineering tools for modulation of the immune response. *Biotechniques*. 51; 4, 239-240, 242, 244 passim. doi: 10.2144/000113754

Cao, J., M. Ehling, S. Marz, J. Seebach, K. Tarbashevich, T. Sixta, et al. (2017). Polarized actin and VE-cadherin dynamics regulate junctional remodelling and cell migration during sprouting angiogenesis. *Nat Commun*. 8; 1, 2210. doi: 10.1038/s41467-017-02373-8

Carmeliet, P. (2005). VEGF as a key mediator of angiogenesis in cancer. *Oncology*. 69 Suppl 3; 4-10. doi: 10.1159/000088478

Casals, G., J. Ros, A. Sionis, M. M. Davidson, M. Morales-Ruiz and W. Jimenez (2009). Hypoxia induces B-type natriuretic peptide release in cell lines derived from human cardiomyocytes. *Am J Physiol Heart Circ Physiol*. 297; 2, H550-555. doi: 10.1152/ajpheart.00250.2009

Chapman, M. A., R. Meza and R. L. Lieber (2016). Skeletal muscle fibroblasts in health and disease. *Differentiation*. 92; 3, 108-115. doi: 10.1016/j.diff.2016.05.007

Chen, S., T. Nakamoto, N. Kawazoe and G. Chen (2015). Engineering multi-layered skeletal muscle tissue by using 3D microgrooved collagen scaffolds. *Biomaterials*. 73; 23-31. doi: 10.1016/j.biomaterials.2015.09.010

Chu, H., N. R. Johnson, N. S. Mason and Y. Wang (2011). A [polycation:heparin] complex releases growth factors with enhanced bioactivity. *J Control Release*. 150; 2, 157-163. doi: 10.1016/j.jconrel.2010.11.025

Cleland, J. G. and J. McGowan (1999). Heart failure due to ischaemic heart disease: epidemiology, pathophysiology and progression. *J Cardiovasc Pharmacol*. 33 Suppl 3; S17-29. doi:

Cook, J. A., K. B. Shah, M. A. Quader, R. H. Cooke, V. Kasirajan, K. K. Rao, et al. (2015). The total artificial heart. *J Thorac Dis*. 7; 12, 2172-2180. doi: 10.3978/j.issn.2072-1439.2015.10.70

Davis, G. E. and D. R. Senger (2005). Endothelial extracellular matrix: biosynthesis, remodeling, and functions during vascular morphogenesis and neovessel stabilization. *Circ Res*. 97; 11, 1093-1107. doi: 10.1161/01.RES.0000191547.64391.e3

De Smet, F., I. Segura, K. De Bock, P. J. Hohensinner and P. Carmeliet (2009). Mechanisms of vessel branching: filopodia on endothelial tip cells lead the way. *Arterioscler Thromb Vasc Biol*. 29; 5, 639-649. doi: 10.1161/ATVBAHA.109.185165

Dejana, E., G. Bazzoni and M. G. Lampugnani (1999). Vascular endothelial (VE)-cadherin: only an intercellular glue? *Exp Cell Res*. 252; 1, 13-19. doi: 10.1006/excr.1999.4601

Detillieux, K. A., F. Sheikh, E. Kardami and P. A. Cattini (2003). Biological activities of fibroblast growth factor-2 in the adult myocardium. *Cardiovasc Res*. 57; 1, 8-19. doi: 10.1016/s0008-6363(02)00708-3

Dib, N., P. McCarthy, A. Campbell, M. Yeager, F. D. Pagani, S. Wright, et al. (2005). Feasibility and safety of autologous myoblast transplantation in patients with ischemic cardiomyopathy. *Cell Transplant*. 14; 1, 11-19. doi: 10.3727/000000005783983296

Dib, N., R. E. Michler, F. D. Pagani, S. Wright, D. J. Kereiakes, R. Lengerich, et al. (2005). Safety and feasibility of autologous myoblast transplantation in patients with ischemic cardiomyopathy: four-year follow-up. *Circulation*. 112; 12, 1748-1755. doi: 10.1161/CIRCULATIONAHA.105.547810

Distler, J. H., A. Hirth, M. Kurowska-Stolarska, R. E. Gay, S. Gay and O. Distler (2003). Angiogenic and angiostatic factors in the molecular control of angiogenesis. *Q J Nucl Med*. 47; 3, 149-161. doi:

Durand, M. J., K. Ait-Aissa and D. D. Gutterman (2017). Regenerative Angiogenesis: Quality Over Quantity. *Circ Res*. 120; 9, 1379-1380. doi: 10.1161/CIRCRESAHA.117.310918

Durrani, S., M. Konoplyannikov, M. Ashraf and K. H. Haider (2010). Skeletal myoblasts for cardiac repair. *Regen Med*. 5; 6, 919-932. doi: 10.2217/rme.10.65

Fafeur, V., B. I. Terman, J. Blum and P. Bohlen (1990). Basic FGF treatment of endothelial cells down-regulates the 85-KDa TGF beta receptor subtype and decreases the growth inhibitory response to TGF-beta 1. *Growth Factors*. 3; 3, 237-245. doi: 10.3109/08977199009043908

Fallah, A., A. Sadeghinia, H. Kahroba, A. Samadi, H. R. Heidari, B. Bradaran, et al. (2019). Therapeutic targeting of angiogenesis molecular pathways in angiogenesis-dependent diseases. *Biomed Pharmacother*. 110; 775-785. doi: 10.1016/j.biopha.2018.12.022

Farjood, F. and E. Vargis (2017). Physical disruption of cell-cell contact induces VEGF expression in RPE cells. *Mol Vis*. 23; 431-446. doi:

Felmeden, D. C., A. D. Blann and G. Y. Lip (2003). Angiogenesis: basic pathophysiology and implications for disease. *Eur Heart J*. 24; 7, 586-603. doi: 10.1016/s0195-668x(02)00635-8

Ferrara, N. and R. S. Kerbel (2005). Angiogenesis as a therapeutic target. *Nature*. 438; 7070, 967-974. doi: 10.1038/nature04483

Freyman, T., G. Polin, H. Osman, J. Crary, M. Lu, L. Cheng, et al. (2006). A quantitative, randomized study evaluating three methods of mesenchymal stem cell delivery following myocardial infarction. *Eur Heart J*. 27; 9, 1114-1122. doi: 10.1093/eurheartj/ehi818

Garmy-Susini, B., E. Delmas, P. Gourdy, M. Zhou, C. Bossard, B. Bugler, et al. (2004). Role of fibroblast growth factor-2 isoforms in the effect of estradiol on endothelial cell migration and proliferation. *Circ Res*. 94; 10, 1301-1309. doi: 10.1161/01.RES.0000127719.13255.81

Gavira, J. J., J. Herreros, A. Perez, M. J. Garcia-Velloso, J. Barba, F. Martin-Herrero, et al. (2006). Autologous skeletal myoblast transplantation in patients with nonacute myocardial infarction: 1-year follow-up. *J Thorac Cardiovasc Surg*. 131; 4, 799-804. doi: 10.1016/j.jtcvs.2005.11.030

Gianni-Barrera, R., N. Di Maggio, L. Melly, M. G. Burger, E. Mujagic, L. Gurke, et al. (2020). Therapeutic vascularization in regenerative medicine. *Stem Cells Transl Med*. 9; 4, 433-444. doi: 10.1002/sctm.19-0319

Guo, R., M. Morimatsu, T. Feng, F. Lan, D. Chang, F. Wan, et al. (2020). Stem cell-derived cell sheet transplantation for heart tissue repair in myocardial infarction. *Stem Cell Res Ther*. 11; 1, 19. doi: 10.1186/s13287-019-1536-y

Haider, H., L. Ye, S. Jiang, R. Ge, P. K. Law, T. Chua, et al. (2004). Angiomyogenesis for cardiac repair using human myoblasts as carriers of human vascular endothelial growth factor. *J Mol Med (Berl)*. 82; 8, 539-549. doi: 10.1007/s00109-004-0546-z

Hasegawa, M., M. Yamato, A. Kikuchi, T. Okano and I. Ishikawa (2005). Human periodontal ligament cell sheets can regenerate periodontal ligament tissue in an athymic rat model. *Tissue Eng*. 11; 3-4, 469-478. doi: 10.1089/ten.2005.11.469

Hata, H., G. Matsumiya, S. Miyagawa, H. Kondoh, N. Kawaguchi, N. Matsuura, et al. (2006). Grafted skeletal myoblast sheets attenuate myocardial remodeling in pacing-induced canine heart failure model. *J Thorac Cardiovasc Surg*. 132; 4, 918-924. doi: 10.1016/j.jtcvs.2006.01.024

Heydarkhan-Hagvall, S., G. Helenius, B. R. Johansson, J. Y. Li, E. Mattsson and B. Risberg (2003). Co-culture of endothelial cells and smooth muscle cells affects gene expression of angiogenic factors. *J Cell Biochem*. 89; 6, 1250-1259. doi: 10.1002/jcb.10583

Huang, A., X. Qi, Y. Cui, Y. Wu, S. Zhou and M. Zhang (2020). Serum VEGF: Diagnostic Value of Acute Coronary Syndrome from Stable Angina Pectoris and Prognostic Value of Coronary Artery Disease. *Cardiol Res Pract*. 2020; 6786302. doi: 10.1155/2020/6786302

Iansante, V., R. R. Mitry, C. Filippi, E. Fitzpatrick and A. Dhawan (2018). Human hepatocyte transplantation for liver disease: current status and future perspectives. *Pediatr Res*. 83; 1-2, 232-240. doi: 10.1038/pr.2017.284

Ichim, T. E., P. O'Heeron and S. Kesari (2018). Fibroblasts as a practical alternative to mesenchymal stem cells. *J Transl Med*. 16; 1, 212. doi: 10.1186/s12967-018-1536-1

Imoukhuede, P. I. and A. S. Popel (2012). Expression of VEGF receptors on endothelial cells in mouse skeletal muscle. *PLoS One*. 7; 9, e44791. doi: 10.1371/journal.pone.0044791

Javerzat, S., P. Auguste and A. Bikfalvi (2002). The role of fibroblast growth factors in vascular development. *Trends Mol Med*. 8; 10, 483-489. doi: 10.1016/s1471-4914(02)02394-8

Jin, H., R. Yang, W. Li, A. K. Ogasawara, R. Schwall, D. A. Eberhard, et al. (2003). Early treatment with hepatocyte growth factor improves cardiac function in experimental heart failure induced by myocardial infarction. *J Pharmacol Exp Ther*. 304; 2, 654-660. doi: 10.1124/jpet.102.041772

Kalladka, D., J. Sinden, K. Pollock, C. Haig, J. McLean, W. Smith, et al. (2016). Human neural stem cells in patients with chronic ischaemic stroke (PISCES): a phase 1, first-in-man study. *Lancet*. 388; 10046, 787-796. doi: 10.1016/S0140-6736(16)30513-X

Kanda, S., Y. Miyata and H. Kanetake (2004). Fibroblast growth factor-2-mediated capillary morphogenesis of endothelial cells requires signals via Flt-1/vascular endothelial growth factor receptor-1: possible involvement of c-Akt. *J Biol Chem*. 279; 6, 4007-4016. doi: 10.1074/jbc.M307569200

Kano, M. R., Y. Morishita, C. Iwata, S. Iwasaka, T. Watabe, Y. Ouchi, et al. (2005). VEGF-A and FGF-2 synergistically promote neoangiogenesis through enhancement of endogenous PDGF-B-PDGFRbeta signaling. *J Cell Sci*. 118; Pt 16, 3759-3768. doi: 10.1242/jcs.02483

Kendall, R. T. and C. A. Feghali-Bostwick (2014). Fibroblasts in fibrosis: novel roles and mediators. *Front Pharmacol*. 5; 123. doi: 10.3389/fphar.2014.00123

Kenji K., S. F. a. I. A. (1990). Solution properties of poly(N-isopropylacrylamide) in water. *Polymer Journal*. 22; 15-20. doi:

Kim, C. K., K. H. Haider and S. J. Lim (2001). Gene medicine : a new field of molecular medicine. *Arch Pharm Res*. 24; 1, 1-15. doi:

Koehl, U., S. Zimmermann, R. Esser, J. Sorensen, H. P. Gruttner, M. Duchscherer, et al. (2002). Autologous transplantation of CD133 selected hematopoietic progenitor cells in a pediatric patient with relapsed leukemia. *Bone Marrow Transplant*. 29; 11, 927-930. doi: 10.1038/sj.bmt.1703558

Kubota, T., A. Namiki, M. Fukazawa, M. Ishikawa, M. Moroi, K. Ebine, et al. (2004). Concentrations of hepatocyte growth factor, basic fibroblast growth factor, and vascular endothelial growth factor in pericardial fluid and plasma. *Jpn Heart J*. 45; 6, 989-998. doi: 10.1536/jhj.45.989

Kwon, Y. W., H. M. Yang and H. J. Cho (2010). Cell therapy for myocardial infarction. *Int J Stem Cells*. 3; 1, 8-15. doi:

Laddha, A. P. and Y. A. Kulkarni (2019). VEGF and FGF-2: Promising targets for the treatment of respiratory disorders. *Respir Med*. 156; 33-46. doi: 10.1016/j.rmed.2019.08.003

Lampugnani, M. G. (2012). Endothelial cell-to-cell junctions: adhesion and signaling in physiology and pathology. *Cold Spring Harb Perspect Med*. 2; 10, doi: 10.1101/cshperspect.a006528

Langer, R. and J. P. Vacanti (1993). Tissue engineering. *Science*. 260; 5110, 920-926. doi: 10.1126/science.8493529

Laschke, M. W., M. Rucker, G. Jensen, C. Carvalho, R. Mulhaupt, N. C. Gellrich, et al. (2008). Incorporation of growth factor containing Matrigel promotes vascularization of porous PLGA scaffolds. *J Biomed Mater Res A*. 85; 2, 397-407. doi: 10.1002/jbm.a.31503

Laschke, M. W., B. Vollmar and M. D. Menger (2009). Inosculation: connecting the life-sustaining pipelines. *Tissue Eng Part B Rev*. 15; 4, 455-465. doi: 10.1089/ten.TEB.2009.0252

Lee, J., D. Shin and J. L. Roh (2018). Development of an in vitro cell-sheet cancer model for chemotherapeutic screening. *Theranostics*. 8; 14, 3964-3973. doi: 10.7150/thno.26439

Lei, J., S. Peng, S. B. Samuel, S. Zhang, Y. Wu, P. Wang, et al. (2016). A simple and biosafe method for isolation of human umbilical vein endothelial cells. *Anal Biochem*. 508; 15-18. doi: 10.1016/j.ab.2016.06.018

Leuning, D. G., N. R. M. Beijer, N. A. du Fosse, S. Vermeulen, E. Lievers, C. van Kooten, et al. (2018). The cytokine secretion profile of mesenchymal stromal cells is determined by surface structure of the microenvironment. *Sci Rep*. 8; 1, 7716. doi: 10.1038/s41598-018-25700-5

Li, M. and M. Kino-Oka (2017). Degradation of endothelial network in disordered tumor-containing cell sheet. *J Biosci Bioeng*. 123; 6, 748-753. doi: 10.1016/j.jbiosc.2017.01.017

Liu, J., P. Wu, Y. Wang, Y. Du, N. A, S. Liu, et al. (2016). Ad-HGF improves the cardiac remodeling of rat following myocardial infarction by upregulating autophagy and necroptosis and inhibiting apoptosis. *Am J Transl Res*. 8; 11, 4605-4627. doi:

Liu, Y., S. Sakai and M. Taya (2016). Engineering tissues with a perfusable vessel-like network using endothelialized alginate hydrogel fiber and spheroid-enclosing microcapsules. *Heliyon*. 2; 2, e00067. doi: 10.1016/j.heliyon.2016.e00067

Madonna, R., C. Cadeddu, M. Deidda, Z. Giricz, C. Madeddu, D. Mele, et al. (2015). Cardioprotection by gene therapy: A review paper on behalf of the Working Group on Drug Cardiotoxicity and Cardioprotection of the Italian Society of Cardiology. *Int J Cardiol*. 191; 203-210. doi: 10.1016/j.ijcard.2015.04.232

Makarevich, P. I., K. V. Dergilev, Z. I. Tsokolaeva, M. A. Boldyreva, E. K. Shevchenko, E. V. Gluhanyuk, et al. (2018). Angiogenic and pleiotropic effects of VEGF165 and HGF combined gene therapy in a rat model of myocardial infarction. *PLoS One*. 13; 5, e0197566. doi: 10.1371/journal.pone.0197566

Mann, C. J., E. Perdiguero, Y. Kharraz, S. Aguilar, P. Pessina, A. L. Serrano, et al. (2011). Aberrant repair and fibrosis development in skeletal muscle. *Skelet Muscle*. 1; 1, 21. doi: 10.1186/2044-5040-1-21

Masaki, I., Y. Yonemitsu, A. Yamashita, S. Sata, M. Tanii, K. Komori, et al. (2002). Angiogenic gene therapy for experimental critical limb ischemia: acceleration of limb loss by overexpression of vascular endothelial growth factor 165 but not of fibroblast growth factor-2. *Circ Res*. 90; 9, 966-973. doi: 10.1161/01.res.0000019540.41697.60

Mastrullo, V., W. Cathery, E. Velliou, P. Madeddu and P. Campagnolo (2020). Angiogenesis in Tissue Engineering: As Nature Intended? *Front Bioeng Biotechnol*. 8; 188. doi: 10.3389/fbioe.2020.00188

Matkar, P. N., R. Ariyagunarajah, H. Leong-Poi and K. K. Singh (2017). Friends Turned Foes: Angiogenic Growth Factors beyond Angiogenesis. *Biomolecules*. 7; 4, doi: 10.3390/biom7040074

Matsumine, H., G. Giatsidis, A. Osada, W. Kamei, H. Fujimaki, Y. Tsukamoto, et al. (2019). Keratinocyte sheets prepared with temperature-responsive dishes show enhanced survival after

in vivo grafting on acellular dermal matrices in a rat model of staged bi-layered skin reconstruction. *Regen Ther*. 11; 167-175. doi: 10.1016/j.reth.2019.07.003

Matsuura, K., Y. Haraguchi, T. Shimizu and T. Okano (2013). Cell sheet transplantation for heart tissue repair. *J Control Release*. 169; 3, 336-340. doi: 10.1016/j.jconrel.2013.03.003

Memon, I. A., Y. Sawa, N. Fukushima, G. Matsumiya, S. Miyagawa, S. Taketani, et al. (2005). Repair of impaired myocardium by means of implantation of engineered autologous myoblast sheets. *J Thorac Cardiovasc Surg*. 130; 5, 1333-1341. doi: 10.1016/j.jtcvs.2005.07.023

Menasche, P. (2007). Skeletal myoblasts as a therapeutic agent. *Prog Cardiovasc Dis*. 50; 1, 7-17. doi: 10.1016/j.pcad.2007.02.002

Menasche, P., A. A. Hagege, M. Scorsin, B. Pouzet, M. Desnos, D. Duboc, et al. (2001). Myoblast transplantation for heart failure. *Lancet*. 357; 9252, 279-280. doi: 10.1016/S0140-6736(00)03617-5

Menasche, P., A. A. Hagege, J. T. Vilquin, M. Desnos, E. Abergel, B. Pouzet, et al. (2003). Autologous skeletal myoblast transplantation for severe postinfarction left ventricular dysfunction. *J Am Coll Cardiol*. 41; 7, 1078-1083. doi: 10.1016/s0735-1097(03)00092-5

Miyagawa, S., K. Domae, Y. Yoshikawa, S. Fukushima, T. Nakamura, A. Saito, et al. (2017). Phase I Clinical Trial of Autologous Stem Cell-Sheet Transplantation Therapy for Treating Cardiomyopathy. *J Am Heart Assoc*. 6; 4, doi: 10.1161/JAHA.116.003918

Mongiat, M., E. Andreuzzi, G. Tarticchio and A. Paulitti (2016). Extracellular Matrix, a Hard Player in Angiogenesis. *Int J Mol Sci*. 17; 11, doi: 10.3390/ijms17111822

Montesano, R., J. D. Vassalli, A. Baird, R. Guillemin and L. Orci (1986). Basic fibroblast growth factor induces angiogenesis in vitro. *Proc Natl Acad Sci U S A*. 83; 19, 7297-7301. doi: 10.1073/pnas.83.19.7297

Morimoto, A., K. Okamura, R. Hamanaka, Y. Sato, N. Shima, K. Higashio, et al. (1991). Hepatocyte growth factor modulates migration and proliferation of human microvascular endothelial cells in culture. *Biochem Biophys Res Commun*. 179; 2, 1042-1049. doi: 10.1016/0006-291x(91)91924-2

Murakami, M., L. T. Nguyen, K. Hatanaka, W. Schachterle, P. Y. Chen, Z. W. Zhuang, et al. (2011). FGF-dependent regulation of VEGF receptor 2 expression in mice. *J Clin Invest*. 121; 7, 2668-2678. doi: 10.1172/JCI44762

Murakami, M. and M. Simons (2008). Fibroblast growth factor regulation of neovascularization. *Curr Opin Hematol*. 15; 3, 215-220. doi: 10.1097/MOH.0b013e3282f97d98

Murtuza, B., K. Suzuki, G. Bou-Gharios, J. R. Beauchamp, R. T. Smolenski, T. A. Partridge, et al. (2004). Transplantation of skeletal myoblasts secreting an IL-1 inhibitor modulates adverse remodeling in infarcted murine myocardium. *Proc Natl Acad Sci U S A*. 101; 12, 4216-4221. doi: 10.1073/pnas.0306205101

Nagamori, E., T. X. Ngo, Y. Takezawa, A. Saito, Y. Sawa, T. Shimizu, et al. (2013). Network formation through active migration of human vascular endothelial cells in a multilayered skeletal myoblast sheet. *Biomaterials*. 34; 3, 662-668. doi: 10.1016/j.biomaterials.2012.08.055

Nagase, K., M. Yamato, H. Kanazawa and T. Okano (2018). Poly(N-isopropylacrylamide)-based thermoresponsive surfaces provide new types of biomedical applications. *Biomaterials*. 153; 27-48. doi: 10.1016/j.biomaterials.2017.10.026

Nakamura, T., S. Mizuno, K. Matsumoto, Y. Sawa, H. Matsuda and T. Nakamura (2000). Myocardial protection from ischemia/reperfusion injury by endogenous and exogenous HGF. *J Clin Invest*. 106; 12, 1511-1519. doi: 10.1172/JCI10226

Newman, A. C., M. N. Nakatsu, W. Chou, P. D. Gershon and C. C. Hughes (2011). The requirement for fibroblasts in angiogenesis: fibroblast-derived matrix proteins are essential for endothelial cell lumen formation. *Mol Biol Cell*. 22; 20, 3791-3800. doi: 10.1091/mbc.E11-05-0393

Ngo, T. X., E. Nagamori, T. Kikuchi, T. Shimizu, T. Okano, M. Taya, et al. (2013). Endothelial cell behavior inside myoblast sheets with different thickness. *Biotechnol Lett*. 35; 7, 1001-1008. doi: 10.1007/s10529-013-1174-x

Nishida, K., M. Yamato, Y. Hayashida, K. Watanabe, K. Yamamoto, E. Adachi, et al. (2004). Corneal reconstruction with tissue-engineered cell sheets composed of autologous oral mucosal epithelium. *N Engl J Med*. 351; 12, 1187-1196. doi: 10.1056/NEJMoa040455

Olanow, C. W., C. G. Goetz, J. H. Kordower, A. J. Stoessl, V. Sossi, M. F. Brin, et al. (2003). A double-blind controlled trial of bilateral fetal nigral transplantation in Parkinson's disease. *Ann Neurol*. 54; 3, 403-414. doi: 10.1002/ana.10720

Olsson, A. K., A. Dimberg, J. Kreuger and L. Claesson-Welsh (2006). VEGF receptor signalling - in control of vascular function. *Nat Rev Mol Cell Biol*. 7; 5, 359-371. doi: 10.1038/nrm1911

Onimaru, M., Y. Yonemitsu, M. Tanii, K. Nakagawa, I. Masaki, S. Okano, et al. (2002). Fibroblast growth factor-2 gene transfer can stimulate hepatocyte growth factor expression irrespective of hypoxia-mediated downregulation in ischemic limbs. *Circ Res*. 91; 10, 923-930. doi: 10.1161/01.res.0000043281.66969.32

Orlic, D., J. Kajstura, S. Chimenti, I. Jakoniuk, S. M. Anderson, B. Li, et al. (2001). Bone marrow cells regenerate infarcted myocardium. *Nature*. 410; 6829, 701-705. doi: 10.1038/35070587

Pagani, F. D., H. DerSimonian, A. Zawadzka, K. Wetzel, A. S. Edge, D. B. Jacoby, et al. (2003). Autologous skeletal myoblasts transplanted to ischemia-damaged myocardium in humans. Histological analysis of cell survival and differentiation. *J Am Coll Cardiol*. 41; 5, 879-888. doi: 10.1016/s0735-1097(03)00081-0

Papetti, M. and I. M. Herman (2002). Mechanisms of normal and tumor-derived angiogenesis. *Am J Physiol Cell Physiol*. 282; 5, C947-970. doi: 10.1152/ajpcell.00389.2001

Piard, C., A. Jeyaram, Y. Liu, J. Caccamese, S. M. Jay, Y. Chen, et al. (2019). 3D printed HUVECs/MSCs cocultures impact cellular interactions and angiogenesis depending on cell-cell distance. *Biomaterials*. 222; 119423. doi: 10.1016/j.biomaterials.2019.119423

Potente, M. and T. Makinen (2017). Vascular heterogeneity and specialization in development and disease. *Nat Rev Mol Cell Biol*. 18; 8, 477-494. doi: 10.1038/nrm.2017.36

Pouzet, B., S. Ghostine, J. T. Vilquin, I. Garcin, M. Scorsin, A. A. Hagege, et al. (2001). Is skeletal myoblast transplantation clinically relevant in the era of angiotensin-converting enzyme inhibitors? *Circulation*. 104; 12 Suppl 1, I223-228. doi:

Presta, M., P. Dell'Era, S. Mitola, E. Moroni, R. Ronca and M. Rusnati (2005). Fibroblast growth factor/fibroblast growth factor receptor system in angiogenesis. *Cytokine Growth Factor Rev*. 16; 2, 159-178. doi: 10.1016/j.cytogfr.2005.01.004

Richardson, T. P., W. L. Murphy and D. J. Mooney (2001). Polymeric delivery of proteins and plasmid DNA for tissue engineering and gene therapy. *Crit Rev Eukaryot Gene Expr*. 11; 1-3, 47-58. doi:

Rinsch, C., P. Quinodoz, B. Pittet, N. Alizadeh, D. Baetens, D. Montandon, et al. (2001). Delivery of FGF-2 but not VEGF by encapsulated genetically engineered myoblasts improves survival and vascularization in a model of acute skin flap ischemia. *Gene Ther*. 8; 7, 523-533. doi: 10.1038/sj.gt.3301436

Robinson, S. D., L. E. Reynolds, V. Kostourou, A. R. Reynolds, R. G. da Silva, B. Tavora, et al. (2009). Alphav beta3 integrin limits the contribution of neuropilin-1 to vascular endothelial growth factor-induced angiogenesis. *J Biol Chem*. 284; 49, 33966-33981. doi: 10.1074/jbc.M109.030700

Romo, P., M. C. Madigan, J. M. Provis and K. M. Cullen (2011). Differential effects of TGF-beta and FGF-2 on in vitro proliferation and migration of primate retinal endothelial and Muller cells. *Acta Ophthalmol*. 89; 3, e263-268. doi: 10.1111/j.1755-3768.2010.01968.x

Rosen, E. M., K. Lamszus, J. Laterra, P. J. Polverini, J. S. Rubin and I. D. Goldberg (1997). HGF/SF in angiogenesis. *Ciba Found Symp*. 212; 215-226; discussion 227-219. doi: 10.1002/9780470515457.ch14

Rucker, M., M. W. Laschke, D. Junker, C. Carvalho, A. Schramm, R. Mulhaupt, et al. (2006). Angiogenic and inflammatory response to biodegradable scaffolds in dorsal skinfold chambers of mice. *Biomaterials*. 27; 29, 5027-5038. doi: 10.1016/j.biomaterials.2006.05.033

Sahni, A. and C. W. Francis (2004). Stimulation of endothelial cell proliferation by FGF-2 in the presence of fibrinogen requires alphavbeta3. *Blood*. 104; 12, 3635-3641. doi: 10.1182/blood-2004-04-1358

Saif, J., T. M. Schwarz, D. Y. Chau, J. Henstock, P. Sami, S. F. Leicht, et al. (2010). Combination of injectable multiple growth factor-releasing scaffolds and cell therapy as an advanced modality to

enhance tissue neovascularization. *Arterioscler Thromb Vasc Biol*. 30; 10, 1897-1904. doi: 10.1161/ATVBAHA.110.207928

Santos, M. I. and R. L. Reis (2010). Vascularization in bone tissue engineering: physiology, current strategies, major hurdles and future challenges. *Macromol Biosci*. 10; 1, 12-27. doi: 10.1002/mabi.200900107

Sanz-Nogues, C. and T. O'Brien (2016). In vitro models for assessing therapeutic angiogenesis. *Drug Discov Today*. 21; 9, 1495-1503. doi: 10.1016/j.drudis.2016.05.016

Sauteur, L., A. Krudewig, L. Herwig, N. Ehrenfeuchter, A. Lenard, M. Affolter, et al. (2014). Cdh5/VE-cadherin promotes endothelial cell interface elongation via cortical actin polymerization during angiogenic sprouting. *Cell Rep*. 9; 2, 504-513. doi: 10.1016/j.celrep.2014.09.024

Sawa, Y. and S. Miyagawa (2013). Present and future perspectives on cell sheet-based myocardial regeneration therapy. *Biomed Res Int*. 2013; 583912. doi: 10.1155/2013/583912

Sawa, Y., Y. Yoshikawa, K. Toda, S. Fukushima, K. Yamazaki, M. Ono, et al. (2015). Safety and Efficacy of Autologous Skeletal Myoblast Sheets (TCD-51073) for the Treatment of Severe Chronic Heart Failure Due to Ischemic Heart Disease. *Circ J*. 79; 5, 991-999. doi: 10.1253/circj.CJ-15-0243

Schlegelmilch, K., M. Mohseni, O. Kirak, J. Pruszak, J. R. Rodriguez, D. Zhou, et al. (2011). Yap1 acts downstream of alpha-catenin to control epidermal proliferation. *Cell*. 144; 5, 782-795. doi: 10.1016/j.cell.2011.02.031

Schumann, P., F. Tavassol, D. Lindhorst, C. Stuehmer, K. H. Bormann, A. Kampmann, et al. (2009). Consequences of seeded cell type on vascularization of tissue engineering constructs in vivo. *Microvasc Res*. 78; 2, 180-190. doi: 10.1016/j.mvr.2009.06.003

Sekiya, N., G. Matsumiya, S. Miyagawa, A. Saito, T. Shimizu, T. Okano, et al. (2009). Layered implantation of myoblast sheets attenuates adverse cardiac remodeling of the infarcted heart. *J Thorac Cardiovasc Surg*. 138; 4, 985-993. doi: 10.1016/j.jtcvs.2009.02.004

Seko, Y., S. Fukuda and R. Nagai (2004). Serum levels of endostatin, vascular endothelial growth factor (VEGF) and hepatocyte growth factor (HGF) in patients with acute myocardial infarction

undergoing early reperfusion therapy. *Clin Sci (Lond)*. 106; 5, 439-442. doi: 10.1042/CS20030365

Severino, P., A. D'Amato, M. Pucci, F. Infusino, F. Adamo, L. I. Birtolo, et al. (2020). Ischemic Heart Disease Pathophysiology Paradigms Overview: From Plaque Activation to Microvascular Dysfunction. *Int J Mol Sci*. 21; 21, doi: 10.3390/ijms21218118

She, Z., C. Wang, J. Li, G. B. Sukhorukov and M. N. Antipina (2012). Encapsulation of basic fibroblast growth factor by polyelectrolyte multilayer microcapsules and its controlled release for enhancing cell proliferation. *Biomacromolecules*. 13; 7, 2174-2180. doi: 10.1021/bm3005879

Shibuya, M. (2011). Vascular Endothelial Growth Factor (VEGF) and Its Receptor (VEGFR) Signaling in Angiogenesis: A Crucial Target for Anti- and Pro-Angiogenic Therapies. *Genes Cancer*. 2; 12, 1097-1105. doi: 10.1177/1947601911423031

Shirasaka, T., S. Miyagawa, S. Fukushima, A. Saito, M. Shiozaki, N. Kawaguchi, et al. (2013). A slow-releasing form of prostacyclin agonist (ONO1301SR) enhances endogenous secretion of multiple cardiotherapeutic cytokines and improves cardiac function in a rapid-pacing-induced model of canine heart failure. *J Thorac Cardiovasc Surg*. 146; 2, 413-421. doi: 10.1016/j.jtcvs.2012.10.003

Siminiak, T., R. Kalawski, D. Fiszer, O. Jerzykowska, J. Rzezniczak, N. Rozwadowska, et al. (2004). Autologous skeletal myoblast transplantation for the treatment of postinfarction myocardial injury: phase I clinical study with 12 months of follow-up. *Am Heart J*. 148; 3, 531-537. doi: 10.1016/j.ahj.2004.03.043

Sottile, J. (2004). Regulation of angiogenesis by extracellular matrix. *Biochim Biophys Acta*. 1654; 1, 13-22. doi: 10.1016/j.bbcan.2003.07.002

Sumide, T., K. Nishida, M. Yamato, T. Ide, Y. Hayashida, K. Watanabe, et al. (2006). Functional human corneal endothelial cell sheets harvested from temperature-responsive culture surfaces. *FASEB J*. 20; 2, 392-394. doi: 10.1096/fj.04-3035fje

Suzuki, K., B. Murtuza, S. Fukushima, R. T. Smolenski, A. Varela-Carver, S. R. Coppen, et al. (2004). Targeted cell delivery into infarcted rat hearts by retrograde intracoronary infusion: distribution,

dynamics, and influence on cardiac function. *Circulation*. 110; 11 Suppl 1, II225-230. doi: 10.1161/01.CIR.0000138191.11580.e3

Suzuki, K., B. Murtuza, R. T. Smolenski, I. A. Sammut, N. Suzuki, Y. Kaneda, et al. (2001). Cell transplantation for the treatment of acute myocardial infarction using vascular endothelial growth factor-expressing skeletal myoblasts. *Circulation*. 104; 12 Suppl 1, I207-212. doi: 10.1161/hc37t1.094524

Tahergorabi, Z. and M. Khazaei (2012). A review on angiogenesis and its assays. *Iran J Basic Med Sci*. 15; 6, 1110-1126. doi:

Takezawa, T., Y. Mori and K. Yoshizato (1990). Cell culture on a thermo-responsive polymer surface. *Biotechnology (N Y)*. 8; 9, 854-856. doi: 10.1038/nbt0990-854

Taylor, D. A., B. Z. Atkins, P. Hungspreugs, T. R. Jones, M. C. Reedy, K. A. Hutcheson, et al. (1998). Regenerating functional myocardium: improved performance after skeletal myoblast transplantation. *Nat Med*. 4; 8, 929-933. doi:

Terajima, Y., T. Shimizu, S. Tsuruyama, H. Sekine, H. Ishii, K. Yamazaki, et al. (2014). Autologous Skeletal Myoblast Sheet Therapy for Porcine Myocardial Infarction Without Increasing Risk of Arrhythmia. *Cell Med*. 6; 3, 99-109. doi: 10.3727/215517913X672254

Thummarati, P. and M. Kino-oka (2020). Effect of Co-culturing Fibroblasts in Human Skeletal Muscle Cell Sheet on Angiogenic Cytokine Balance and Angiogenesis. *Frontiers in Bioengineering and Biotechnology*. 8; 1121, doi: 10.3389/fbioe.2020.578140

Ueda, H., T. Nakamura, K. Matsumoto, Y. Sawa, H. Matsuda and T. Nakamura (2001). A potential cardioprotective role of hepatocyte growth factor in myocardial infarction in rats. *Cardiovasc Res*. 51; 1, 41-50. doi: 10.1016/s0008-6363(01)00272-3

Xin, X., S. Yang, G. Ingle, C. Zlot, L. Rangell, J. Kowalski, et al. (2001). Hepatocyte growth factor enhances vascular endothelial growth factor-induced angiogenesis in vitro and in vivo. *Am J Pathol*. 158; 3, 1111-1120. doi: 10.1016/S0002-9440(10)64058-8

Xuan, N. T. (2013). Study on Endothelial Network Formation in Fluidic Multilayered Myoblast Sheet. doi: 10.18910/26216

Yang, J., M. Yamato, C. Kohno, A. Nishimoto, H. Sekine, F. Fukai, et al. (2005). Cell sheet engineering: recreating tissues without biodegradable scaffolds. *Biomaterials*. 26; 33, 6415-6422. doi: 10.1016/j.biomaterials.2005.04.061

Yuan, B., Z. Zhao, Y. R. Zhang, C. T. Wu, W. G. Jin, S. Zhao, et al. (2008). Short-term safety and curative effect of recombinant adenovirus carrying hepatocyte growth factor gene on ischemic cardiac disease. *In Vivo*. 22; 5, 629-632. doi:

Yun, Y. R., S. Lee, E. Jeon, W. Kang, K. H. Kim, H. W. Kim, et al. (2012). Fibroblast growth factor 2-functionalized collagen matrices for skeletal muscle tissue engineering. *Biotechnol Lett*. 34; 4, 771-778. doi: 10.1007/s10529-011-0812-4

Yun, Y. R., J. E. Won, E. Jeon, S. Lee, W. Kang, H. Jo, et al. (2010). Fibroblast growth factors: biology, function, and application for tissue regeneration. *J Tissue Eng*. 2010; 218142. doi: 10.4061/2010/218142

Zachary, I. and G. Gliki (2001). Signaling transduction mechanisms mediating biological actions of the vascular endothelial growth factor family. *Cardiovasc Res*. 49; 3, 568-581. doi: 10.1016/s0008-6363(00)00268-6

Zhang, F., W. X. Peng, L. Wang, J. Zhang, W. T. Dong, J. H. Wu, et al. (2018). Role of FGF-2 Transfected Bone Marrow Mesenchymal Stem Cells in Engineered Bone Tissue for Repair of Avascular Necrosis of Femoral Head in Rabbits. *Cell Physiol Biochem*. 48; 2, 773-784. doi: 10.1159/000491906

Zubilewicz, A., C. Hecquet, J. C. Jeanny, G. Soubrane, Y. Courtois and F. Mascarelli (2001). Two distinct signalling pathways are involved in FGF2-stimulated proliferation of choriocapillary endothelial cells: a comparative study with VEGF. *Oncogene*. 20; 12, 1403-1413. doi: 10.1038/sj.onc.1204231

List of publications

Original papers

1. **Thummarati, P**. and M. Kino-oka (2020). Effect of Co-culturing Fibroblasts in Human Skeletal Muscle Cell Sheet on Angiogenic Cytokine Balance and Angiogenesis. *Frontiers in Bioengineering and Biotechnology*. 8; 1121, doi: 10.3389/fbioe.2020.578140
2. **Thummarati, P**. and M. Kino-oka (2021). Exogenous FGF-2 prolongs endothelial connection in multilayered human skeletal muscle cell sheet. *J. Biosci. Bioeng.* Epub.30.03.2021, doi: 10.1016/j.jbiosc.2021.02.005

Conferences

1. **Thummarati, P**. and M. Kino-oka (2019). "Effect of fibroblast population on VEGF secretion in human skeletal muscle myoblast sheet". ISCT 2018 Montreal Annual Meeting, Montréal, Montréal, Canada. May 2^{nd} – 5^{th}, 2018
2. **Thummarati, P**. and M. Kino-oka (2019). "Effect of fibroblast population on cytokine productions in skeletal muscle myoblast sheet". The 18th APCChE Congress (APCChE 2019), Sapporo, Japan. September 23^{rd} – 27^{th}, 2019.

Acknowledgments

First and foremost, I would like to express my deepest appreciation and gratitude to my esteemed supervisor, Prof. Dr. Masahiro Kino-oka, Department of Biotechnology, Graduate School of Engineering, Osaka University, for constant encouragement and valuable suggestions.

I also profoundly grateful for all the help and valuable advice with this Ph.D. thesis from Prof. Dr. Takeshi Omasa and Prof. Dr. Takayoshi Watanabe. Without your guidance and constant feedback, this Ph.D. would not have been achievable.

I also gratefully acknowledge Assoc. Prof. Dr. Mae Hee Kim, Department of Biotechnology, Graduate School of Engineering, Osaka University, and Assoc. Prof. Dr. Eiji Nagamori, Department of Biomedical Engineering, Osaka Institute of Technology, for their helpfulness and sincere suggestion of my study.

I am heartily thankful and owe my deepest gratitude to Dr. Li Menglu, Mr. Tadashi Nakamura, and Mr. Motoki Yagi, my excellent trainers, for tremendous and moral support to conquer the impossible difficulties for me to do alone. I would also like to give warm thanks to Iwata Toshihiko and Iwahashi Atsushi to support the experiment.

I wish to express my deep sense of gratitude to Dr. Chaiyong Koaykul for his constant support, care, affection, and excellent advice. Special thanks are extended to BioProcess Systems Engineering Laboratory members for their excellent helpfulness and great friendship.

I also thank the Ministry of Education, Culture, Sports, Science, and Technology (MEXT) Japanese Government for supporting my study at the Graduate School of Engineering, Osaka University under the Japanese Government (Monbukagakusho) scholarship student.

Finally, I am grateful appreciation to my family, beloved Thai teachers, and friends for their infinite love, understanding, supporting all my pursuits and believing in me, which will never be forgotten.

Thummarati Parichut

September 2021